LONG-TERM PERFORMANCE OF RECYCLED STEEL FIBRE REINFORCED CONCRETE FOR PAVEMENT APPLICATIONS

(Volume 2)

A thesis submitted for the degree of Doctor of Philosophy in the Faculty of Engineering of the University of Sheffield

By

Ângela Gaio Graeff

(BSc, MSc)

Centre for Cement and Concrete
Department of Civil and Structural Engineering
The University of Sheffield

Sheffield

April 2011

CHAPTER 11

11. CLOSURE

This chapter deals with the main conclusions arrived from the results presented in this thesis. The chapter provides answers for the research questions asked in Chapter 1. It also provides some recommendations for future work, aiming to understand the aspects of the durability of recycled SFRC that were not addressed in this work.

11.1 DISCUSSION AND CONCLUDING REMARKS

This thesis aimed at understanding the long-term performance of concrete reinforced with recycled steel fibres recovered from post-consumer tyres. The main conclusions that can be drawn from the work carried in the thesis are presented in this section.

For the literature review described in Chapters 2 and 3, the following can be concluded:

- Sustainability is a key element that is increasingly taken into account in the design of concrete structures. The use of recycled steel fibres recovered from post-consumer tyres as reinforcement for concrete pavements can make construction more sustainable. The fibres are a good quality manufactured product that can be reused to improve some properties of plain concrete. By improving the mechanical properties of the concrete, this leads to other sustainable benefits, such as the reduction of the pavement depth, which uses less natural resources. In addition, the energy consumed to sort and process the recycled fibres is much lower than the energy used to produce new fibres.

- The design codes for road pavements do not take into account the post-cracking behaviour of SFRC, and more work should be undertaken to include the advantages of SFRC in design procedures. The TR 34 (The Concrete Society, 2003) considers the post-cracking behaviour of SFRC for industrial floors. However, it does not account for the fatigue and other concrete pavement failure criteria. More studies in this field would encourage the extended use of steel fibres in concrete, including the ones recovered from post-consumer tyres, and also lead to indirect benefits, such as cost reductions and minimal use of natural resources.

- The literature review on the use of recycled steel fibres as reinforcement for concrete shows that very few studies were undertaken on the subject. The University of Sheffield is leading the studies on the use of recycled fibres in concrete, and no studies prior to this thesis can be found on the durability and long-term performance of recycled SFRC.

The results from this study in terms of mechanical properties of control specimens show that recycled fibres tend to enhance some of the properties of the concrete, especially in terms of flexural post-cracking behaviour.

- Compressive strength is slightly increased by the addition of fibres and fibres (approximately by 10%), especially in wet mixes, and fibres help to keep the integrity of the specimens even after failure.

- Flexural behaviour is greatly affected by the inclusion of recycled fibres. When they are added at higher amounts (e.g. 6% by mass), the concrete has similar behaviour as that containing 2% industrial fibres, in both flexural strength and post-cracking behaviour. The amount of 2% recycled fibres shows a well-defined post-cracking behaviour, however much lower than 6% (residual flexural strength results are less than half the strength observed for 2I and 6R).

- The use of recycled fibres (for both fibre contents analysed – 2% and 6%) fulfil the BS EN 14889-1 (2006a) requirements in terms of the effect of fibres on the strength of concrete, which says that the residual strength at 0.5 mm and 3.5 CMOD should be higher than 1.5 and 1.0 MPa, respectively.

- LEC mixes have higher flexural strength (ultimate and at the limit of proportionality) than CIP mixes (usually around 5-20% higher), which is probably due to enhanced adhesion between the fibres and the matrix. On the other hand, CIP and LEC mixes show similar flexural post-cracking behaviour, which means that LEC presents a more brittle pull-out behaviour than CIP cementitious material, especially when the fibre starts debonding from the matrix (friction phase).

The results for some pore-structure related properties (density, porosity and free-shrinkage) show that the inclusion of recycled fibres, in general, does not influence the pore structure of the concrete. Exceptions apply for situations where the high amount of fibres (around 6%) leads to compaction limitations and high amount of trapped air, for RCC mixes, and to a reduction of air entrained bubbles, for wet mixes. Other findings related to pore-structure related properties are described below:

- The LEC mixes seem to have finer pore size than CIP mixes, based only on indirect measurements of pore fineness. More accurate tests should be undertaken to obtain the influence of the cementitious material on the pore structure of concrete.

- LEC mixes are up to 10% denser than CIP mixes, which is probably due to LEC mixes having finer size of pores than CIP mixes, and also because the LEC itself may be denser than CIP. On the other hand, porosity results show that LEC mixes are sometimes up to 50% more porous than CIP mixes. This is probably because LEC has less reactivity than CIP, which leads to less C-S-H products at the age they were tested (28 days). This probably changes with age as further hydration takes place for LEC mixes.

- 6R wet mixes have higher density (approximately 3%) than the corresponding mixes with lower amount of fibres. This is due to the higher amount of steel in the mix, which has higher specific density compared to the other constituents of the mix. However, the opposite is observed for the 6R RCC mixes (a reduction in approximately 3%). This is because of the boundary conditions of RCC specimens which, due to the *springiness* of the fibres and to the compaction procedures, lead to a more porous area in the outer parts of the specimens.

- RCC mixes can have more than 2 times higher porosity than wet mixes. This is due to the high amount of trapped air in the mix, caused by compaction limitations, especially close to boundaries of the specimens.

- The mechanical properties are more easily correlated with density than other pore-structure-related properties, and this is especially true for wet mixes.

- Regarding the temperature for the preconditioning of specimens prior to density, porosity and other transport mechanisms properties, it could be observed that the temperature does play an important role on the results. Higher temperatures are more effective in eliminating water from the pores, while lower temperatures allow more water to remain in the concrete thus blocking the pores and affecting the results. Based on experimental data, the temperature of 80 C appears to be the most appropriate for the preconditioning of specimens.

The transport mechanisms results show that steel fibres do not influence the transport of aggressive agents into concrete. Exceptions apply when high contents of fibres lead to compaction limitations and to changes in the rheological characteristics of the mix. The main factors influencing the transport mechanisms are the mix constituents (other than fibres), compaction and curing procedures. In particular, the tests carried out in this thesis showed that the cementitious material plays an important role in the transport mechanism results, as explained below.

- LEC mixes are considerably more permeable than CIP mixes (which can be up to 100 times more). Sorptivity results of LEC mixes are also slightly higher than CIP mixes. This is probably due to the lower amount of C-S-H products of LEC mixes at 28 days and also due to the size of CIP particles, which seems to fit better the RCC aggregate gradation curve, thus contributing to a better packing of the particles. However, the size of the LEC and CIP particles was not investigated in this thesis and further studies should be carried out on the characterisation of the cementitious materials. The higher values of permeability and sorptivity of LEC mixes may lead to durability problems of mixes using such cementitious material type. This is mainly because the specimens were tested at 28 days and, hence, this behaviour should change due to further hydration of the cement.

- LEC mixes have, in general, lower diffusion coefficient than CIP mixes, which appears to be due to the lower reactivity and lower C_3A of the cement, which binds less chloride than CIP. Diffusion coefficient of CIP mixes are less than half of the diffusion coefficient of the corresponding LEC mixes.

- RCC mixes have usually 2-3 times more sorptivity than wet mixes. Again, this is due to the higher amount of trapped air during casting.

The corrosion analysis shows that, after 10 months of wet-dry cycles, only superficial rust in fibre reinforced concrete could be observed. Other findings are explained as follows.

- The mechanical properties were enhanced due to 5 and 10 months of wet-dry cycles, however, they seem to stabilise after 5 months of wet-dry cycles. This is due to further hydration of the cementitious material. The increase in the compressive strength varied from 15-50%, with the LEC mixes being the ones that presented the highest increase in strength. The increase in the flexural strength was lower than in the compressive strength, and maximum increase was up to 35% compared to control specimens (at 28 days).

- Pre-cracked specimens were also exposed to wet-dry cycles and the results show that cracks with a maximum width of 0.2 mm appear to regain some of the concrete continuity due to autogeneous healing of the concrete.

- There seems to be a correlation of mechanical properties after wet-dry cycles with pore-structure and transport mechanisms properties. Higher permeability, porosity and sorptivity leads to a higher rate of moisture transport into concrete, which improves curing, and enhances the hydration rate of the cement, thus leading to higher increase in the mechanical properties.

- Specimens exposed to 10 months of wet-dry cycles showed lower residual flexural strength results after 2.5 mm of crack mouth opening displacement than the ones exposed at 28 days and 5 months. This is probably not due to corrosion but to the higher hydration level and improved curing of the specimens, that appears to lead to a more brittle pull-out behaviour, especially when the fibre starts debonding from the matrix.

- Specimens were exposed up to 10 months of wet-dry cycles, which is not sufficient to provide full understanding of the corrosion behaviour of SFRC. Longer periods of exposure and combined effects with loading and other deterioration processes may give a better understanding of the real effects of chloride ingress into SFRC.

The freeze-thaw results are affected by the inclusion of recycled fibres. The way fibres affect the freeze-thaw behaviour is not in terms of avoiding the ingress of water and other freeze-thaw aggressive agents into concrete, but by restraining the stresses caused by freezing of the pore solution, thus controlling crack propagation. This occurs mainly in concrete with advanced level of freeze-thaw deterioration (higher than 2% scaling). At the superficial scaling, fibres are not knitted in such a way to keep the integrity of the concrete. This effect is mainly observed for recycled SFRC, due to the high amount and shape of fibres. Other conclusions on the freeze-thaw results are explained below.

- RCC specimens are more susceptible to deterioration (up to 10 times higher scaling) than wet mixes due to the larger amount of voids caused by trapped air, which are coarser and not well spaced as air-entrained pores. The larger sorptivity and permeability of RCC mixes also contributes for the high freeze-thaw deterioration.

- The inclusion of 6R in RCC mixes keeps the integrity of the concrete at an accelerated level of deterioration, thus slowing down the degradation process. In this case, 6R had better performance than 2I mixes.

- The addition of 6R in wet mixes reduced the air entrained content of the fresh mix by 50% (probably by mechanically breaking the fresh formed bubbles), which led to higher deterioration than the corresponding 2I wet mix. However, since wet mixes had much lower deterioration than RCC mixes, in this case the knitted effect of the fibres was not triggered.

- Both wet and RCC mixes had their flexural behaviour reduced after freeze-thaw exposure. The latter was more severely affected, with flexural strength reductions varying from 50% to 85% compared with the non-damaged specimens. This is because damage caused by freeze-thaw is also observed in terms of internal damage. Even though measurements of internal damage were not taken, the residual flexural behaviour gives a good indication of such damage.

- The mechanical freeze-thaw resistance of concrete is clearly influenced by the characteristics of the pore structure of the material. High values of porosity, sorptivity and permeability increase the degree of saturation of specimens during freeze-thaw cycles, which leads to higher stresses during freezing of concrete, accelerating the damage and reducing strength.

- The method used to accelerate freeze-thaw cycles is quite aggressive since specimens are fully-immersed in chloride solution during the tests, which is not realistic, especially when dealing with concrete pavements. Hence, a less aggressive test should be considered in future works.

The fatigue analysis shows that steel fibres improve the behaviour of both wet and RCC mixes. Other issues on the fatigue behaviour were also raised:

- There seems to be an optimum fibre content that gives the best fatigue performance, which seems to be between 2 and 6% for recycled fibres. However, since only these two fibre contents were examined, further studies should be undertaken.

- The aggregate interlock effect improves the fatigue resistance of RCC mixes compared with wet mixes, especially at high stress levels (higher than 0.7).

- Recycled fibres are more efficient in arresting the propagation of micro-cracks, while industrial fibres are more effective in controlling the propagation of macro-cracks. Thus, a combination of both recycled and industrially produced fibres should give the best fatigue performance, and increase the fatigue life of the concrete. Further investigations should be carried to find out the ideal combination of both fibres that gives the longest fatigue life.

- Recycled fibres show a more brittle pull-out behaviour than for industrially produced fibres, caused by their low ability in arresting meso and macro-cracks. For this reason, the use of recycled fibres alone as reinforcement is more effective when the concrete is subjected to lower stress levels (such as when the concrete is not initially cracked).

- A simplified practical example explained some advantages of considering the fatigue post-cracking behaviour and the probabilistic analysis in the design guidelines of concrete pavements. This showed that, if the inclusion of fibres is taken into account, especially by allowing pavements to be subjected to higher stress levels, this could diminish the thickness of the pavements up to around 20% and contribute for less use of resources.

The analysis in terms of probabilistic analysis leads to the following findings:

- A simplified probabilistic method was proposed to correlate results of chloride ingress from wet-dry cycles with fully-saturated conditions. The method is not fully validated in this thesis and requires some further investigations in this subject. If validated, the method may be used to estimate a correlation between wet-dry cycles and specific environments.

- The fully-saturated condition of chloride ingress (based on Fick's second law of diffusion) was used to perform a parametric study to compare the depth of chloride ingress into concrete for various mixes. The results show that the amount of 2% of fibres has the lowest chloride ingress depth compared to other fibre contents. Same behaviour was observed from wet over RCC mixes and from LEC over CIP mixes.

- The freeze-thaw probabilistic analysis proposes a methodology for calculating the service life of concrete pavements exposed to freeze-thaw cycles. The method is based on the scaling resistance of the concrete, and also takes into account climate data. A practical example was used for the model, based on the mixes tested experimentally. However, there is still a need to understand the correlation between the accelerated tests with more realistic situations. Other input parameters are still unknown in the model, and should be determined in the future to fully validate the model.

- The fatigue probabilistic analysis can be used used in practice, for design purposes. However, the low of data prevented clearer conclusions.

11.2 ANSWER TO QUESTIONS

This section provides answers to the research questions raised in Chapter 1. The following responses can be drawn from the understanding of the thesis.

On the use of recycled fibres as reinforcement for concrete pavements: Recycled fibres improve the post-cracking flexural behaviour of the concrete and, when used at a higher content, they can lead to similar mechanical performance as for industrially produced fibres. If well sorted (e.g. ideal fibre length distribution and textile-free) and up to a certain content, recycled fibres can be added to concrete without causing agglomeration. For these reasons and for many others described in the next responses, recycled fibres appear to be a suitable alternative for reinforcement for both conventional and RCC pavements.

On the use of recycled SFRC against asphalt and common used pavement technique: Even though asphalt pavements are the most widely used pavement technique, the use of concrete pavements is increasing significantly due to the improvement of concrete technology and to durability benefits compared to asphalt pavements. The use of recycled steel fibres in concrete pavements shows similar benefits as for conventional concrete pavements, with the addition of collaborating with the sustainability in road construction. Fibres can be added to conventional concrete and placed with concrete pavers or they can also be added to RCC and placed with asphalt pavers. The inclusion of fibres does not need any alteration in the paving system, except for an extra step of adding and mixing the fibres into the concrete. If the design guidelines start accounting for the post-cracking behaviour of recycled SFRC (pavement can be cracked while in operation), the design depth will reduce and, as a result, the use of natural resources could be reduced and the costs diminished. This could lead to a more competitive use for concrete pavements.

On the influence of recycled fibres in the pore structure of the concrete: Recycled fibres affect the pore structure of the concrete only when used at higher contents, as for any other steel fibre type. For wet and RCC mixes, fibre contents higher than 6% lead to balling of the fibres, which causes large voids and discontinuities in the pore structure of the concrete. RCC is more affected by higher amounts of recycled fibres due to the 'springiness' effect of the fibres combined with the compaction procedures used, especially close to the boundaries of the specimens, which lead to discontinuities and voids in those regions. The influence of recycled fibres in the pore structure properties of the concrete are associated with the amount of trapped air, the formation of balling and the compaction procedures when high amount of fibres are added to the concrete. There seems to be an ideal fibre content that does not affect the pore structure of the concrete. This seems to be in-between 2 and 6% for both wet and RCC mixes, since 2% did not cause any changes in both mixes and 6% caused compaction limitation in RCC and reduction of air content in fresh wet mixes.

On the response of recycled SFRC against the main deterioration processes of concrete pavements: Recycled SFRC reacted well against the three deterioration processes investigated in this thesis. 1) The corrosion of fibres is not an issue since fibres do not get corroded while inside the concrete, and only superficial rust can be observed. Corrosion through the cracks may be a problem depending on the crack width. For cracks opening smaller than 0.2 mm, autogeneous healing seems to heal the cracks after certain period of time. Larger crack widths were not studied in this thesis and for this reason should be analysed in further investigations. 2) The addition of recycled fibres in wet mixes does not influence the freeze-thaw performance of the concrete, whilst in RCC mixes, the recycled fibres control cracking, keep the integrity of the material and slow down the deterioration process. 3) Recycled fibres contribute to avoid propagation of micro-cracks into meso-cracks when subjected to fatigue and, for this reason, improve the fatigue behaviour of the concrete. However, the ideal situation would be the combination of both recycled and industrial fibres in order to significantly increase the fatigue life of the concrete.

On models to predict service life of recycled SFRC pavements: Specific models to predict the service life of concrete pavements subjected to specific deterioration processes can be used. Due to many uncertain factors influencing the deterioration processes, probabilistic models seem to be the most appropriate. In this thesis, a new model to predict the service life of concrete pavements subjected to freeze-thaw is proposed. A model based on the fully-saturated condition is also discussed to evaluate the depth of chloride ingress into concrete. Fatigue probabilistic analysis is also shown based on the number of cycles that pavements can endure for a certain stress level. Due to a lack of methods specific for recycled SFRC, the models are based on experimental results carried out in this thesis, and further investigation should be carried out to verify the accuracy of the models. There is also a need to combine the various deterioration processes in a single deterioration model for recycled SFRC.

On the benefits of recycled SFRC on the design and maintenance of concrete pavements: If the post-cracking and the fatigue behaviours of SFRC (including both recycled and industrially produced) are accounted for in the design guidelines, the depth of the concrete pavements would reduce and this would lead to a reduction of costs and natural resources. In terms of maintenance procedures, the addition of fibres does not seem to reduce the long-term performance of concrete pavements. On the contrary, in some cases such as when subjected to freeze-thaw attack, fibres seem to slow down the deterioration process. They also improve the fatigue performance of the concrete. Fibres are protected inside the concrete against corrosion and no major effect on the structural performance is observed in un-cracked or thinned cracked concrete. If the concrete is well designed to account for the addition of fibres in a rational way, this could lead to a reduction in the maintenance procedures of the concrete structures.

11.3 RECOMMENDATIONS FOR FUTURE WORK

The following items are recommendations for future work, aiming to understand some issues that, mainly by time restriction, were not addressed in this thesis.

On the variables of the research: More recycled fibre contents should be studied to find out the ideal content that provides the best performance in terms of mechanical and durability behaviour. More fibre types from other recycling units should be considered, to account for various sorting processes and fibre geometries, which may significantly influence the results.

Apart from the recycled fibre content and type, there is a need to understand the influence of the various constituents of the mix proportions on the long-term and mechanical performance of recycled SFRC, such as the use of different w/c ratios and cement contents. Curing and casting procedures should also be accounted for. This could be carried out by a parametric study.

The use of LEC should be further investigated, especially in terms of characterisation of the cement and strength development of concrete and its pore structure.

On the casting procedures: When dealing with RCC, another casting procedure should be developed since it seems that the boundary conditions of the specimens influence the results. Ideally, cores should be extracted from a real RCC slab and compared with the results obtained by the compaction procedure used in this thesis.

On the mechanical performance: Ageing development in the strength of LEC mixes should be examined in more details. Aspects on the bond behaviour of LEC matrix and fibres should also be better understood.

The assumed brittle bond behaviour in recycled SFRC due to improved curing conditions and/or enhanced adhesion between the fibres and the matrix should be investigated in more detail. Pull-out tests could be performed to assess such characteristics.

On the pore structure-related properties: The pore size distribution of reinforced and plain concrete should be studied by specific experimental procedures such as the use of MIP (mercury intrusion porosimetry), electronic microscopy, etc. This contributes to find out if the inclusion of fibres causes discontinuities in the concrete matrix. Moreover, this could provide a better understanding of the influence of the cementitious material on the pores structure of the concrete. It could also provide more precise information on the boundary conditions of RCC mixes.

There is a need to understand the restrained shrinkage behaviour of recycled SFRC. Shrinkage behaviour is an important parameter for the design of concrete pavements.

On the deterioration processes: Deterioration processes other than the ones studied in this thesis should be taken into account. This includes sulphate attack, corrosion due to carbonation, roughness deterioration, shrinkage stresses, among others.

Diffusivity should be evaluated by using a larger number of samples to account for the variability usually encountered when dealing with experimental tests. Moreover, the new released draft standard DD CEN/TS 12390-11 (2010) for the calculation of diffusion should be followed.

The coupled effects of different deterioration processes should be understood. This includes, for example, the simulation of corrosion, fatigue and freeze-thaw simultaneously.

On the corrosion analysis: The use of wet-dry cycles should be studied in further detail to understand how accelerated is the method compared to real situations. This can be done by modelling the non-saturated ingress of chloride into concrete by considering the coupled effect of diffusion and convection. Other methods of accelerating chloride ingress should also be considered, such as the exposure to mist chambers.

Specimens should be exposed to longer periods of corrosion accelerated methods, to verify whether longer periods may lead to deterioration other than superficial rust.

The effect of different crack widths on the corrosion resistance of SFRC through the cracks should be investigated. This is especially important when dealing with the coupled effect of fatigue and corrosion.

On the freeze-thaw analysis: Efforts should be made to verify the correlation between the accelerated tests with real conditions. This would contribute for a better use of the proposed service life method. In addition, more work should be performed on other parameters affecting the service life prediction of freeze-thaw exposed specimens, such as the resistance temperature and the limit scaling.

A more realistic method to simulate freeze-thaw in concrete pavements should be used other than the fully-saturation method chosen in this thesis.

<u>On the fatigue analysis:</u> The combination of both industrially produced and recycled fibres should be investigated to verify whether the fatigue life of the concrete increases or not, as it was postulated in Chapter 10.

More efforts should be undertaken to understand the toughness behaviour during fatigue cycles. For that, a specific methodology should be developed to accurately and simultaneously measure the load and displacements of specimens.

<u>On the design guidelines recommendations:</u> This thesis was mainly focused on the experimental tests carried out to understand the long-term behaviour of recycled SFRC. However, there is a need to apply the experimental findings in terms of guidelines for the design of concrete pavements. For that, a larger database of results should be grouped together to provide accurate recommendations for the design codes.

REFERENCES

AASHTO (1993) *AASHTO Guide for design of pavement structures*, Washington, DC, American Association of State Highway and Transportation Officials.

AASHTO (1998) *Supplement to the AASHTO Guide for design of pavement structures*, Washington, DC, American Association of State Highway and Transportation Officials.

Ababneh, A.; Benboudjema, F. & Xi, Y. (2003) 'Chloride penetration in nonsaturated concrete.' *Journal of Materials in Civil Engineering,* 15, 2, 183-191.

Abbas, A.; Carcasses, M. & Ollivier, J-P. (1999) 'Gas permeability of concrete in relation to its degree of saturation.' *Materials and Structures,* 32, 3-8.

ACPA (2010a) *Why concrete pavement.* [online]. Available at: <URL: http://www.pavement.com/concrete_pavement/About_Concrete/Why_Concrete_Pavement/index.asp> [Acessed 21 March 2010].

ACPA (2010b) Differences between concrete and asphalt pavement [online]. Available at: <URL: http://www.pavement.com/Concrete_Pavement/Technical/Fundamentals/Differences_Between_Concrete_and_Asphalt.asp> [Acessed 16 June 2010].

ACPA (2011) Concrete pavement fundamentals [online]. Available at: <URL: http://www.pavement.com/Concrete_Pavement/Technical/Fundamentals/index.asp> [Acessed 28 March 2011].

ACPA (2008) 'The economics of concrete pavements.' *Concrete Pavement Progress*, 44, 3.

Adnan, A. B. & Al-Balbissi, A. H. (1989) 'Probabilistic design of flexible and rigid pavements using AASHTO equations.' *Transportation Research Record,* 1227, 34-43.

Aggregate Industries (2010) Aggregate Industries UK [online]. Available at: <URL: http://www.aggregate.com> [Acessed 05 May 2010].

Aiello, M. A., Leuzzi, F., Centonze, G. & Maffezzoli, A. (2009) 'Use of steel fibres recovered from waste tyres as reinforcement in concrete: Pull-out behaviour, compressive and flexural strength.' *Waste Management,* Article in Press.

Alavi-Fard, M. & Marzouk, H. (2004) 'Bond of high-strength concrete under monotonic pull-out loading.' *Magazine of Concrete Research*, 56, 9, 545-557.

Albuquerque, A. C. (2009) *Estudo das propriedades de concreto massa com adição de partículas de borracha de pneu,* Doctorate Thesis, Federal University of Rio Grande do Sul. In Portuguese.

Aldea, C-M.; Shah, S. P. & Karr, A. (1999a) 'Effect of cracking on water and chloride permeability of concrete.' *Journal of Materials in Civil Engineering,* 11, 3, 181-187.

Aldea, C-M.; Shah, S. P. & Karr, A. (1999b) 'Permeability of cracked concrete.' *Materials and Structures,* 32, 370-376.

Alonso, M. C. & Sanchez, M. (2009) 'Analysis of the variability of chloride threshold values in the literature.' *Materials and Corrosion,* 60, 8, 631-637.

Al-Oraimi, S. K. & Seibi, A. C. (1995) 'Mechanical characterisation and impact behaviour of concrete reinforced with natural fibres.' *Composite Structures,* 32, 165-171.

Altun, F.; Haktanir, T. & Ari, K. (2007) 'Effects of steel fiber addition on mechanical properties of concrete and RC beams.' *Construction and Building Materials,* 21, 654-661.

Alwan, J. M.; Naaman, A. E. & Hansen, W. (1991) 'Pull-out work of steel fibers from cementitious composites: analytical investigation.' *Cement and Concrete Composites,* 13, 247-255.

Aly, T.; Sanjayan, J. G. & Collins, F. (2008) 'Effect of polypropylene fibers on shrinkage and cracking of concretes.' *Materials and Structures,* 41, 1741-1753.

American Concrete Institute (2008) ACI 544.3R-08. *Guide for specifying, proportioning, and production of fiber-reinforced concrete,* Detroit, USA.

American Concrete Institute (2002) ACI 211.3R-02. *Guide for selecting proportions for no-slump concrete,* Detroit, USA.

American Concrete Institute (1999) ACI 207.5R-99. *Roller-compacted mass concrete,* Detroit, USA.

American Concrete Institute (1996) ACI 544.1R-96. *Report on fiber reinforced concrete,* Detroit, USA.

American Concrete Institute (1995) ACI 325.10R-95. *Report on Roller-Compacted Concrete Pavements,* reapproved 2001, Detroit, USA.

American Concrete Institute (1989) ACI 544.2R-89. *Measurement of properties of fiber reinforced concrete,* Detroit, USA.

American Concrete Institute (1988) ACI 544.4R-88. *Design considerations for steel fiber reinforced concrete,* Detroit, USA.

American Concrete Institute (1982) ACI 544.1R-82. *State-of-the-art report on fiber reinforced concrete,* Detroit, USA.

American Standardization of Testing Material (2010a) ASTM C114. *Standard test methods for chemical analysis of hydraulic cement,* Philadelphia, U.S.

American Standardization of Testing Material (2010b) ASTM C1202. *Standard test method for electrical indication of concrete's ability to resist chloride ion penetration,* Philadelphia, U.S.

American Standardization of Testing Material (2009a) ASTM C490. *Standard practice for use of apparatus for the determination of length change of hardened cement paste, mortar and concrete,* Philadelphia, U.S.

American Standardization of Testing Material (2009b) ASTM C1581. *Standard test method for electrical determining age at cracking and induced tensile stress characteristics of mortar and concrete under restrained shrinkage,* Philadelphia, U.S.

American Standardization of Testing Material (2008a) ASTM C215. *Standard specification for fundamental transverse, longitudinal, and torsional frequencies of concrete specimens,* Philadelphia, U.S.

American Standardization of Testing Material (2008b) ASTM C1435. *Standard practice for molding roller-compacted concrete in cylinder molds using a vibrating hammer,* Philadelphia, U.S.

American Standardization of Testing Material (2006a) ASTM A820. *Standard specification for steel fibers for fiber-reinforced concrete,* Philadelphia, U.S.

American Standardization of Testing Material (2006b) ASTM C642. *Standard test method for density, absorption, and voids in hardened concrete,* Philadelphia, U.S.

American Standardization of Testing Material (2006c) ASTM C341. *Standard practice for length change of cast, drilled, or sawed specimens of hydraulic-cement mortar and concrete,* Philadelphia, U.S.

American Standardization of Testing Material (2006d) ASTM C1579. *Standard test method for evaluating plastic shrinkage cracking of restrained fiber reinforced concrete (using a steel form insert),* Philadelphia, U.S.

American Standardization of Testing Material (2004) ASTM C1585. *Standard test method for measurement of rate of absorption of water by hydraulic-cement concretes,* Philadelphia, U.S.

American Standardization of Testing Material (2003a) ASTM C666. *Standard test method for resistance of concrete to rapid freezing and thawing,* Philadelphia, U.S.

American Standardization of Testing Material (2003b) ASTM C1556. *Standard test methods for determining the apparent chloride diffusion coefficient of cementitious mixtures by bulk diffusion,* Philadelphia, U.S.

American Standardization of Testing Material (1997) ASTM C1018. *Standard test method for flexural toughness and first-crack strength of fiber-reinforced concrete (using beam with third-point loading)*, Philadelphia, U.S.

Amgai, T. (2004) 'Burning tires: health hazards' *Nepal news*, 24, 10.

Andrade, C. & Whiting, D. (1996) 'A comparison of chloride ion diffusion coefficients derived from concentration gradients and non-steady state accelerated ionic migration.' *Materials and Structures*, 29, 476-484.

Andrade, C.; Sanjuan, M. A.; Recuero, A. & Rio, O. (1994) 'Calculation of chloride diffusivity in concrete from migration experiments, in non steady-state conditions.' *Cement and Concrete Research*, 24, 7, 1214-1228.

Andrade, C. (1993) 'Calculation of chloride diffusion coefficients in concrete from ionic migration measurements.' *Cement and Concrete Research*, 23, 724-742.

Angelakopoulos, H. (2011) *Steel fibre reinforced roller compacted concrete pavements.* Doctorate Thesis, The University of Sheffield.

Angelakopoulos, H., Neocleous, K. & Pilakoutas, K. (2008a) 'Steel fibre reinforced roller compacted concrete pavements.' *Challenges for Civil Construction 2008.* Proceedings of Challenges for Civil Construction 2008, Porto, Portugal, ISBN: 978-972-752-100-5, pp 238 (CD proceedings).

Angelakopoulos H., Neocleous K. & Pilakoutas K. (2008b) Flexural testing of SFRC for all different types of fibres supplied. *Deliverable Report 2.5, FP6 EU STREP Project EcoLanes (031530), Ref. ECO/D2.5,* October 2008.

Angelakopoulos, H. (2007) Trial experiments for EcoLanes Project. Not published. The University of Sheffield, UK.

Antiohos, S. K.; Papageorgiou, D.; Chaniotakis, E. & Tsimas, S. (2007) 'Mechanical and durability characteristics of gypsium-free blended cements incorporating sulphate-rich reject fly ash.' *Cement and Concrete Composites*, 29, 550-558.

ANTT (2006) 'Anuário Estatístico dos Transportes Terrestres.' *Agência Nacional de Transportes Terrestres*, 1, 1. Brasília: ANTT. In Portuguese.

ArcelorMittal (2008) Technical data sheet for total anchorage steel fibres: twincone® 1/54 [online]. Available at: <URL: http://www.constructalia.com> [Acessed 10 June 2010].

Assié, S.; Escadeillas, G. & Waller, V. (2007) 'Estimates of self-compacting concrete 'potential' durability.' *Construction and Building Materials*, 21, 1909-1917.

Associação Brasileira de Normas Técnicas (2007a) ABNT NBR 15530. *Fibras de aço para concreto - Especificação,* Rio de Janeiro, RJ. In Portuguese.

Associação Brasileira de Normas Técnicas (2007b) ABNT NBR 6118. *Projeto de estruturas de concreto - procedimento,* Rio de Janeiro, RJ. In Portuguese.

Asokan, P., Osmani, M. & Price, A. D. F. (2009) 'Assessing the recycling potential of glass fibre reinforced plastic waste in concrete and cement composites.' *Journal of Cleaner Production,* article in press.

Auchey, F. L. (1998) 'The use of recycled polymer fibers as secondary reinforcement in concrete structures.' *Journal of Construction Education,* 3, 2, 131-140.

Ayerra, J. L., Grau, J. S. & Ibáñez, E. M. (2010) 'Behaviour of asphalt pavements made with waste tyres.' *Carreteras,* 174, 4, 63-73. In Spanish.

Balbo, J. T. (2003) 'Análise crítica dos métodos para dimensionamento estrutural de pavimentos de concreto simples.' *Anais do V Simpósio Epusp sobre Estruturas de Concreto,* São Paulo, Brazil. In Portuguese.

Balouch, S. U.; Forth, J. P. & Granju, J. L. (2010) 'Surface corrosion of steel fibre reinforced concrete.' *Cement and Concrete Research,* 40, 410-414.

Banthia, N. & Sappakittipakornm M. (2007) 'Toughness enhancement in steel fiber reinforced concrete through fiber hybridization.' *Cement and Concrete Research,* 37, 1366-1372.

Barluenga, G. & Hernandez-Olivares, F. (2007) 'Cracking control of concretes modified with short AR-glass fibers at early age. Experimental results on standard concrete and SCC.' *Cement and Concrete Research,* 37, 1624-1638.

Barnett, S. J., Soutsos, M. N., Millard, S. G. & Bungey, J. H. (2006) 'Strength development of mortars containing ground granulated blast-furnace slag: effect of curing temperatures and determination of apparent activation energies.' *Cement and Concrete Research,* 36, 434-440.

Barnett, S. J.; Soutsos, M. N., Bungey, J. H. & Millard, S. G. (2004) 'Fast-track concrete construction using cement replacement materials.' *ACI Special Publication,* 221, 135-152.

Barr, B. & Swamy, R. N. (1989) *Fibre Reinforced Cements and Concretes – Recent Developments.* Essex: Elsevier Science Publishers Ltd.

BASF (2008) Products: readymix / mortar / site batch. [online]. Available at: <URL: http://www.basf-admixtures.co.uk/EN/PRODUCTS/READYMIXMORTARITEBATCH/> [Acessed 7 July 2010].

Batayneh, M. K.; Marie, I. & Asi, I. (2008) 'Promoting the use of crumb rubber concrete in developing countries.' *Waste Management,* 28, 2171-2176.

Bayasi, Z. & Gebman, M. (2002) 'Reduction of lateral reinforcement in seismic beam-column connection via application of steel fibers.' *ACI Structural Journal,* 99, 6, 772-780.

Bayasi, M. Z. & Soroushian, P. (1992) 'Effect of steel fiber reinforcement on fresh mix properties of concrete.' *ACI Materials Journal,* 89, 4, 369-374.

Bazant, Z. P. & Najjar, L. J. (1972) 'Nonlinear water diffusion in nonsaturated concrete.' *Materials and Structures,* 5, 25, 3-20.

Bentur, A. & Mindess, S. (2007) *Fibre reinforced cementitious composites,* 2ed. London, Taylor & Francis.

Bentur, A. (2003) 'Long term performance of fibre reinforced cements and concretes.' *Role of Cement Science in Sustainable Development.* Proceedings of International Symposium Celebrating Concrete: People and Practice, Dundee, Thomas Telford LTD.

Bhalla, G.; Kumar, A. & Bansal, A. (2010) 'Performance of scrap tire shreds as a potential leachate collection medium.' *Geotechnical and Geological Engineering,* Article in press.

Bloom, R. & Bentur, A. (1995) 'Free and restrained shrinkage of normal and high-strength concretes.' *ACI Materials Journal,* 92, 2, 211-217.

Boel, V.; Audenaert, K.; De Schutter, G.; Heirman, G.; Vandewalle, L.; Desmet, B. & Vantomme, J. (2007) 'Transport properties of self-compacting concrete with limestone filler or fly ash.' *Materials and Structures,* 40, 507-516.

Boulekbache, B.; Hamrat, M.; Chemrouk, M. & Amziane, S. (2010) 'Flowability of fibre-reinforced concrete and its effect on the mechanical properties of the material.' *Construction and Building Materials,* Article in press.

BRE (1997) *Design of normal concrete mixes,* Teychenné, D. C.; Franklin, R. E. & Erntroy, H. C. (authors) 2ed. London, BRE.

Bridgegate Tyres (2009) Tyre Section [online]. Available at: <URL: http://www.bridgegatetyres.com/tyres/tyre-section.aspx> [Acessed 22 June 2010].

British Standard Institution (2010) DD CEN/TS 12390-11. *Testing hardened concrete – Part 11: Determination of the chloride resistance of concrete, unidirectional diffusion,* London, UK.

British Standard Institution (2009a) BS EN 12350-3. *Testing fresh concrete – Part 3: Vebe test,* London, UK.

British Standard Institution (2009b) BS EN 12350-4. *Testing fresh concrete – Part 4: Degree of compactability,* London, UK.

British Standard Institution (2009c) DD CEN/TS 12390-8. *Testing hardened concrete – Part 8: Depth of penetration of water under pressure*, London, UK.

British Standard Institution (2009d) BS EN 12390-7. *Testing hardened concrete – Part 7: Density of hardened concrete*, London, UK.

British Standard Institution (2009e) BS EN 12350-7. *Testing fresh concrete – Part 7: Air content – Pressure mehods*, London, UK.

British Standard Institution (2009f) BS ISO 1920-8. *Testing of concrete – Part 8: Determination of drying shrinkage of concrete for samples prepared in the field or in the laboratory*, London, UK.

British Standard Institution (2009g) BS EN 12390-3. *Testing hardened concrete – Part 3: Compressive strength of test specimens*, London, UK.

British Standard Institution (2007a) BS EN 14845-1. *Test method for fibres in concrete – Part 1: Reference concretes*, London, UK.

British Standard Institution (2007b) BS prEN 12350-8. *Testing fresh concrete – Part 4: Self-compacting concrete – Slump-flow test*, London, UK.

British Standard Institution (2007c) BS EN 14629. *Products and systems for the protection and repair of concrete structure – Test methods – Determination of chloride content in hardened concrete*, London, UK.

British Standard Institution (2006a) BS EN 14889-1. *Fibres for concrete – Part 1: Steel fibres – definitions, specifications and conformity*, London, UK.

British Standard Institution (2006b) BS EN 14488-3. *Testing sprayed concrete – Part 3: Flexural strengths (first peak, ultimate and residual) of fibre reinforced beam specimens*, London, UK.

British Standard Institution (2006c) DD CEN/TS 12390-9. *Testing hardened concrete – Part 9: Freeze-thaw resistance – scaling*, London, UK.

British Standard Institution (2006d) PD CEN/TR 15177. *Testing the freeze-thaw resistance of concrete – internal structural damage*, London, UK.

British Standard Institution (2006e) BS 8500-1. *Concrete – complementary British Standard to BS EN 206-1 – Part 1: Method of specifying and guidance for the specifier*, London, UK.

British Standard Institution (2005a) BS EN 14651. *Test method for metallic fibre concrete – Measuring the flexural tensile strength (limit of proportionality (LOP), residual)*, London, UK.

British Standard Institution (2005b) BS EN 14487-1. *Sprayed concrete – Part 1: Definitions, specifications and conformity*, London, UK.

British Standard Institution (2005c) BS EN 450-1. *Fly ash for concrete – Part 1: Definition, specifications and conformity criteria,* London, UK.

British Standard Institution (2004a) BS EN 13396. *Products and systems for the protection and repair of concrete structures – Test methods – Measurement of chloride ion ingress,* London, UK.

British Standard Institution (2004b) BS EN 1992-1-1. *Eurocode 2: Design of concrete structures – Part 1-1: General rules and rules for buildings,* London, UK.

British Standard Institution (2002a) BS EN 13057. *Products and systems for the protection and repair of concrete structures – Test methods – Determination of resistance of capillary absorption,* London, UK.

British Standard Institution (2002b) BS EN 12617-4. *Products and systems for the protection and repair of concrete structures – Test methods – Part 4: Determination of shrinkage and expansion,* London, UK.

British Standard Institution (2002c) BS EN 1990. *Basis of structural design,* London, UK.

British Standard Institution (2001) BS EN 934-2. *Admixtures for concrete, mortar and grout – Concrete admixtures – Definitions, requirements, conformity, marking and labelling,* London, UK.

British Standard Institution (2000a) BS EN 197-1. *Cement – Part 1: Composition, specifications and conformity criteria for common cements,* London, UK.

British Standard Institution (2000b) BS EN 12390-1. *Testing hardened concrete – Part 1: Shape, dimensions and other requirements for specimens and moulds,* London, UK.

British Standard Institution (2000c) BS EN 12390-2. *Testing hardened concrete – Part 2: Making and curing specimens for strength tests,* London, UK.

British Standard Institution (2000d) BS EN 12350-2. *Testing fresh concrete – Part 2: Slump test,* London, UK.

British Standard Institution (2000e) BS EN 206-1. *Concrete. Specification, performance and conformity,* London, UK.

British Standard Institution (1990) BS 1377-4. *Methods of test for soils for civil engineering purposes – Part 4: Compaction-related tests,* London, UK.

British Standard Institution (1983) BS 1881-122. *Testing concrete – Part 122: Method for determination of water absorption,* London, UK.

Cabrera, J.G. & Lynsdale, C.J. 'New gas permeameter for measuring the permeability of mortar and concrete'. *Magazine of Concrete Research,* 40, 177-182.

Cai, H. & Liu, X. (1998) 'Freeze-thaw durability of concrete: ice formation process in pores.' *Cement and Concrete Research,* 28, 9, 1281-1287.

Cantin, R. & Pigeon, M. (1996) 'Deicer salt scaling resistance of steel-fiber-reinforced concrete.' *Cement and Concrete Research,* 26, 11, 1639-1648.

Carcassès, M.; Abbas, A.; Ollivier, J-P. & Verdier, J. (2002) 'An optimised preconditioning procedure for gas permeability measurement.' *Materials and Structures,* 35, 22-27.

CEB-FIP (1993) *CEB-FIP Model Code 1990 – Design Code.* London, Thomas Telford.

CEB (1992) *Durable concrete structures,* 2ed. London, Thomas Telford.

Chang, D-I. & Chai, W-K. (1995) 'Flexural fracture and fatigue behaviour of steel-fiber-reinforced concrete structures.' *Nuclear Engineering and Design,* 156, 201-207.

Charron, J. P.; Denarié, E. & Brühwiler, E. (2008) 'Transport properties of water and glycol in an ultra high performance fiber reinforced concrete (UHPFRC) under high tensile deformation.' *Cement and Concrete Research,* 38, 689-698.

Chatterji, S. (2003) 'Freezing of air-entrained cement-based materials and specific actions of air-entraining agents.' *Cement and Concrete Composites,* 25, 759-765.

Che, Y. (2010) *The development and behaviour of premix GRC suitable for mass produced structural elements,* PhD Thesis, University of Sheffield.

Chern, J-C. & Young, C-H. (1989) 'Compressive creep and shrinkage of steel fibre reinforced concrete.' *The International Journal of Cement Composites and Lightweight Concrete,* 11, 4, 205-214.

Christensen, R. M. (1979) *Mechanics of composite materials,* Willey, New York.

Claisse, P. (2005) 'Transport properties of concrete.' *Concrete International,* 27, 1, 43-48.

CMAX (2009) *Products* [online]. Available at: <URL: http://www.engineeringfiber.com/index.asp?bigclassname=PRODUCTS> [Acessed 23 March 2009].

CONAMA (2009a) *Resolução Conama nº 301.* In Portuguese.

CONAMA (2009b) *Resolução Conama nº 416.* In Portuguese.

CONAMA (1999) *Resolução Conama nº 258.* In Portuguese.

CONAMA (1998) *Resolução Conama nº 235.* In Portuguese.

CONAMA (1996) *Resolução Conama nº 23.* In Portuguese.

Concepa (2009) Dados de tráfego – 3 praças da Rodovia BR-290. Not published. In Portuguese.

Corinaldesi, V. & Moriconi, G. (2004) 'Durable fiber reinforced self-compacting concrete.' *Cement and Concrete Research*, 34, 249-254.

Crank, J. (1979) *The mathematics of diffusion*, 2ed. Oxford, Clarendon Press.

Darter, M. I. & Barenberg, E. J. (1977) Design of zero-maintenance plain jointed concrete. *Report no. FHWA-RD-77-111*. Cited in.: Sotelino, E.; Asgari, A.; Saksa, A. & Cedeno, G. (2005) Damage analysis of jointed plain concrete pavements in Indiana, Part I: finite element modeling and damage analysis, Part II: INDISLAB, a software for jointed plain concrete pavement design. *Final Report, FHWA/INJTRP-2004/30, SPR 2643.*

Delagrave, A.; Marchand, J.; Ollivier, J-P.; Julien, S. & Hazrati, K. (1997) 'Chloride binding capacity of various hydrated cement paste systems.' *Advanced Cement Based Materials*, 6, 28-35.

Delatte, N. (2008) *Concrete pavement design, construction, and performance*. London, Taylor & Francis.

Department for Transport (2010) *Annual average daily traffic flows.* Available at: <URL: http://www.dft.gov.uk/matrix/> [Acessed 6 July 2010].

DNIT (2005) *Manual de pavimentos rígidos, 2ed.* Rio de Janeiro, Departamento Nacional de Infra-Estrutura de Transportes. In Portuguese.

DuraCrete (1998) Modelling of Degradation. *Brite EuRam III Project BE95-1347, Report R4-5.* Cited in.: Lay, S.; Schiebl, P. & Cairns, J. (2003) Life cycle management of concrete infrastructures for improved sustainability. *Deliverable Report 3.2, G1RD-CT-2000-00378 Lifecon, Ref. D3.2,* November 2003.

Edil, T. B.; Park, J. K. & Kim, J. Y. (2004) 'Effectiveness of scrap tire chips as sorptive drainage material.' *Journal of Environmental Engineering,* 130, 7, 824-831.

Edinçlider, A.; Baykal, G. & Saygili, A. (2010) 'Influence of different processing techniques on the mechanical properties of used tires in embankment construction.' *Waste Management,* 30, 1073-1080.

Edvardsen, C. (1999) 'Water permeability and autogeneous healing of cracks in concrete.' *ACI Materials Journal*, 96, 4, 448-455.

El-Dieb, A. S. (2009) 'Mechanical, durability and microstructural characteristics of ultra-high-strength self-compacting concrete incorporating steel fibres.' *Materials and Design,* 30, 4286-4292.

El-Dieb, A. S. & Hooton, R. D. (1995) 'Water-permeability measurement of high performance concrete using a high-pressure triaxial cell.' *Cement and Concrete Research,* 25, 6, 1199-1208.

ETRA (2010) 'Introduction to Tyre Recycling: 2010'. Prepared and edited by Valerie L. Shulman, Paris.

ETRMA (2010) *End of tyres management in Europe.* Available at: <URL: http://www.etrma.org/public/activitieseofltrenf.asp> [Acessed 6 May 2010].

European Technical Approval (2008) *Cemroc®, TSC 52.5N LH HSR LA, TSC 42.5N LH HSR LA.* ETA-08/0019.

European Union (2008) *Council Directive on waste and repealing certain Directives.* Council Directive 2008/98/EC.

European Union (2000a) *Council Directive on end-of life vehicles.* Council Directive 2000/53/EC.

European Union (2000b) *Council Directive on incineration of waste.* Council Directive 2000/76/EC.

European Union (1999) *Council Directive on the landfill of waste.* Council Directive 1999/31/EC.

Fagerlund, G. (2004) A service life model for internal forst damage in concrete. *Report TCBM-3119,* Division of Building Materials, Lund Institute of Technology. Cited in.: Lay, S.; Schiebl, P. & Cairns, J. (2003) Life cycle management of concrete infrastructures for improved sustainability. *Deliverable Report 3.2, G1RD-CT-2000-00378 Lifecon, Ref. D3.2,* November 2003.

Fanella, D. & Naaman, A. E. (1985) 'Stress-strain properties of fiber reinforced concrete in compression.' *Journal of American Concrete Institute,* 82, 475-483.

Farage, M. C. R.; Sercombe, J. & Gallé, C. (2003) 'Rehydration and microstructure of cement paste after heating at temperatures up to 300 °C.' *Cement and Concrete Research,* 33, 1047-1056.

Fattuhi, N. I. & Clark, L. A. (1996) 'Cement-based materials containing shredded scrap truck tyre rubber.' *Construction and Building Materials*, 10, 4, 229-236.

Fedération Internationale du Béton (2007) *FRP reinforcement in RC structures,* fib bulletin 40. Stuttgart, Sprint-Digital-Druck.

Fedération Internationale du Béton (2006) *Model code for service life design,* fib bulletin 34. Stuttgart, Sprint-Digital-Druck.

Feldman, R. F. & Ramachandran, V. S. (1971) 'Differentiation of interlayer and adsorbed water in hydrated Portland cement by thermal analysis.' *Cement and Concrete Research,* 1, 607-620.

Fiksel, J.; Bakshi, B. R.; Baral, A.; Guerra, E. & DeQuervain, B. (2010) 'Comparative life cycle assessment of beneficial applications for scrap tires.' *Clean Technologies and Environmental Policies*, Article in Press.

Furlan Jr., S. & Hanai, J. B. (1997) 'Shear behaviour of fiber reinforced concrete beams.' *Cement and Concrete Composites*, 19, 359-366.

Gardner, D. R.; Lark, R. J. & Barr, B. (2005) 'Effect of conditioning temperature on the strength and permeability of normal- and high-strength concrete.' *Cement and Concrete Research*, 35, 1400-1406.

Gao, P.; Wu, S.; Lin, P.; Wu, Z. & Tang, M. 'The characteristics of air void and frost resistance of RCC with fly ash and expansive agent.' *Construction and Building Materials*, 20, 586-590.

Glass, G. K. & Buenfeld, N. R. (1997) 'The presentation of the chloride threshold level for corrosion of steel in concrete.' *Corrosion Science*, 39, 5, 1001-1013.

Graeff, A. G., Lynsdale, C., Neocleous, K. & Pilakoutas, K. (2010) 'Permeability behaviour of recycled SFRC and its implications in the durability resistance of rigid pavements.' *11th International Symposium on Concrete Roads*, Seville, Spain (CD proceedings).

Graeff, A. G., Lynsdale, C., Neocleous, K. & Pilakoutas, K. (2009) 'Analysis of the durability of SFRC and SFR-RCC against corrosion and freeze-thaw effects.' *Concrete: 21st Century Superhero – Building a Sustainable Future.* Proceedings of Concrete: 21st Century Superhero, London (CD proceedings).

Granju, J. L. & Balouch, S. U. (2005) 'Corrosion of steel fibre reinforced concrete from the cracks.' *Cement and Concrete Research*, 35, 572-577.

Gray, R. J. (1984) 'Analysis of the effect of embedded fibre length of fibre debonding and pull-out from an elastic matrix.' *Journal of Materials Science*, 19, 861-870.

Griffiths, G. & Thom, N. (2007) *Concrete pavement design guidance notes.* London, Taylor and Francis.

Grzybowski, M. & Shah, S. P. (1990) 'Shrinkage cracking of fiber reinforced concrete.' *ACI Materials Journal*, 87, 2, 138-148.

Hale, W. M., Bush Jr, T. D., Russell, B. W. & Freyne, S. F. (2005) 'Effect of curing temperature on hardened concrete properties: mixtures of ground granulated blast furnace slag, fly ash, or a combination of both.' *Transportation Research Record*, 1914, 97-104.

Hannant, D. J. (1978) *Fibre Cements and Fibre Concretes*, Salisbury, John Wiley & Sons LTD.

Hannant, D. J. (1975) 'The effect of post cracking ductility on the flexural strength of fibre cement and fibre concrete.' Neville, A.N., Hannant, D. J., Majumdar, A. J., Pomeroy, C. D. & Swamy,

R. N. (eds) *Fibre Reinforced Cement & Concrete.* Lancaster, The Construction Press LTD, 499-508.

Harrison, T. A., Dewar, J. D. & Brown, B. V. (2001) Freeze-thaw resisting concrete: its achievement in the UK. *Concrete Society, Ciria C559*, London, Ciria.

HBM (2003) PC measurement electronics – Spider 8, Spider 8-30 and Spider 8-01. *Operating Manual*, Darmstadt, Germany.

HBM (2010) Catman Easy/AP Version 3.1. *Quick start guide*, Darmstadt, Germany.

Hearn, N. (1998) 'Self-sealing, autogeneous healing and continued hydration: what's the difference?.' *Materials and Structures*, 31, 563-567.

Highways Agency (2006a) HD 26/06. *Design Manual for Roads and Bridges, Volume 7 – Pavement Design and Maintanance, Section 2 – Pavement Design and Construction, Part 3 – Pavement Design*, London, UK.

Highways Agency (2006b) HD 24/06. *Design Manual for Roads and Bridges, Volume 7 – Pavement Design and Maintanance, Section 2 – Pavement Design and Construction, Part 1 – Traffic Assessment*, London, UK.

Hover, K. C. (2006) 'Air content and density of hardened concrete' Joseph, L. F. (ed) *Significance of tests and properties of concrete and concrete-making materials.* Philadelphia, ASTM International, 288-308.

IBAMA (2008) 'Dados estatísticos da reciclagem de pneus no Brasil'. Brasília, 3p.

Jansen, D. J. & Snyder, M. B. (1994) 'Resistance of concrete to freezing and thawing.' *Report SHRP-C-391.* Strategic Highway Research Program, Washington, DC.

Japan Concrete Institute (2003) JCI-S-002. *Method of test for load-displacement curve of fiber reinforced concrete by use of notched beam*, Tokio, Japan.

Japan Concrete Institute (1984) JCI SF-4. *Method of test for flexural strength and flexural toughness of steel fiber reinforced concrete*, Tokio, Japan.

Johnston, C. D. & Zemp, R. W. (1991) 'Flexural fatigue performance of steel fiber reinforced concrete – influence of fiber content, aspect ratio and type.' *ACI Materials Journal*, 88, 4, 374-383.

Johnston, C. D. (1974) 'Steel fiber reinforced mortar and concrete: a review of mechanical properties.' Proceedings of an International Symposium on Fiber Reinforced Concrete, *ACI Special Publication*, SP 44-7, 127-142.

Johnston, C. D. & Coleman, R. A. (1974) 'Strength and deformation of steel fiber reinforced mortar in uniaxial tension.' Proceedings of an International Symposium on Fiber Reinforced Concrete, *ACI Special Publication,* SP 44-10, 177-193.

Kendall, D. (1999) 'The selection of reinforcing fibres for strengthening concrete and steel structures using reinforced plastics.' Proceedings of the International Structural Faults and Repair, London, Engineering Technics Press, 8. CD-ROM. Cited in.: Beber, A. J. (2003) *Comportamento estrutural de vigas de concreto armado reforçadas com compósitos de fibras de carbono,* Doctorate Thesis, Federal University of Rio Grande do Sul. In Portuguese.

Khajuria, A. & Balaguru, P. (1992) 'Plastic shrinkage characteristics of fiber reinforced cement composites.' Swamy, R. N. (ed) *Fibre Reinforced Cement & Concrete.* Proceedings of the Fourth Rilem International Symposium, Suffolk, St. Edmundsbury Press, 82-90.

Kim, G. B., Pilakoutas, K. & Waldron, P. (2008) 'Thin FRP/GFRC structural elements.' *Cement and Concrete Composites,* 30, 122-137.

Kim, J. H. J., Park, C. G., Lee, S. W., Lee, S. W. & Won, J. P. (2008) 'Effects of the geometry of recycled PET fiber reinforcement on shrinkage cracking of cement-based composites.' *Composites Part B: Engineering,* 39, 442-450.

Kosa, K. & Naaman, A. E. (1990) 'Corrosion of steel fiber reinforced concrete.' *ACI Materials Journal,* 87, 1, 27-37.

Koutselas K (2007) *Aggregate type and gradation proposed for roller-compacted concrete.* Aggregate Industries UK, Personal Communication, January 2007.

Kraai, P. P. (1985) 'A proposed test to determine the cracking potential due to drying shrinkage of concrete.' *Concrete Construction,* 30, 775-778.

Krenchel, H. (1975) 'Fibre spacing and specific fibre surface.' Neville, A.N., Hannant, D. J., Majumdar, A. J., Pomeroy, C. D. & Swamy, R. N. (eds) *Fibre Reinforced Cement & Concrete.* Lancaster, The Construction Press LTD, 69-79.

Kukubu, K.; Cabrera, J. G. & Ueno, A. (1996) 'Compaction properties of roller compacted concrete.' *Cement and Concrete Composites,* 18, 109-117.

Kwon, S. J.; Na, U. J.; Park, S. S. & Jung, S. H. (2009) 'Service life prediction of concrete wharves with early-aged crack: probabilistic approach for chloride diffusion.' *Structural Safety,* 31, 75-83.

Larbi, J. A. (1993) 'Microstructure of the interfacial zone around aggregate particles in concrete.' *Heron,* 38, 1, 1993.

Lay, S.; Schiebl, P. & Cairns, J. (2003) Life cycle management of concrete infrastructures for improved sustainability. *Deliverable Report 3.2, G1RD-CT-2000-00378 Lifecon, Ref. D3.2,* November 2003.

Lee, M. K. & Barr, B. I. G. (2004) 'An overview of the fatigue behaviour of plain and fibre reinforced concrete.' *Cement and Concrete Composites*, 26, 4, 299-305.

Li, V. C. & Matsumoto, T. (1998) 'Fatigue crack growth analysis of fiber reinforced concrete with effect of interfacial bond degradation.' *Cement and Concrete Composites*, 20, 339-351.

Li, Z. & Chau, C-K. (2000) 'New water permeability test scheme for concrete.' *ACI Materials Journal*, 97, 1, 1-7.

Lima, R. C. A. (2005) *Investigação do comportamento de concretos em temperaturas elevadas,* Doctorate Thesis, Federal University of Rio Grande do Sul. In Portuguese.

Lin, X., Silsbee, M. R., Roy, D. M., Kessler, K. & Blankenhorn, P. R. (1994) 'Approaches to improve the properties of wood fiber reinforced cementitious composites.' *Cement and Concrete Research,* 24, 8, 1558-1566.

Love (1888) 'The small free vibrations and deformation of a thin elastic shell.' *Philosophical Transactions of the Royal Society – A,* 179, 491-546.

Luhr, D. R. (2005) 'RCC applications for pavements.' *RCC Design Seminar.* Presentation, Atlanta.

Luping, T. & Gulikers, J. (2007) 'On the mathematics of time-dependent apparent chloride diffusion coefficient in concrete.' *Cement and Concrete Research,* 37, 589-595.

Luping, T. & Nilsson, L.-O. (1993) 'Chloride binding capacity and binding isotherms of OPC pastes and mortars.' *Cement and Concrete Research,* 23, 247-253.

Lynsdale, C. (2008) 'Rheology of concrete – Lecture Notes.' *Sustainable Concrete – CIV6610.* The University of Sheffield.

Mailhot, T.; Bissonnette, F.; Saucier, F. & Pigeon, M. (2001) 'Flexural fatigue behaviour of steel fibre reinforced concrete before and after cracking.' *Materials and Structures*, 34, 351-359.

Malhotra, V. M. (1970) 'Concrete rings for determining tensile strength of concrete.' *ACI Journal*, 67, 4, 354-361.

Mallick, R. B. & El-Korchi, T. (2009) *Pavement Engineering: Principles and practice*, New York, Taylor and Francis Group.

Mangat, P. S.; Molloy, B. T. & Gurusamy, K. (1989) 'Marine durability of steel fibre reinforced concrete of high water/cement ratio.' Swamy, R. N. & Barr, B. (eds) *Fibre Reinforced Cements and Concretes, Recent Developments.* London, Elsevier Science Publisher LTD, 553-562.

Mangat, P. S. & Gurusamy, K. (1988) 'Corrosion resistance of steel fibres in concrete under marine exposure.' *Cement and Concrete Research,* 18, 1, 44-54.

Mangat, P. S. & Gurusamy, K. (1987a) 'Chloride diffusion in steel fibre reinforced marine concrete.' *Cement and Concrete Research,* 17, 385-396.

Mangat, P. S. & Gurusamy, K. (1987b) 'Permissible crack widths in steel fibre reinforced marine concrete.' *Materials and Structures*, 20, 338-347.

Mangat, P. S. & Gurusamy, K. (1987c) 'Chloride diffusion in steel fibre reinforced concrete containing PFA.' *Cement and Concrete Research*, 17, 640-650.

Mangat, P. S. & Azari, M. M. (1984) 'A theory for the free shrinkage of steel fibre reinforced cement matrices.' *Journal of Materials Science,* 19, 2183-2194.

Mangat, P. S. (1976) 'Tensile strength of steel fiber reinforced concrete.' *Cement and Concrete Research,* 6, 245-252.

Mansur, M. A.; Chin, M. S. & Wee, T. H. (1999) 'Stress-strain relationship of high-strength fiber concrete in compression.' *Journal of Materials in Civil Engineering,* 11, 1, 21-29.

Marchand, J. & Samson, E. (2009) 'Predicting the service-life of concrete structures – limitations of simplified models.' *Cement and Concrete Composites*, article in press.

Markeset, G. (2009) 'Critical chloride content and its influence on service life predictions.' *Materials and Corrosion*, 60, 8, 593-596.

Martin-Perez, B.; Pantazopoulou, S. J. & Thomas, M. D. A. (2001) 'Numerical solution of mass transport equations in concrete structures.' *Computers and Structures,* 79, 1251-1264.

Martys, N. S. (1995) Survey of concrete transport properties and their measurement. *Nistir 5592, U.S. Department of Commerce.*

Martys, N. S.; Torquato, S. & Bentz, D. P. (1994) 'Universal scaling of fluid permeability for sphere packings.' *Physical Review E,* 50, 1, 403-408.

MathWorks (2010) R2010b MathWorks documentation. Online documentation for Matlab and The Mathworks products [online]. Available at: <URL:www.mathworks.com/help/> [Acessed 29 November 2010].

McCall, J. T. (1958) 'Probability of fatigue failure of plain concrete.' *ACI Journal Proceedings*, 55, 8, 233-244.

Meda, A.; Minelli, F.; Plizzari, G. A. & Riva, P. (2005) 'Shear behaviour of steel fibre reinforced concrete beams.' *Materials and Structures,* 38, 343-351.

Mehta, P. K. & Monteiro, P. J. M. (2006) *Concrete: microstructure, properties, and materials,* 3ed. New York, McGraw-Hill.

MetOffice (2010) UK climate and weather statistics [online]. Available at: <URL: http://www.metoffice.gov.uk/weather/uk/climate.html> [Acessed 15 November 2010].

Meyer, C. (2009) 'The greening of the concrete industry.' *Cement and Concrete Composites,* 31, 601-605.

Miao, C.; Mu, R.; Tian, Q. & Sun, W. (2002) 'Effect of sulfate solution on the frost resistance of concrete with and without steel fiber reinforcement.' *Cement and Concrete Research,* 32, 31-34.

Milwaukee (2010) Hammer – breaker Kango 900 K – Features. [online]. Available at: <URL: http://www.milwaukeetool.co.uk/int/uk/uk_products.nsf/vwToolsLink/1B9A664AAE47F32BC12577DC003DAC25?OpenDocument&nav1=pro> [Acessed 18 November 2010].

Mitchell, D. W. & Marzouk, H. (2007) 'Bond characteristics of high-strength lightweight concrete.' *ACI Structural Journal,* 104, 1, 22-29.

Motta, F. G. (2008) 'A cadeia de destinação dos pneus inservíveis – o papel da regulação e do desenvolvimento tecnológico.' *Ambiente & Sociedade,* XI, 1, 167-184. In Portuguese.

Mu, R.; Miao, C.; Luo, X. & Sun, W. (2002) 'Interaction between loading, freeze-thaw cycles, and chloride salt attack of concrete with and without steel fiber reinforcement.' *Cement and Concrete Research,* 32, 1061-1066.

Musacchi, E.; Iacobucci, P. & Pierfelice, M. (2008) Potential process for cleaning and sorting the fibres. *Deliverable Report 1.3, FP6 EU STREP Project EcoLanes (031530), Ref. ECO/D1.3,* April 2008.

Naaman, A. E.; Namur, G. G.; Alwan, J. M. & Najm, H. S. (1991) 'Fiber pullout and bond slip. I: analytical study.' *Journal of Structural Engineering,* 117, 9, 2769-2790.

Naaman, A. E. & Gopalaratnam, V. S. (1983) 'Impact properties of steel fibre reinforced concrete in bending.' *The International Journal of Cement Composites and Lightweight Concrete,* 5, 4, 225-233.

Naaman, A. E.; Argon, A. S. & Moavenzadeh, F. (1973) 'A fracture model for fiber reinforced cementitious materials.' *Cement and Concrete Research,* 3, 397-411.

Nanni, A. (1989) 'Properties and design of fiber reinforced roller compacted concrete.' *Transportation Research Record,* 1226, 61-68.

Nanni, A. & Johari, A. (1989) 'RCC pavement reinforced with steel fibers.' Concrete International, 11, 3, 64-69.

Nataraja, M. C.; Nagaraj, T. S. & Basavaraja, S. B. (2005) 'Reproportioning of steel fibre reinforced concrete mixes and their impact resistance.' *Cement and Concrete Research,* 35, 2350-2359.

National Instruments Corporation (2008) *Products: LabView 8.6 software.*

NCHRP (2002) *Guide for mechanistic-empirical design of new and rehabilitated pavement structures,* NCHRP Project 1-37A. Champaign, IL, Transportation Research Board.

NCHRP (1995) *Support Under Portland Cement Concrete Pavements,* NCHRP Report 372, Project 1-30. Darter, M. I.; Hall, K. T. & Kuo, C. M. (authors) Washington, DC, Transportation Research Board.

Neocleous, K., Angelakopoulos, H., Pilakoutas, K. & Guadanini, M. (2011) 'Fibre reinforced roller compacted concrete transport pavements.' *Proceedings of the ICE – Transport,* 164, 2, 97-109.

Neocleous, K., Tlemat, H. & Pilakoutas, K. (2006) 'Design issues for concrete reinforced with steel fibers, including fibers recovered from used tires.' *Journal of Materials in Civil Engineering,* 18, 5, 677-685.

Neves, R. D. & Almeida, J. C. O. F. (2005) 'Compressive behaviour of steel fibre reinforced concrete.' *Structural Concrete,* 6, 1.

Neville, A. M. (2003) *Properties of concrete,* 4ed. Edinburgh, Pearson Education Limited.

notoxinburning.org (2006) November 2006 update [online]. Available at: <URL: http://www.notoxicburning.org/> [Acessed 28 May 2010].

Ochi, T., Okubo, S. & Fukui, K. (2007) 'Development of recycled PET fiber and its application as concrete-reinforcing fibers.' *Cement and Concrete Composites,* 29, 448-455.

Odriozola, M. A. B. & Gutierrez, P. A. (2008) 'Comparative study of different test methods for reinforced concrete durability assessment in marine environment.' *Materials and Structures,* 41, 527-541.

Ogi, K., Shinoda, T. & Mizui, M. (2005) 'Strength in concrete reinforced with recycled CFRP pieces.' *Composites Part A: Applied Science and Manufacturing,* 36, 893-902.

Oh, B. H. (1986) 'Fatigue analysis of plain concrete in flexure.' *Journal of Structural Engineering,* 112, 2, 273-288.

Osipov, A. D.; Sharkunov, S. V.; Semenenok, S. N. & Magiton, A. S. 'Roller compacted concrete with high values of strength, frost resistance, and impermeability.' *Hydrotechnical Construction,* 26, 7, 400-404.

Packard, R. G. & Tayabji, S. D. (1985) 'New PCA thickness design procedure for concrete highway and street pavement'. *3rd International Conference on Concrete Pavement Design and Rehabilitation,* Purdue University, 225-236. Cited in.: Sotelino, E.; Asgari, A.; Saksa, A. & Cedeno, G. (2005) Damage analysis of jointed plain concrete pavements in Indiana, Part I: finite element modeling and damage analysis, Part II: INDISLAB, a software for jointed plain concrete pavement design. *Final Report, FHWA/INJTRP-2004/30, SPR 2643.*

Page, C. L.; Short, N. R. & El Tarras, A. (1981) 'Diffusion of chloride ions in hardened cement pastes.' *Cement and Concrete Research,* 11, 395-406.

Papakonstantinou, C. G. & Tobolski, A. J. (2006) 'Use of waste tire steel beads in Portland cement concrete.' *Cement and Concrete Research,* 36, 1686-1691.

Paragon Materials (2005) *Health and safety guidelines – Portland Cements – CEM1.* COSHH Data Sheet.

Pavement Interactive (2007) Modulus of subgrade reaction [online]. Available at: <URL: http://pavementinteractive.org/index.php?title=Modulus_of_Subgrade_Reaction> [Acessed 29 June 2010].

PCA (2010a) Roller-compacted concrete (RCC) performance [online]. Available at: <URL: http://www.cement.org/pavements/pv_rcc_chart.asp> [Acessed 18 May 2010].

PCA (2010b) Frequently asked RCC questions – what types of aggregates can be used to create a quality RCC mix for pavements [online]. Available at: <URL: http://www.cement.org/pavements/pv_rcc_faq.asp> [Acessed 30 July 2010].

PCA (2010c) Concrete technology, durability, freeze-thaw resistance [online]. Available at: <URL: http://www.cement.org/tech/cct_dur_freeze-thaw.asp> [Acessed 15 December 2010].

PCA (2004) *Roller compacted concrete density: principles and practice.* Skokie, Portland Cement Association.

PCA (1984) *Thickness design for concrete highway and street pavements,* Packard, P. E. (author) Skokie, Portland Cement Association.

PCA (1966) *Thickness design for concrete pavements,* Chicago, Portland Cement Association.

Perdikaris, P.; Calomino, A. M. & Chudnovsky, A. (1986) 'Effect of fatigue on fracture toughness of concrete.' *Journal of Engineering Mechanics,* 112, 8, 1986.

Perlman, A. (2010) 'Paving the way for economic recovery.' *New Reality Media, PCA perspectives.* Washington, DC, USA, Portland Cement Association.

Petkovski, M. (2008) *Software based on LabView to control freeze-thaw chamber,* Internal Publication, The University of Sheffield, UK.

Picandet, V.; Khelidj, A. & Bellegou, H. (2009) 'Crack effects on gas and water permeability of concretes.' *Cement and Concrete Research,* 39, 537-547.

Pickett, G. & Ray, G. K. (1951) 'Influence charts for concrete pavements.' *Transactions of the American Society of Civil Engineers,* 116, paper 2425, 49-73.

Pigeon, M.; Azzabi, M. & Pleau, R. (1996) 'Can microfibers prevent frost damage?' *Cement and Concrete Research,* 26, 8, 1163-1170.

Pilakoutas, K. (2008) 'Fibre Reinforced Concrete – Lecture Notes.' *Advanced Concrete Design Notes.* The University of Sheffield.

Pilakoutas, K., Neocleous, K. & Tlemat, H. (2004) 'Reuse of tyre steel fibres as concrete reinforcement.' *Engineering Sustainability Journal,* 157, ES3, 131-138.

Pilakoutas, K. & Strube, R. (2001) 'Re-use of tyre fibres in concrete.' *International Symposium Recycling and Re-use of used tyres*, Dundee, Thomas Telford, 225-236.

Pittman, D. W. & Ragan, S. A. (1998) 'Drying shrinkage of roller-compacted concrete for pavement applications.' *ACI Materials Journal*, 95, 1, 19-26.

Poulsen, E. (1990) *The chloride diffusion characteristics of concrete – approximative determination by linear regression analysis,* Publication 9, Nordic concrete research. Oslo, Norway, The Nordic Concrete Federation. Cited in: Caré, S. (2008) 'Effect of temperature on porosity and on chloride diffusion in cement pastes.' *Construction and Building Materials,* 22, 1560-1573.

Powers, T. C. (1954) 'Void spacing as a basis for producing air-entrained concrete.' *Journal of the American Concrete Institute,* 25, 9, 741-760.

Pyreco (2010) About Pyreco [online]. Available at: <URL: http://www.pyreco.com/about.php> [Acessed 24 May 2010].

Ramakrishnan, V.; Wu, G. Y. & Hosalli, G. (1989) 'Flexural fatigue strength, endurance limit, and impact strength of fiber reinforced concretes.' *Transportation Research Record*, 1226, 17-24.

Ramakrishnan, V.; Oberling, G. & Tatnall, P. (1987) 'Flexural fatigue strength of steel fiber reinforced concrete.' Fibre reinforced concrete – Properties and Applications. *ACI Special Publication*, SP-105-13, 225-245.

Ramakrishnan, V. (1984) 'Superplasticized fiber-reinforced concretes for the rehabilitation of bridges and pavements.' *Transportation Research Record,* 1003, 4-11.

Ramakrishnan, V., Coyle, W. V., Kulandaisamy, V. & Schrader, E. K. (1981) 'Performance characteristics of fiber reinforced concrete with low fiber contents.' *ACI Journal*, 78, 5, 388-394.

Rao, G. V. & Dutta, R. K. (2006) 'Compressibility and strength behaviour of sand-tyre choip mixtures.' *Geotechnical and Geological Engineering,* 24, 711-724.

Reciclanip (2009) *Press Release – Supremo Tribunal Federal proíbe entrada de pneus usados no Brasil* [online]. Available at: <URL: http://www.reciclanip.com.br/?cont=press_release&tipo=interno&id=377> [Acessed 7 May 2010]. In Portuguese.

Reddy, K. R.; Stark, T. D. & Marella, A. (2010) 'Beneficial use of shredded tires as drainage material in cover systems for abandoned landfills.' *Waste Management,* 14, 1, 47-60.

RILEM (2004a) 'Test methods of frost resistance of concrete: CIF-test: capillary suction, internal damage and freeze-thaw test – Reference method and alternative methods A and B. Internal damage of concrete due to frost action. Final Reccomendation.' RILEM TC 176-IDC. *Materials and Structures,* 37, 743-753.

RILEM (2004b) 'Slab test: freeze/thaw resistance of concrete – Internal deterioration. Internal damage of concrete due to frost action. Final Reccomendation.' RILEM TC 176-IDC. *Materials and Structures,* 37, 754-759.

RILEM (2002) 'Test and design methods for steel fibre reinforced concrete. Bending test. Final Reccomendation.' RILEM TC 162-TDF. *Materials and Structures,* 35, 579-582.

RILEM (1999) 'Test for gas permeability of concrete. A, B and C. Recommendations.' RILEM TC 116-PCD: Permeability of concrete as a criterion of its durability. *Materials and Structures,* 32, 174-179.

RILEM (1997) 'Freeze-thaw and deicing resistance of concrete. Report.' RILEM TC 117-FDC. *Materials and Structures,* Supplement, 3-6.

RILEM (1984) 'Absorption of water by concrete by immersion under vacuum' RILEM TC 14-CPC 11.3. *Materials and Structures,* 17, 101, 391-394.

RILEM (1975) 'Density of hardened concrete' RILEM TC 14-CPC 10.2.

Ribeiro, A. C. B. & Almeida, I. R (2000) 'Study on high-performance roller compacted concrete.' *Materials and Structures,* 33, 398-402.

RMA (2009) *Scrap tire markets in the United States.* 9th Biennal Report. 2009ed. Washington, DC., RMA.

Roesler, J. R.; Hiller, J. E. & Littleton, P. C. (2005) 'Large-scale airfield concrete slab fatigue tests.' *International Journal of Concrete Pavements,* ISCP, 1, 1, 66-87.

Roesler, J. R. & Barenberg, B. J. (1998) Fatigue of concrete beams and slabs. *Report FHWA-IL-UI-265, IHR-535,* June 1998.

Romualdi, J. P. & Mandel, J. A. (1964) 'Tensile strength of concrete affected by uniformly distributed and closely spaced short lengths of wire reinforcement.' Journal of the American Concrete Institute, 61, 6, 657-672.

Rossi, P. & Parant, E. (2008) 'Damage mechanisms analysis of a multi-scale fibre reinforced cement-based composite subjected to impact and fatigue loading conditions.' *Cement and Concrete Research,* 38, 413-421.

Rossi, P. & Harrouche, N. (1990) 'Mix design and mechanical behaviour of some steel-fibre-reinforced concretes used in reinforced concrete structures.' *Materials and Structures,* 23, 4, 256-266.

Rossi, P.; Acker, P. & Malier, Y. (1987) 'Effect of steel fibres at two different stages: the material and the structure.' *Materials and Structures,* 20, 436-439.

RWE Power international (2007) *Certificate of analysis.* Sheet no. 38, authorised by R. Coombs, July, 2007.

Saetta, A. V.; Scotta, R. V. & Vitaliani, R. V. (1993) 'Analysis of chloride diffusion into partially saturated concrete.' *ACI Materials Journal,* 90, 5, 441-451.

Sahmaran, M.; Li, M. & Li, V. C. (2007) 'Transport properties of engineered cementitious composites under chloride exposure.' *ACI Materials Journal,* 104, 6, 604-611.

Samaha, H. R. & Hover, K. C. (1992) 'Influence of microcracking on the mass transport properties of concrete.' *ACI Materials Journal,* 89, 4, 416-424.

Sanjuán, M. A. & Muñoz-Martialay, R. (1996) 'Oven-drying as a preconditioning method for air permeability test on concrete.' *Materials Letters,* 27, 263-268.

Savastano Jr., H., Santos, S. F., Radonjic, M. & Soboyejo, W. O. (2009) 'Fracture and fatigue of natural fiber-reinforced cementitious composites.' *Cement and Concrete Composites,* article in press.

Setzer, M. J. (1977) 'Einfluss des wassergehalts auf die eigenschaften des erhaerteten betons.' *Deutscher Ausschuss fur Stahlbeton,* 280, 43-117. In German.

Shah, S. P. & Rangan, B. V. (1971) 'Fiber reinforced concrete properties.' *ACI Journal,* 68, 2, 126-137.

Shakya, P. R.; Shrestha, P.; Tamrakar, C. S. & Bhattarai, P. K. (2008) 'Studies on potential emission of hazardous gases due to uncontrolled open-air burning of waste vehicle tyres and their possible impacts on the environment.' *Atmospheric Environment,* 42, 6555-6559.

Sheffield Weather (2011) *Weather Data* [online]. Available at: <URL: http://www.sheffieldweather.co.uk/Weather%20Data.htm> [Acessed 4 March 2011].

Shi, X. P.; Fwa, T. F. & Tan, S. A. (1993) 'Flexural fatigue strength of plain concrete.' *ACI Materials Journal,* 90, 5, 435-440.

Siddique, R. & Naik, T. R. (2004) 'Properties of concrete containing scrap-tire rubber – na overview.' *Waste Management,* 24, 563-569.

Silva, D. A., Betioli, A. M., Gleize, P. J. P., Roman, H. R., Gómez, L. A. & Ribeiro, J. L. D. (2005) 'Degradation of recycled PET fibers in Portland cement-based materials.' *Cement and Concrete Research,* 35, 1741-1746.

Singh, S. P. (2010) 'Procedures to calculate the coefficients a, b and c for mathematical model to predict fatigue life cycle of concrete.' *Personal notes.*

Singh, S. P.; Ambedkar, B. R.; Mohammadi, Y. & Kaushik, S. K. (2008) 'Flexural fatigue strength prediction of steel fibre reinforced concrete beams.' *Electronic Journal of Structural Engineering,* 8, 46-54.

Singh, S. P.; Mohammadi, Y. & Madan, S. K. (2006) 'Flexural fatigue strength of steel fibrous concrete containing mixed steel fibres.' *Journal of Zhejiang University Science A*, 7, 8, 1329-13335.

Singh, S. P.; Singh, B. & Kaushik, S. K. (2005a) 'Probability of failure of steel fibrous concrete.' *Magazine of Concrete Research*, 57, 2, 65-72.

Singh, S. P.; Mohammadi, Y. & Kaushik, S. K. (2005b) 'Flexural fatigue analysis of steel fibrous concrete containing mixed fibers.' *ACI Materials Journal,* 102, 6, 438-444.

Singh, S. P. & Kaushik, S. K. (2003) 'Fatigue strength of steel fibre reinforced concrete in flexure.' *Cement and Concrete Composites*, 25, 7, 779-786.

Singh, S. P. & Kaushik, S. K. (2001) 'Flexural fatigue analysis of steel fiber-reinforced concrete.' *ACI Materials Journal*, 98, 4, 306-312.

Singh, S. P. & Kaushik, S. K. (2000) 'Flexural fatigue life distributions and failure probability of steel fibrous concrete.' *ACI Materials Journal*, 97, 6, 658-667.

Snyder, K. A. (1998) 'A numerical test of air void spacing equations.' *Advanced Cement Based Materials,* 8, 1, 28-44.

Song, P. S.; Wu, J. C.; Hwang, S. & Sheu, B. C. (2005) 'Assessment of statistical variations in impact resistance of high-strength concrete and high-strength steel fiber-reinforced concrete.' *Cement and Concrete research*, 35, 393-399.

Soroushian, P., Shah, Z. & Won, J. P. (1995) 'Optimization of wastepaper fiber-cement composites, *ACI Materials Journal,* 92, 1, 1-11.

Soroushian, P. & Lee, C-D. (1990a) 'Tensile strength of steel fiber reinforced concrete: correlation with some measures of fiber spacing.' *ACI Materials Journal,* 87, 6, 541-546.

Soroushian, P. & Lee, C-D. (1990b) 'Distribution and orientation of fibers in steel fiber reinforced concrete.' *ACI Materials Journal,* 87, 5, 433-439.

Soroushian, P. & Bayasi, Z. (1987) 'Prediction of the tensile strength of fiber reinforced concrete: a critique of the composite material concept.' Proceedings of an International Symposium on Fiber Reinforced Concrete – Properties and Applications, *ACI Special Publication,* SP 105-4, 71-84.

Sotelino, E.; Asgari, A.; Saksa, A. & Cedeno, G. (2005) Damage analysis of jointed plain concrete pavements in Indiana, Part I: finite element modeling and damage analysis, Part II: INDISLAB, a software for jointed plain concrete pavement design. *Final Report, FHWA/INJTRP-2004/30, SPR 2643.*

Soutsos, M. N.; Barnett, S. J.; Millard, S. G. & Bungey, J. H. (2009) 'The effect of temperature on the rate of strength development of slag cement.' *ACI Special Publication,* 263, 111-126.

Specht, L. P. (2004) *Avaliação de misturas asfálticas com incorporação de borracha reciclada de pneus,* PhD Thesis, Federal University of Rio Grande do Sul. In portuguese.

Sullivan, E. (2009) 'Update: paving, new realities.' *Flash Report*, Breaking Analysis of the Economy, Construction and Cement Industries. PCA: Washington, DC, USA.

Sun, W.; Mu, R.; Luo, X. & Miao, C. (2002) 'Effect of chloride salt, freeze-thaw cycling and externally applied load on the performance of the concrete.' *Cement and Concrete Research,* 32, 1859-1864.

Suryavanshi, A. K.; Scantlebury, J. D. & Lyon, S. B. (1995) 'The binding of chloride ions by sulphate resistance Portland cement.' *Cement and Concrete Research,* 25, 3, 581-592.

Swamy, R. N. & Al-Ta'an, S. A. (1981) 'Deformation and ultimate strength in flexure of reinforced concrete beams made with steel fiber concrete.' *ACI Journal,* 78, 5, 395-405.

Swamy, R. N. & Stavrides, V. (1979) 'Influence of fiber reinforcement on restrained shrinkage and cracking.' *ACI Journal,* 76, 3, 443-460.

Swamy, R. N. & Stavrides, V. (1975) 'Some properties of high workability steel fibre concrete.' Hannant, D. J., Majumdar, A. J., Pomeroy, C. D. & Swamy, R. N. (eds) *Rilem Symposium 1975 Fibre Reinforced Cement and Concrete.* Lancaster, The Construction Press Ltd, 197-208

Swamy, R. N. & Mangat, P. S. (1974) 'Influence of fibre-aggregate interaction on some properties of steel fibre reinforced concrete.' *Materials and Structures,* 7, 5, 307-314.

Swamy, R. N. (1974) 'The technology of steel fibre reinforced concrete for practical applications.' *Proceedings, Institution of Civil Engineers,* 56, 143-159.

Tan, K-H. & Saha, M-K. (2007) 'Glass FRP-bonded RC beams under cyclic loading.' *International Journal of Concrete Structures and Materials,* 1, 1, 51-61.

Tan, K-H.; Paramasivam, P. & Tan, K-C. (1994) 'Creep and shrinkage deflections of RC beams with steel fibres.' *Journal of Materials in Civil Engineering,* 6, 4, 474-494.

The Concrete Society (2008) 'Permeability testing of site concrete.' *A review of methods and experience. Technical Report 31.*

The Concrete Society (2004) 'Enhancing reinforced concrete durability.' *Guidance on selecting measures for minimising the risk of corrosion of reinforcement in concrete. Technical Report 61,* written by Bamforth, P. B.

The Concrete Society (2003) 'Concrete industrial ground floors.' *A guide to the design and construction. Technical Report 34,* 3ed.

Thomas, D. (2006) 'Choosing between asphalt and concrete pavement.' *Public Works Magazine.*

Thom, N. H.; Thompson, I. & Peaston, C. H. (2000) 'Use of steel fibre reinforcement in cement treated base.' *4th International RILEM Conference on Reflective Cracking in Pavements,* Ottawa, U.S.A., pp. 413-422.

Tilles, R. S.; Glebova, F. E. & Khokhlova, N. A. (1990) 'Selection of the composition of roller-compacted concrete.' *Hydrotechnical Construction,* 24, 1, 17-21.

Timoshenko, S. P. & Goodier, J. N. (1970) *Theory of elasticity,* New York, McGraw-Hill.

Tlemat, H., Pilakoutas, K & Neocleous, K. (2006) 'Stress-strain characteristic of SFRC using recycled fibres.' *Materials and Structures,* 39, 365-377.

Tlemat, H. (2004) *Steel Fibres from Waste Tyres to Concrete; Testing, Modelling and Design,* PhD Thesis, University of Sheffield.

Tlemat, H., Pilakoutas, K. & Neocleous, K. (2004a) 'Flexural toughness of SFRC made with fibres extracted from tyres.' Newlands, M. D., Dhir, R. K. & Halliday, J. E. (eds) *Recycling and Reuse of Waste Materials.* London, American Society of Civil Engineers, 365-374.

Tlemat, H., Pilakoutas, K. & Neocleous, K. (2004b) 'Pull-out behaviour of steel fibres recycled from used tyres.' Newlands, M. D., Dhir, R. K. & Csetenyi, L. J. (eds) *Role of Cement Science in Sustainable Development.* London, American Society of Civil Engineers, 175-184.

Tongaroonsri, S. & Tangtermsirikul, S. (2009) 'Effect of mineral admixtures and curing periods shrinkage and cracking age under restrained condition.' *Construction and Building Materials,* 23, 1050-1056.

Torrijos, M. C.; Barragan, B. E. & Zerbino, R. L. (2010) 'Placing conditions, mesostructural characteristics and post-cracking response of fibre reinforced self-compacting concretes.' *Construction and Building Materials,* 24, 1078-1085.

Turatsinze, A., Bonnet, S. & Granju, J. L. (2005) 'Mechanical characterisation of cement-based mortar incorporating rubber aggregates from recycled worn tyres.' *Building and Environment,* 40, 221-226.

Turer, A. & Gölalmis, M. (2008) 'Scrap tire ring as a low-cost post-tensioning material for masonry strengthening.' *Materials and Structures,* 41, 1345-1361.

Tyner, J. S.; Wright, W. C. & Dobbs, P. A. (2009) 'Increasing exfiltration from pervious concrete and temperature monitoring.' *Journal of Environmental Management,* 90, 2636-2641.

TRL (2005) *New continuously reinforced concrete pavement design,* Hassan, K. E.; Chandler, J. W. E.; Harding, H. M. & Dudgeon, R. P. (authors) Workingham, Transport Research Laboratory.

TRRL (1987) *Thickness design of concrete roads,* Mayhew, H. C. & Harding, H.M. (authors) Workingham, Transport and Road Research Laboratory.

USFD (2001) 'Thin wire reinforcement for concrete'. *British Patent Application* No 0130852.7 and 0511012.7 filed by the University of Sheffield on 24/12/01 and published on 9/11/2005, Sheffield UK.

U. S. Department of Transportation (2008) *National Transportation Statistics*, Research and Innovative Technology Administration, Bureau of Transportation Statistics, Washington, DC.

U. S. Environmental Protection Agency (2008) *Laws/Statutes* [online]. Available at: <URL: http://www.epa.gov/osw/conserve/materials/tires/laws.htm> [Acessed 4 May 2010].

U. S. Environmental Protection Agency (2009) *Frequent questions – what is the current status of tire recycling and disposal in the US?* [online]. Available at: <URL: http://www.epa.gov/osw/conserve/materials/tires/faq.htm> [Acessed 3 March 2009].

UTWD (2009) *Statistics – download 2005 UTWG (Used Tyre Working Group) statistics document.* [online]. Available at: <URL: http://www.tyredisposal.co.uk/stats.html> [Acessed 19 November 2010].

Val, D. V. & Trapper, P. A. (2008) 'Probabilistic evaluation of initiation time of chloride-induced corrosion.' *Reliability Engineering & System Safety,* 93, 364-372.

Vassou, V. C.; Short, N. R.; Kettle, R. J. (2009) 'Microstructural investigation into the abrasion resistance of fiber-reinforced concrete floors.' *Journal of Materials in Civil Engineering,* 20, 2, 157-168.

Verbeck, G. & Copeland, L. E. (1972) 'Some physical and chemical aspects of high-pressure steam-curing.' *Menzel Symposium on High-Pressure Steam-Curing,* ACI Special Publication – SP-32, 1-13. Cited in.: Farage, M. C. R.; Sercombe, J. & Gallé, C. (2003) 'Rehydration and microstructure of cement paste after heating at temperatures up to 300 °C.' *Cement and Concrete Research,* 33, 1047-1056.

Verbeck, G. & Helmuth, R. (1968) 'Structures and physical properties of cement paste.'*Fifth International Symposium on the Chemistry of Cement*, Tokio, China, pp. 1-32. Cited in.: Farage, M. C. R.; Sercombe, J. & Gallé, C. (2003) 'Rehydration and microstructure of cement paste after heating at temperatures up to 300 °C.' *Cement and Concrete Research,* 33, 1047-1056.

Verdier, J. & Carcassès, M. (2004) 'Equivalent gas permeability of concrete samples subjected to drying.' *Magazine of Concrete Research,* 56, 4, 223-230.

Voigt, T.; Bui, V. K. & Shah, S. P. (2004) 'Drying shrinkage of concrete reinforced with fibers and welded-wire fabric.' *ACI Materials Journal,* 101, 3, 233-241.

Wang, K.; Shah, S. P. & Phuaksuk, P. (2001) 'Plastic shrinkage cracking in concrete materials – influence of fly ash and fibers.' *ACI Materials Journal,* 98, 6, 458-464.

Wang, X. (1997) 'Concrete reinforcement with recycled fibers from carpet industrial waste.' *Journal of Materials in Civil Engineering,* 103-104.

Wang, Y., Wu, H. C. & Li, V. C. (2000) 'Concrete reinforcement with recycled fibers.' *Journal of Materials in Civil Engineering,* 2000.

Westergaard, H. M. (1927) 'Analysis of stresses in concrete pavements caused by variations of temperature.' *Public works,* 8, 3, 54-60.

Westergaard, H. M. (1926) 'Stresses in concrete pavements computed by theoretical analysis.' *Public Roads*, 7, 2, 25-35.

Whalley, C. P. & Neville, A. M. (1973) 'Non-elastic deformation of concrete under cyclic compression.' *Magazine of Concrete Research,* 25, 84, 145-154. Cited in: Balaguru, P. & Shah, S. P. (1982) 'A method of predicting crack widths and deflections for fatigue loadings.' *ACI Special Publication.* SP-75-7, 153-175.

Wiggenraad, P. B. L. (2007) 'Geometrical and structural design of roads and railways.' Chapter 5 – Concrete Pavements. *Students' notes for MSc course.* Delft University of Technology.

Wikipedia (2009) *Fiber reinforced concrete* [online]. Available at: <URL: http://en.wikipedia.org/wiki/Fiber_reinforced_concrete> [Acessed 25 February 2009].

Williams, P. T.; Boottrill, R. P.; Brindle, A. J. & Cunliffe, A. M. (2001) 'The potential of pyrolysis to recycle used tyres,' in Dhir, R., Limbachiya, M. & Paine, K. (eds) *Recycling and reuse of used tyres.* London, Thomas Telford, 187-202.

Williamson, G. R. (1974) 'The effect of steel fibers on the compressive strength of concrete.' Proceedings of an International Symposium on Fiber Reinforced Concrete, *ACI Special Publication,* SP 44-11, 195-207.

Wilson, M. A.; Carter, M. A. & Hoff, W. D. (1999) 'Bristish standard and RILEM water absorption tests: a critical evaluation.' *Materials and Structures,* 32, 571-578.

WRAP (2007) 'Markets for steel and fibre from used tyre processing.' *WRAP tyres Programme. Report TYR022,* written by Archer, E. and Boyarkina, N., June 2007.

Wu, H. C., Lim, Y. M. & Li, V. C. (1996) 'Application of recycled tyre cord in concrete for shrinkage crack control.' *Journal of Materials Science Letters,* 15, 1828-1831.

Xi, Y. & Bazant, Z. P. (1999) 'Modeling chloride penetration in saturated concrete.' *Journal of Materials in Civil Engineering,* 11, 1, 58-65.

Xiao, F.; Zhao, P. E. W. & Amikhanian, S. N. (2009) 'Fatigue behaviour of rubberized asphalt concrete mixtures containing warm asphalt additives.' *Construction and Building Materials,* 23, 3144-3151.

Xiao, J. & Falkner, H. (2006) 'On residual strength of high-performance concrete with and without polypropylene fibres at elevated temperatures.' *Fire Safety Journal,* 41, 115-121.

Xu, B. W. & Shi, H. S. (2009) 'Correlations among mechanical properties of steel fibre reinforced concrete.' *Construction and Building Materials,* 23, 3468-3474.

Yang, H. H. (1993) *Kevlar Aramid Fiber,* Wiley. Cited in.: Bernardi, S. T. (2003) *Avaliação do comportamento de materiais compósitos de matrizes cimentícias reforçadas com fibra de aramida kevlar,* Doctorate Thesis, Federal University of Rio Grande do Sul. In Portuguese.

Yang, C. C. (2005) 'A comparison of transport properties for concrete using the ponding test and the accelerated chloride migration test.' *Materials and Structures,* 38, 313-320.

Yang, C. C. & Wang, L. C. (2004) 'The diffusion characteristic of concrete with mineral admixtures between salt ponding test and accelerated chloride migration test.' *Materials, Chemistry and Physics,* 85, 266-272.

Yazici, S.; Inan, G. & Tabak, V. (2007) 'Effect of aspect ratio and volume fraction of steel fiber on the mechanical properties of SFRC.' *Construction and Building Materials,* 21, 1250-1253.

Yilmaz, A. & Degirmenci, N. (2009) 'Possibility of using waste tire rubber and fly ash with Portland cement as construction material.' *Waste Management,* 29, 1541-1546.

Yoder, E. G. & Witczak, M. W. (1975) Principles of pavement design. 2ed. New York, John Wiley and Sons.

Yoder, E. (1969) 'Selection of soil strength values for the design of flexible pavements.' *Highway Research Record,* 276, 1-13. Cited in.: Adnan, A. B. & Al-Balbissi, A. H. (1989) 'Probabilistic design of flexible and rigid pavements using AASHTO equations.' *Transportation Research Record,* 1227, 34-43.

Yoon, S.; Prezzi, M.; Siddiki, N. Z. & Kim, B. (2006) 'Construction of a test embankment using a sand-tyre shred mixture as fill material.' *Waste Management,* 26, 1033-1044.

Zhang, B.; Phillips, D. V. & Wu, K. (1996) 'Effect of loading frequency and stress reversal on fatigue life of plain concrete.' *Magazine of Concrete Research,* 48, 177, 361-375.

Zhang, J. & Li, V. C. (2001) 'Influencing of supporting base characteristics on shrinkage-induced stresses in concrete pavements.' *Journal of Transportation Engineering,* 127, 6, 455-462.

Zheng, L.; Huo, X. S. & Yuan, Y. (2008) 'Strength, modulus of elasticity, and brittleness index of rubberized concrete.' *Journal of Materials in Civil Engineering,* 20, 11, 692-699.

APPENDIX A

APPENDIX A. ECOLANES PROJECT

A.1 DESCRIPTION AND OBJECTIVES

EcoLanes (Economical and Sustainable Pavement Infrastructure for Surface Transport) was a three year European Union Funded Project (2006-2009) on the Sixth Framework Programme (contract number 031530).

The strategic objectives of the project were to reduce the manufacturing costs of surface transport by 10% to 20%, the production times by 15% and energy by 40% based on the use of new materials, advance design and new processes.

The main objectives of EcoLanes was to develop: 1) techniques and equipment for post-processing steel fibres extracted from tyres to use them as suitable reinforcement for concrete; 2) techniques and equipments for dispersing the fibres into wet and RCC mixes; 3) SFRC mixes suitable for slip forming and roller compaction; 4) models for the design of long-lasting rigid pavements made with SFRC; 5) life-cycle tools to determine cost, energy, efficiency and environmental impact of the new infrastructure; 6) full-scale demonstration projects.

A.2 PARTNERS

EcoLanes was a consortium composed of 11 partners described below.

1) The University of Sheffield, United Kingdom
2) Akdeniz University, Turkey
3) Technical University 'Gheorghe Asachi' Iasi, Romania
4) European Tyre Recycling Association, France
5) Aggregate Industries UK LTD, United Kingdom
6) Antalya Greater Municipality, Turkey
7) Compania Nationala di Drumuri Nationale din Romania, prin DRDP Iasi, Romania
8) Adriatica Riciclagio e Ambiente s.r.l, Italy
9) Ministry of Communications and Works – Cyprus, Public Works Department, Cyprus
10) Cyprus University of Technology, Cyprus
11) Scott Wilson LTD, United Kingdom

A.3 WORK-PACKAGES AND TASKS

EcoLanes was composed of 9 work-packages, which were divided in 32 tasks (in total), described in Table A.1.

Table A.1 – Work-packages and tasks of EcoLanes Project.

Work-package	Tasks
1 – Fibre sorting	1.1 Composition and classification study 1.2 Fibre cleaning and sorting 1.3 Hardware prototypes 1.4 Fibre supply
2 – Fibre-reinforced concrete	2.1 Fibre characteristics 2.2 Concrete optimisation 2.3 SFRC experimental characterisation 2.4 Chemical durability 2.5 Modelling of SFRC
3 – Pavement testing, analysis and design	3.1 Development of the concept of long lasting rigid pavements 3.2 Laboratory accelerated load testing (ALT) 3.3 Numerical analysis and parametric study 3.4 Design of pavements
4 – Environmental studies and site processes	4.1 Environmental impact and energy consumption 4.2 Life-cycle methodology 4.3 Fibre dispersing in concrete 4.4 Roller compaction of SFRC 4.5 Hardware prototypes
5 – Demonstration in Western European Environment	5.1 Problem investigation 5.2 Design and construction of demonstration 5.3 Monitoring and testing of pavement behaviour
6 – Demonstration in Eastern European Environment	6.1 Problem investigation 6.2 Design and construction of demonstration 6.3 Monitoring and testing of pavement behaviour
7 – Demonstration in Eastern Mediterranean Environment	7.1 Problem investigation 7.2 Design and construction of demonstration 7.3 Monitoring and testing of pavement behaviour
8 – Dissemination and exploitation of results	8.1 Dissemination website and industrial seminars 8.2 Technology implementation plan
9 – Project management	9.1 Project coordination 9.2 Technical and management meetings

A.4 DELIVERABLES

D1.1 – Tyre Recycling Technologies and Environmental Issues. Authors: Kyriacos Neocleous, Valerie Shulman, Harris Angelakopoulos.

D1.2 – Classification of fibres from different mechanical treatments and the reasons for fibre balling. Authors: Ettore Musacchi, Pierluigi Iacobucci, Kyriacos Neocleous, Harris Angelakopoulos and Kypros Pilakoutas.

D1.3 – Potential process for cleaning and sorting the fibres. Authors: Ettore Musacchi, Pierluigi Iacobucci and Marco Pierfelice.

D1.4 – A prototype attachment for producing fibres suitable for concrete. Authors: Ettore Musacchi and Marco Pierfelice.

D1.4b – A prototype attachment for producing fibres suitable for concrete. Author: Ettore Musacchi.

D1.4c – Attachment - Fibre production guideline. Author: Ettore Musacchi.

D1.4d – Specification for Classifying Steel Tyre-Cord Fibres. Authors: Kyriacos Neocleous, Kypros Pilakoutas, Peter Waldron and Jim Goulding.

D1.5 – Fibre Supply. Author: Ettore Musacchi.

D2.1a – Use and Design of Steel Fibres in Concrete Pavements. Authors: Harris Angelakopoulos, Kyriacos Neocleous and Kypros Pilakoutas.

D2.1b – State-of-the-art on roller-compacted concrete. Authors: Angelakopoulos, Kyriacos Neocleous and Kypros Pilakoutas.

D2.2 – Characteristics of fibres from post-consumer tyres and other sources. Authors: Angelakopoulos, Kyriacos Neocleous, Kypros Pilakoutas.

D2.3 – Wet Concrete Mix Optimisation for Selected Fibres. Authors: Nicolae Vlad, Nicolae Taranu, Radu Andrei, Marius Muscalu, Radu Cojocaru, Oana Ionita and Mioara Nerges.

D2.3b – Wet Concrete Mix Optimisation for Selected Fibres. Authors: Angelakopoulos, Kyriacos Neocleous and Kypros Pilakoutas.

D2.4 – Concrete Mix Optimisation for Roller Compacted Concrete. Authors: Harris Angelakopoulos, Kyriacos Neocleous and Kypros Pilakoutas.

D2.4b – Parametric investigation on the compressive strength of Steel Fibre Reinforced Roller Compacted Concrete. Authors: Harris Angelakopoulos, Kyriacos Neocleous and Kypros Pilakoutas.

D2.5 – Flexural testing of SFR-RCC and SFRC for all different types of fibres supplied. Authors: Harris Angelakopoulos, Kyriacos Neocleous and Kypros Pilakoutas.

D2.5b – Parametric investigation on the flexural behaviour of plain and SFR-RCC. Authors: Harris Angelakopoulos, Kyriacos Neocleous and Kypros Pilakoutas.

D2.5c – Fatigue Tests on SFR-RCC with Recycled Fibres. Authors: Angela Graeff, Kyriacos Neocleous and Kypros Pilakoutas.

D2.6 – Chemical Durability for Dry and Wet Steel Fibre Reinforced Concrete. Authors: Angela Graeff, Kyriacos Neocleous and Kypros Pilakoutas.

D2.6b – Durability properties of SFRC and SFR-RCC with recycled fibres. Authors: Angela Graeff, Kyriacos Neocleous and Kypros Pilakoutas.

D2.7 – Modelling of SFRC. Authors: Harris Angelakopoulos, Angela Graeff, Naeimeh Jafarifar, Kyriacos Neocleous and Kypros Pilakoutas.

D2.7b – Modelling of SFRC. Authors: Harris Angelakopoulos, Angela Graeff, Kyriacos Neocleous and Kypros Pilakoutas.

D3.1 – State-of-the-art report on design and construction of LLRP. Authors: R. Andrei, N. Taranu, H. Gh. Zarojanu, N. V. Vlad, V. Boboc and I. D. Vrancianu.

D3.2 – Accelerated load testing 1-200K passes. Authors: B. Cososchi, N. Taranu, H. Gh. Zarojanu, R. Andrei, V. Boboc, M. Muscalu and O. M. Ionita.

D3.3a – Numerical and Analytical Study of Long-Lasting-Rigid-Pavements – Linear Elastic Analysis. Authors: Naeimeh Jafarifar, Kypros Pilakoutas and Kyriacos Neocleous.

D3.3b – Numerical and Analytical Study of Long-Lasting-Rigid-Pavements – Non-Linear Analysis. Authors: Naeimeh Jafarifar and Kypros Pilakoutas.

D3.3c – Numerical analysis and parametric study of SFRC pavements subjected to traffic. Authors: Nicolae Taranu, Horia Gh. Zarojanu, Radu Andrei, Vasile Boboc, Radu Cojocaru, Marius Muscalu, Oana Mihaela Banu and Elena Puslau.

D3.4 – Algorithms and software for the design of SFRC pavements. Authors: Nicolae Taranu, Horia Gh. Zarojanu, Radu Andrei, Vasile Boboc, Radu Cojocaru, Marius Muscalu, Oana Mihaela Banu and Elena Puslau.

D3.5 – Accelerated load testing 200K-1.5m passes. Authors: B. Cososchi, N. Taranu, H. Gh. Zarojanu, R. Andrei, V. Boboc, M. Muscalu and O. M. Banu.

D3.6 – Developing of guidelines for the design of SFRC pavements. Authors: Nicolae Taranu, Horia Gh. Zarojanu, Radu Andrei, Vasile Boboc, Radu Cojocaru, Marius Muscalu, Oana Mihaela Banu and Elena Puslau.

D4.1a – Environmental Impact and Energy Consumption of Transport Pavements. Authors: Laura Dumitrescu, Nicolae Taranu and Mioara Nerges.

D4.1b – Methodology for environmental impact and energy consumption of transport pavements. Authors: Diofantos Hadjimitsis and Kyriacos Themistocleous.

D4.2a – Life Cycle Costing. Authors: Laura Dumitrescu, Nicolae Taranu and Mioara Nerges.

D4.2b – Methodology for Life Cycle Costing. Authors: Diofantos Hadjimitsis, Kyriacos Themistocleous and Laura Dumitrescu.

D4.3 – Fibre dispersion techniques. Author: Kostas Koutselas.

D4.4 – Roller Compaction Equipment. Author: Kostas Koutselas and John Donegan.

D4.4b – Specification for Production of Steel Fibre-reinforced Roller Compacted Concrete Pavements. Authors: Kostas Koutselas, Kyriacos Neocleous and Kypros Pilakoutas.

D4.5 – Prototype Machines or Attachments to Disperse Fibres and Compact SFRC. Author: Kostas Koutselas.

D4.6 – Environmental impact and energy consumption of demonstrations. Authors: Constantia Achilleos, Diofantos Hadjimitsis and Kyriacos Themistocleous.

D4.7 – Life-cycle costing of demonstrations. Authors: Constantia Achilleos, Diofantos Hadjimitsis and Kyriacos Themistocleous.

D5.1 – Problems in the specific environment. Author: Kostas Koutselas.

D5.2 – Design of the road using new techniques to solve the defined problems. Author: Kostas Koutselas, John Donegan and Paul Phillips.

D6.1 – Problems in specific environment. Authors: Camelia Bulau, Tudor Varlan, Constantin Zbarnea, Irina Lungu, Vasile Boboc, Nicolae Taranu, Radu Cojocaru and Marius Muscalu.

D6.2 – Design of the road using new techniques to solve the defined problems. Authors: Camelia Bulau, Tudor Varlan, Constantin Zbarnea, Irina Lungu, Vasile Boboc, Andrei Radu, Nicolae Taranu, Radu Cojocaru and Marius Muscalu.

D6.3 – Construction of road using new techniques. Authors: Camelia Bulau, Tudor Varlan and Constantin Zbarnea.

D6.4 – Feedback on the design, construction and service of the new road. Assessment of the cost, environmental and energy benefits of the project. Authors: Camelia Bulau, Tudor Varlan, Constantin Zbarnea and Laura Dumitrescu.

D7.1a – Problems in the specific environment (Turkey). Author: Gülbahar Budak.

D7.1b – Problems in the specific environment (Cyprus). Section of the old road to Galataria village – F624. Author: Pavlos Neofytou.

D7.2a – Design of the road using new techniques to solve the defined problems (Turkey). Author: Gülbahar Budak.

D7.2b – Design of the road using new techniques to solve the defined problems. (Section of the old road to Galataria village – F624, Pafos, Cyprus). Author: Pavlos Neofytou.

D7.3a – Construction of the road in Turkey using new techniques. Author: Gülbahar Budak.

D7.3b – Construction of the road using new techniques to solve the defined problems. (Section of the old road to Galataria village – F624, Pafos, Cyprus). Author: Pavlos Neofytou.

D8.1 – Dissemination Website. Authors: Kypros Pilakoutas and Kyriacos Neocleous.

D8.1b – Dissemination Website. Authors: Kypros Pilakoutas and Kyriacos Neocleous.

D8.2 – Industrial Seminar. Authors: Kypros Pilakoutas, Valerie Shulman, Kyriacos Neocleous, Radu Andrei, Laura Dumitrescu.

D8.2b – Industrial Seminar. Authors: Kypros Pilakoutas, Valerie Shulman, Kyriacos Neocleous, Radu Andrei, Laura Dumitrescu, Kyriacos Themistocleous, John Donegan and Tudor Varlan.

D8.4 – Technology Implementation Plan. Authors: Jim Goulding, Valerie Shulman, Kyriacos Neocleous, Kypros Pilakoutas and and Radu Andrei.

D8.5 – Partnership Agreement on Detailed Business Plans and Funding Routes. Authors: Jim Goulding, Kyriacos Neocleous, Kypros Pilakoutas, Valerie Shulman, and Radu Andrei.

D9.1 – Management Website. Authors: Kypros Pilakoutas and Kyriacos Neocleous.

D9.2 – Minutes of management meetings and progress reports. Authors: Kypros Pilakoutas and Kyriacos Neocleous.

APPENDIX B

APPENDIX B. EQUATIONS AND CHARTS OF RIGID PAVEMENT DESIGN METHODS

B.1 WESTERGAARD (1926) EQUATIONS

The main equations proposed by Westergaard (1926) to calculate stresses in concrete pavements are shown below, converted to International System of Units (SI).

$$\sigma = \frac{0.316 \times Q}{h^2} \times \left[4 log\left(\frac{l}{b}\right) + 1.069\right] \ [\text{N/mm}^2] \qquad (B.1)$$

$$\sigma = \frac{0.572 \times Q}{h^2} \times \left[4 log\left(\frac{l}{b}\right) + 0.359\right] \ [\text{N/mm}^2] \qquad (B.2)$$

$$\sigma = \frac{3 \times Q}{h^2} \times \left[1 - \left(\frac{a\sqrt{2}}{l}\right)^{0.6}\right] \ [\text{N/mm}^2] \qquad (B.3)$$

Where:

b = equivalent radius of the effective resisting section: $b = (1.6a^2 + h^2)^{0,5} - 0.675h$ [mm]

a = radius of distributed load [mm]

h = thickness of concrete slab [mm]

Q = Total load [N]

L = radius of relative stiffness (relation between the radius of plate stiffness and the module of subgrade reaction k) ($l = \sqrt[4]{\frac{E \times h^3}{12 \times (1-\mu^2) \times k}}$)

Each one of the above equation refers to a specific load position in the concrete plate, as shown in Figure B.1. The "a" arrow refers to load at considerable distance from the edges (Equation B.1), "b" arrow refers to load in one of the plate edges (Equation B.2) and the "c" arrow represents the wheel load in the corner of the plate (Equation B.3).

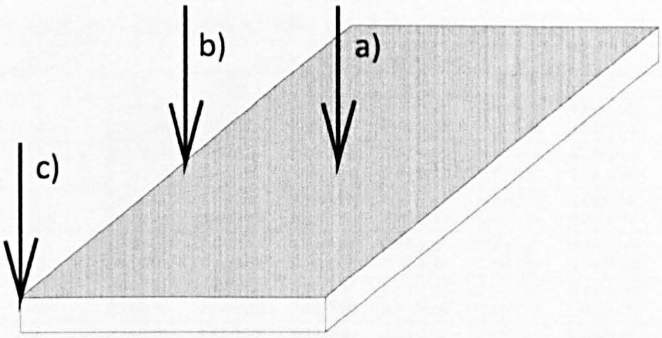

Figure B.1 – Three cases of loading investigation according to Westergaard (1926).

B.2 DESIGN CHARTS AND TABLES OF PCA (1984)

Table B.1 – Equivalent stress – no concrete shoulder (single axle/tandem axle).

Slab thickness, in.	*k* of subgrade-subbase, pci						
	50	100	150	200	300	500	700
4	825/679	726/585	671/542	634/516	584/486	523/457	484/443
4.5	699/586	616/500	571/460	540/435	498/406	448/378	417/363
5	602/516	531/436	493/399	467/376	432/349	390/321	363/307
5.5	526/461	464/387	431/353	409/331	379/305	343/278	320/264
6	465/416	411/348	382/316	362/296	336/271	304/246	285/232
6.5	417/380	367/317	341/286	324/267	300/244	273/220	256/207
7	375/349	331/290	307/262	292/244	271/222	246/199	231/186
7.5	340/323	300/268	279/241	265/224	246/203	224/181	210/169
8	311/300	274/249	255/223	242/208	225/188	205/167	192/155
8.5	285/281	252/232	234/208	222/193	206/174	188/154	177/143
9	264/264	232/218	216/195	205/181	190/163	174/144	163/133
9.5	245/248	215/205	200/183	190/170	176/153	161/134	151/124
10	228/235	200/193	186/173	177/160	164/144	150/126	141/117
10.5	213/222	187/183	174/164	165/151	153/136	140/119	132/110
11	200/211	175/174	163/155	154/143	144/129	131/113	123/104
11.5	188/201	165/165	153/148	145/136	135/122	123/107	116/98
12	177/192	155/158	144/141	137/130	127/116	116/102	109/93
12.5	168/183	147/151	136/135	129/124	120/111	109/97	103/89
13	159/176	139/144	129/129	122/119	113/106	103/93	97/85
13.5	152/168	132/138	122/123	116/114	107/102	98/89	92/81
14	144/162	125/133	116/118	110/109	102/98	93/85	88/78

Table B.2 – Equivalent stress – concrete shoulder (single axle/tandem axle).

Slab thickness, in.	*k* of subgrade-subbase, pci						
	50	100	150	200	300	500	700
4	640/534	559/468	517/439	489/422	452/403	409/388	383/384
4.5	547/461	479/400	444/372	421/356	390/338	355/322	333/316
5	475/404	417/349	387/323	367/308	341/290	311/274	294/267
5.5	418/360	368/309	342/285	324/271	302/254	276/238	261/231
6	372/325	327/277	304/255	289/241	270/225	247/210	234/203
6.5	334/295	294/251	274/230	260/218	243/203	223/188	212/180
7	302/270	266/230	248/210	236/198	220/184	203/170	192/162
7.5	275/250	243/211	226/193	215/182	201/168	185/155	176/148
8	252/232	222/196	207/179	197/168	185/155	170/142	162/135
8.5	232/216	205/182	191/166	182/156	170/144	157/131	150/125
9	215/202	190/171	177/155	169/146	158/134	146/122	139/116
9.5	200/190	176/160	164/146	157/137	147/126	136/114	129/108
10	186/179	164/151	153/137	146/129	137/118	127/107	121/101
10.5	174/170	154/143	144/130	137/121	128/111	119/101	113/95
11	164/161	144/135	135/123	129/115	120/105	112/95	106/90
11.5	154/153	136/128	127/117	121/109	113/100	105/90	100/85
12	145/146	128/122	120/111	114/104	107/95	99/86	95/81
12.5	137/139	121/117	113/106	108/99	101/91	94/82	90/77
13	130/133	115/112	107/101	102/95	96/86	89/78	85/73
13.5	124/127	109/107	102/97	97/91	91/83	85/74	81/70
14	118/122	104/103	97/93	93/87	87/79	81/71	77/67

Table B.3 – Erosion factors – doweled joints, no concrete shoulder (single axle/tandem axle).

Slab thickness, in.	k of subgrade-subbase, pci					
	50	100	200	300	500	700
4	3.74/3.83	3.73/3.79	3.72/3.75	3.71/3.73	3.70/3.70	3.68/3.67
4.5	3.59/3.70	3.57/3.65	3.56/3.61	3.55/3.58	3.54/3.55	3.52/3.53
5	3.45/3.58	3.43/3.52	3.42/3.48	3.41/3.45	3.40/3.42	3.38/3.40
5.5	3.33/3.47	3.31/3.41	3.29/3.36	3.28/3.33	3.27/3.30	3.26/3.28
6	3.22/3.38	3.19/3.31	3.18/3.26	3.17/3.23	3.15/3.20	3.14/3.17
6.5	3.11/3.29	3.09/3.22	3.07/3.16	3.06/3.13	3.05/3.10	3.03/3.07
7	3.02/3.21	2.99/3.14	2.97/3.08	2.96/3.05	2.95/3.01	2.94/2.98
7.5	2.93/3.14	2.91/3.06	2.88/3.00	2.87/2.97	2.86/2.93	2.84/2.90
8	2.85/3.07	2.82/2.99	2.80/2.93	2.79/2.89	2.77/2.85	2.76/2.82
8.5	2.77/3.01	2.74/2.93	2.72/2.86	2.71/2.82	2.69/2.78	2.68/2.75
9	2.70/2.96	2.67/2.87	2.65/2.80	2.63/2.76	2.62/2.71	2.61/2.68
9.5	2.63/2.90	2.60/2.81	2.58/2.74	2.56/2.70	2.55/2.65	2.54/2.62
10	2.56/2.85	2.54/2.76	2.51/2.68	2.50/2.64	2.48/2.59	2.47/2.56
10.5	2.50/2.81	2.47/2.71	2.45/2.63	2.44/2.59	2.42/2.54	2.41/2.51
11	2.44/2.76	2.42/2.67	2.39/2.58	2.38/2.54	2.36/2.49	2.35/2.45
11.5	2.38/2.72	2.36/2.62	2.33/2.54	2.32/2.49	2.30/2.44	2.29/2.40
12	2.33/2.68	2.30/2.58	2.28/2.49	2.26/2.44	2.25/2.39	2.23/2.36
12.5	2.28/2.64	2.25/2.54	2.23/2.45	2.21/2.40	2.19/2.35	2.18/2.31
13	2.23/2.61	2.20/2.50	2.18/2.41	2.16/2.36	2.14/2.30	2.13/2.27
13.5	2.18/2.57	2.15/2.47	2.13/2.37	2.11/2.32	2.09/2.26	2.08/2.23
14	2.13/2.54	2.11/2.43	2.08/2.34	2.07/2.29	2.05/2.23	2.03/2.19

Table B.4 – Erosion factors – aggregate-interlock joints, no concrete shoulder (single axle/tandem axle).

Slab thickness, in	k of subgrade-subbase, pci					
	50	100	200	300	500	700
4	3.94/4.03	3.91/3.95	3.88/3.89	3.86/3.86	3.82/3.83	3.77/3.80
4.5	3.79/3.91	3.76/3.82	3.73/3.75	3.71/3.72	3.68/3.68	3.64/3.65
5	3.66/3.81	3.63/3.72	3.60/3.64	3.58/3.60	3.55/3.55	3.52/3.52
5.5	3.54/3.72	3.51/3.62	3.48/3.53	3.46/3.49	3.43/3.44	3.41/3.40
6	3.44/3.64	3.40/3.53	3.37/3.44	3.35/3.40	3.32/3.34	3.30/3.30
6.5	3.34/3.56	3.30/3.46	3.26/3.36	3.25/3.31	3.22/3.25	3.20/3.21
7	3.26/3.49	3.21/3.39	3.17/3.29	3.15/3.24	3.13/3.17	3.11/3.13
7.5	3.18/3.43	3.13/3.32	3.09/3.22	3.07/3.17	3.04/3.10	3.02/3.06
8	3.11/3.37	3.05/3.26	3.01/3.16	2.99/3.10	2.96/3.03	2.94/2.99
8.5	3.04/3.32	2.98/3.21	2.93/3.10	2.91/3.04	2.88/2.97	2.87/2.93
9	2.98/3.27	2.91/3.16	2.86/3.05	2.84/2.99	2.81/2.92	2.79/2.87
9.5	2.92/3.22	2.85/3.11	2.80/3.00	2.77/2.94	2.75/2.86	2.73/2.81
10	2.86/3.18	2.79/3.06	2.74/2.95	2.71/2.89	2.68/2.81	2.66/2.76
10.5	2.81/3.14	2.74/3.02	2.68/2.91	2.65/2.84	2.62/2.76	2.60/2.72
11	2.77/3.10	2.69/2.98	2.63/2.86	2.60/2.80	2.57/2.72	2.54/2.67
11.5	2.72/3.06	2.64/2.94	2.58/2.82	2.55/2.76	2.51/2.68	2.49/2.63
12	2.68/3.03	2.60/2.90	2.53/2.78	2.50/2.72	2.46/2.64	2.44/2.59
12.5	2.64/2.99	2.55/2.87	2.48/2.75	2.45/2.68	2.41/2.60	2.39/2.55
13	2.60/2.96	2.51/2.83	2.44/2.71	2.40/2.65	2.36/2.56	2.34/2.51
13.5	2.56/2.93	2.47/2.80	2.40/2.68	2.36/2.61	2.32/2.53	2.30/2.48
14	2.53/2.90	2.44/2.77	2.36/2.65	2.32/2.58	2.28/2.50	2.25/2.44

Table B.5 – Erosion factors – doweled joints, concrete shoulder (single axle/tandem axle).

Slab thickness, in.	k of subgrade-subbase, pci					
	50	100	200	300	500	700
4	3.28/3.30	3.24/3.20	3.21/3.13	3.19/3.10	3.15/3.09	3.12/3.08
4.5	3.13/3.19	3.09/3.08	3.06/3.00	3.04/2.96	3.01/2.93	2.98/2.91
5	3.01/3.09	2.97/2.98	2.93/2.89	2.90/2.84	2.87/2.79	2.85/2.77
5.5	2.90/3.01	2.85/2.89	2.81/2.79	2.79/2.74	2.76/2.68	2.73/2.65
6	2.79/2.93	2.75/2.82	2.70/2.71	2.68/2.65	2.65/2.58	2.62/2.54
6.5	2.70/2.86	2.65/2.75	2.61/2.63	2.58/2.57	2.55/2.50	2.52/2.45
7	2.61/2.79	2.56/2.68	2.52/2.56	2.49/2.50	2.46/2.42	2.43/2.38
7.5	2.53/2.73	2.48/2.62	2.44/2.50	2.41/2.44	2.38/2.36	2.35/2.31
8	2.46/2.68	2.41/2.56	2.36/2.44	2.33/2.38	2.30/2.30	2.27/2.24
8.5	2.39/2.62	2.34/2.51	2.29/2.39	2.26/2.32	2.22/2.24	2.20/2.18
9	2.32/2.57	2.27/2.46	2.22/2.34	2.19/2.27	2.16/2.19	2.13/2.13
9.5	2.26/2.52	2.21/2.41	2.16/2.29	2.13/2.22	2.09/2.14	2.07/2.08
10	2.20/2.47	2.15/2.36	2.10/2.25	2.07/2.18	2.03/2.09	2.01/2.03
10.5	2.15/2.43	2.09/2.32	2.04/2.20	2.01/2.14	1.97/2.05	1.95/1.99
11	2.10/2.39	2.04/2.28	1.99/2.16	1.95/2.09	1.92/2.01	1.89/1.95
11.5	2.05/2.35	1.99/2.24	1.93/2.12	1.90/2.05	1.87/1.97	1.84/1.91
12	2.00/2.31	1.94/2.20	1.88/2.09	1.85/2.02	1.82/1.93	1.79/1.87
12.5	1.95/2.27	1.89/2.16	1.84/2.05	1.81/1.98	1.77/1.89	1.74/1.84
13	1.91/2.23	1.85/2.13	1.79/2.01	1.76/1.95	1.72/1.86	1.70/1.80
13.5	1.86/2.20	1.81/2.09	1.75/1.98	1.72/1.91	1.68/1.83	1.65/1.77
14	1.82/2.17	1.76/2.06	1.71/1.95	1.67/1.88	1.64/1.80	1.61/1.74

Table B.6 – Erosion factors – aggregate-interlock joints, concrete shoulder (single axle/tandem axle).

Slab thickness, in.	k of subgrade-subbase, pci					
	50	100	200	300	500	700
4	3.46/3.49	3.42/3.39	3.38/3.32	3.36/3.29	3.32/3.26	3.28/3.24
4.5	3.32/3.39	3.28/3.28	3.24/3.19	3.22/3.16	3.19/3.12	3.15/3.09
5	3.20/3.30	3.16/3.18	3.12/3.09	3.10/3.05	3.07/3.00	3.04/2.97
5.5	3.10/3.22	3.05/3.10	3.01/3.00	2.99/2.95	2.96/2.90	2.93/2.86
6	3.00/3.15	2.95/3.02	2.90/2.92	2.88/2.87	2.86/2.81	2.83/2.77
6.5	2.91/3.08	2.86/2.96	2.81/2.85	2.79/2.79	2.76/2.73	2.74/2.68
7	2.83/3.02	2.77/2.90	2.73/2.78	2.70/2.72	2.68/2.66	2.65/2.61
7.5	2.76/2.97	2.70/2.84	2.65/2.72	2.62/2.66	2.60/2.59	2.57/2.54
8	2.69/2.92	2.63/2.79	2.57/2.67	2.55/2.61	2.52/2.53	2.50/2.48
8.5	2.63/2.88	2.56/2.74	2.51/2.62	2.48/2.55	2.45/2.48	2.43/2.43
9	2.57/2.83	2.50/2.70	2.44/2.57	2.42/2.51	2.39/2.43	2.36/2.38
9.5	2.51/2.79	2.44/2.65	2.38/2.53	2.36/2.46	2.33/2.38	2.30/2.33
10	2.46/2.75	2.39/2.61	2.33/2.49	2.30/2.42	2.27/2.34	2.24/2.28
10.5	2.41/2.72	2.33/2.58	2.27/2.45	2.24/2.38	2.21/2.30	2.19/2.24
11	2.36/2.68	2.28/2.54	2.22/2.41	2.19/2.34	2.16/2.26	2.14/2.20
11.5	2.32/2.65	2.24/2.51	2.17/2.38	2.14/2.31	2.11/2.22	2.09/2.16
12	2.28/2.62	2.19/2.48	2.13/2.34	2.10/2.27	2.06/2.19	2.04/2.13
12.5	2.24/2.59	2.15/2.45	2.09/2.31	2.05/2.24	2.02/2.15	1.99/2.10
13	2.20/2.56	2.11/2.42	2.04/2.28	2.01/2.21	1.98/2.12	1.95/2.06
13.5	2.16/2.53	2.08/2.39	2.00/2.25	1.97/2.18	1.93/2.09	1.91/2.03
14	2.13/2.51	2.04/2.36	1.97/2.23	1.93/2.15	1.89/2.06	1.87/2.00

Table B.7 – Simplified method – allowable ADTT, Axle-load category 1 – Pavements with aggregate-interlock joints

	No Concrete Shoulder or Curb				Concrete Shoulder or Curb			
	Slab thickness, in.	Subgrade-subbase support			Slab thickness, in.	Subgrade-subbase support		
		Low	Medium	High		Low	Medium	High
MR = 650 psi					4		0.2	0.9
	4.5			0.1	4.5	2	8	25
	5	0.1	0.8	3	5	30	130	330
	5.5	3	15	45	5.5	320		
	6	40	160	430				
	6.5	330						
MR = 600 psi	5		0.1	0.4	4			0.1
	5.5	0.5	3	9	4.5	0.2	1	5
	6	8	36	98	5	6	27	75
	6.5	76	300	760	5.5	73	290	730
	7	520			6	610		
MR = 550 psi	5.5	0.1	0.3	1	4.5		0.2	0.6
	6	1	6	18	5	0.8	4	13
	6.5	13	60	160	5.5	13	57	150
	7	110	400		6	130	480	
	7.5	620						

Table B.8 – Simplified method – allowable ADTT, Axle-load category 2 – Pavements with doweled joints

	No Concrete Shoulder or Curb					Concrete Shoulder or Curb				
	Slab thickness, in.	Subgrade-subbase support				Slab thickness, in.	Subgrade-subbase support			
		Low	Medium	High	Very high		Low	Medium	High	Very high
MR = 650 psi						5		3	9	42
	5.5				5	5.5	9	42	120	450
	6		4	12	59	6	96	380	970	3400
	6.5	9	43	120	490	6.5	710	2600		
	7	80	320	840	3100	7	4200			
	7.5	490	1900							
	8	2500								
MR = 600 psi	6				11	5			1	8
	6.5		8	24	110	5.5	1	8	23	98
	7	15	70	190	750	6	19	84	220	810
	7.5	110	440	1100		6.5	160	620	1500	5200
	8	590	2300			7	1000	3600		
	8.5	2700								
MR = 550 psi	6.5			4	19	5.5			3	17
	7		11	34	150	6	3	14	41	160
	7.5	19	84	230	890	6.5	29	120	320	1100
	8	120	470	1200		7	210	770	1900	
	8.5	560	2200			7.5	1100	4000		
	9	2400								

Table B.9 – Simplified method – allowable ADTT, Axle-load category 2 – Pavements with aggregate-interlock joints

	No Concrete Shoulder or Curb					Concrete Shoulder or Curb				
	Slab thickness, in.	Subgrade-subbase support				Slab thickness, in.	Subgrade-subbase support			
		Low	Medium	High	Very high		Low	Medium	High	Very high
MR = 650 psi						5		3	9	42
	5.5				5	5.5	9	42	120	450
	6		4	12	59	6	96	380	700**	970**
	6.5	9	43	120	490	6.5	650**	1000**	1400**	2100**
	7	80	320	840	1200**	7	1100**	1900**		
	7.5	490	1200**	1500**						
	8	1300**	1900**							
MR = 600 psi	6				11	5			1	8
	6.5		8	24	110	5.5	1	8	23	98
	7	15	70	190	750	6	19	84	220	810
	7.5	110	440	1100	2100**	6.5	160	620	1400**	2100**
	8	590	1900**			7	1000	1900**		
	8.5	1900**								
MR = 550 psi	6.5			4	19	5.5			3	17
	7		11	34	150	6	3	14	41	160
	7.5	19	84	230	890	6.5	29	120	320	1100
	8	120	470	1200		7	210	770	1900	
	8.5	560	2200			7.5	1100			
	9	2400								

Table B.10 – Simplified method – allowable ADTT, Axle-load category 3 – Pavements with doweled joints

	No Concrete Shoulder or Curb					Concrete Shoulder or Curb				
	Slab thickness, in.	Subgrade-subbase support				Slab thickness, in.	Subgrade-subbase support			
		Low	Medium	High	Very high		Low	Medium	High	Very high
MR = 650 psi	7.5				250	6.5			83	320
	8		130	350	1,300	7	52	220	550	1,900
	8.5	160	640	1,600	6,200	7.5	320	1,200	2,900	9,800
	9	700	2,700	7,000	11,500**	8	1,600	5,700	13,800	
	9.5	2,700	10,800			8.5	6,900	23,700**		
	10	9,900								
MR = 600 psi						6.5				67
	8			73	310	7			120	440
	8.5		140	380	1,500	7.5		270	680	2,300
	9	160	640	1,700	6,200	8	370	1,300	3,200	10,800
	9.5	630	2,500	6,500		8.5	1,600	5,800	14,100	
	10	2,300	9,300			9	6,600			
	10.5	7,700								
MR = 550 psi						7				82
	8.5			70	300	7.5			130	480
	9		120	340	1,300	8	67	270	670	2,300
	9.5	120	520	1,300	5,100	8.5	330	1,200	2,900	9,700
	10	460	1,900	4,900	19,100	9	1,400	4,900	11,700	
	10.5	1,600	6,500	17,400		9.5	5,100	18,600		
	11	4.900								

Table B.11 – Simplified method – allowable ADTT, Axle-load category 3 – Pavements with aggregate interlock joints

No Concrete Shoulder or Curb

MR	Slab thickness, in.	Subgrade-subbase support: Low	Medium	High	Very high
MR = 650 psi	7.5			60**	250**
	8		130**	350**	830
	8.5	160**	640**	900	1,300
	9	680	1,000	1,300	2,000
	9.5	960	1,500	2,000	2,900
	10	1,300	2,100	2,800	4,300
	10.5	1,800	2,900	4,000	6,300
	11	2,500	4,000	5,700	9,200
	11.5	3,300	5,500	7,900	
	12	4,400	7,500		
MR = 600 psi	8			73**	310**
	8.5		140**	380**	1,300
	9	160**	640**	1,300	2,000
	9.5	630**	1,500	2,000	2,900
	10	1,300	2,100	2,800	4,300
	10.5	1,800	2,900	4,000	6,300
	11	2,500	4,000	5,700	9,200
	11.5	3,300	5,500	7,900	
	12	4,400	7,500		
MR = 550 psi	8				56**
	8.5			70**	300**
	9		120**	340**	1,300**
	9.5	120**	520**	1,300**	2,900
	10	460**	1,900**	2,800	4,300
	10.5	1,600**	2,900	4,000	6,300
	11	2,500	4,000	5,700	9,200
	11.5	3,300	5,500	7,900	
	12	4,400	7,500		

Concrete Shoulder or Curb

MR	Slab thickness, in.	Subgrade-subbase support: Low	Medium	High	Very high
MR = 650 psi	7		220**	510	750
	7.5	320**	640	890	1,400
	8	610	1,100	1,500	2,500
	8.5	950	1,800	2,700	4,700
	9	1,500	2,900	4,600	8,700
	9.5	2,300	4,700	8,000	
	10	3,500	7,700		
	10.5	5,300			
	11	8,100			
MR = 600 psi	7			120**	440**
	7.5	67**	270**	680**	1,400
	8	370**	1,100	1,500	2,500
	8.5	950	1,800	2,700	4,700
	9	1,500	2,900	4,600	8,700
	9.5	2,300	4,700	8,000	
	10	3,500	7,700		
	10.5	5,300			
	11	8,100			
MR = 550 psi	7				82**
	7.5			130**	480**
	8	67**	270**	670**	2,300**
	8.5	330**	1,200**	2,700	4,700
	9	1,400**	2,900	4,600	8,700
	9.5	2,300	4,700	8,000	
	10	3,500	7,700		
	10.5	5,300			
	11	8,100			

Table B.12 – Simplified method – allowable ADTT, Axle-load category 4 – Pavements with doweled joints

No Concrete Shoulder or Curb

MR	Slab thickness, in.	Subgrade-subbase support: Low	Medium	High	Very high
MR = 650 psi	8				270
	8.5		120	340	1,300
	9	140	580	1,500	5,600
	9.5	570	2,300	5,900	14,700**
	10	2,000	8,200	18,700**	25,900**
	10.5	6,700	24,100**	31,800**	45,800**
	11	21,600	39,600**		
	11.5	39,700**			
MR = 600 psi	8.5				300
	9		120	340	1,300
	9.5	120	530	1,400	5,200
	10	480	1,900	5,100	19,300
	10.5	1,600	6,500	17,500	45,900**
	11	4,900	21,400	53,800**	
	11.5	14,500	65,000**		
	12	44,000			
MR = 550 psi	9				260
	9.5			280	1,100
	10		390	1,100	4,000
	10.5	320	1,400	3,600	13,800
	11	1,000	4,300	11,600	46,600
	11.5	3,000	13,100	37,200	
	12	8,200	40,000		

Concrete Shoulder or Curb

MR	Slab thickness, in.	Subgrade-subbase support: Low	Medium	High	Very high
MR = 650 psi	7				400
	7.5		240	620	2,100
	8	330	1,200	3,000	9,800
	8.5	1,500	5,300	12,700	41,100**
	9	5,900	21,400	44,900**	
	9.5	22,500	52,000**		
	10	45,200**			
MR = 600 psi	7.5			130	490
	8		270	690	2,300
	8.5	340	1,300	3,000	9,900
	9	1,400	5,000	12,000	40,200
	9.5	5,200	18,800	45,900	
	10	18,400			
MR = 550 psi	8			130	480
	8.5		250	620	2,100
	9	280	1,000	2,500	8,200
	9.5	1,100	3,900	9,300	30,700
	10	3,800	13,600	32,900	
	10.5	12,400	46,200		
	11	40,400			

Table B.13 – Simplified method – allowable ADTT, Axle-load category 4 – Pavements with aggregate interlock joints

	No Concrete Shoulder or Curb					Concrete Shoulder or Curb				
	Slab thickness, in.	Subgrade-subbase support: Low	Medium	High	Very high	Slab thickness, in.	Subgrade-subbase support: Low	Medium	High	Very high
MR = 650 psi	8				270**	7			100**	400**
	8.5		120**	340**	990	7.5		240**	620**	810
	9	140**	580**	1,100	1,500	8	330**	770	1,100	1,700
	9.5	570**	1,200	1,600	2,300	8.5	720	1,300	1,900	3,100
	10	1,100	1,700	2,200	3,400	9	1,100	2,100	3,200	5,700
	10.5	1,500	2,300	3,200	4,900	9.5	1,700	3,400	5,500	10,200
	11	2,000	3,300	4,500	7,200	10	2,600	5,500	9,200	17,900
	11.5	2,700	4,500	6,300	10,400					
	12	3,600	6,100	8,800	14,900	11	5,900	13,600	24,200	
	13	6,300	11,100	16,800		12	12,800			
	14	10,800								
MR = 600 psi	8.5				300**	7.5			130**	490**
	9		120**	340**	1,300**	8		270**	690**	1,700
	9.5	120**	530**	1,400**	2,300	8.5	340**	1,300**	1,900	3,100
	10	480**	1,700	2,200	3,400	9	1,100	2,100	3,200	5,700
	10.5	1,500	2,300	3,200	4,900	9.5	1,700	3,400	5,500	10,200
	11	2,000	3,300	4,500	7,200	10	2,600	5,500	9,200	17,900
	11.5	2,700	4,500	6,300	10,400					
	12	3,600	6,100	8,800	14,900	11	5,900	13,600	24,200	
	13	6,300	11,100	16,800		12	12,800			
	14	10,800								
MR = 550 psi	9				260**	8			130**	480**
	9.5			280**	1,100**	8.5		250**	620**	2,100**
	10		390**	1,100**	3,400	9	280**	1,000**	2,500**	5,700
	10.5	320**	1,400**	3,200	4,900	9.5	1,100**	3,400	5,500	10,200
	11	1,000**	3,300	4,500	7,200	10	2,600	5,500	9,200	17,900
	11.5	2,700	4,500	6,300	10,400					
	12	3,600	6,100	8,800	14,900	11	5,900	13,600	24,200	
	13	6,300	11,100	16,800		12	12,800			
	14	10,800								

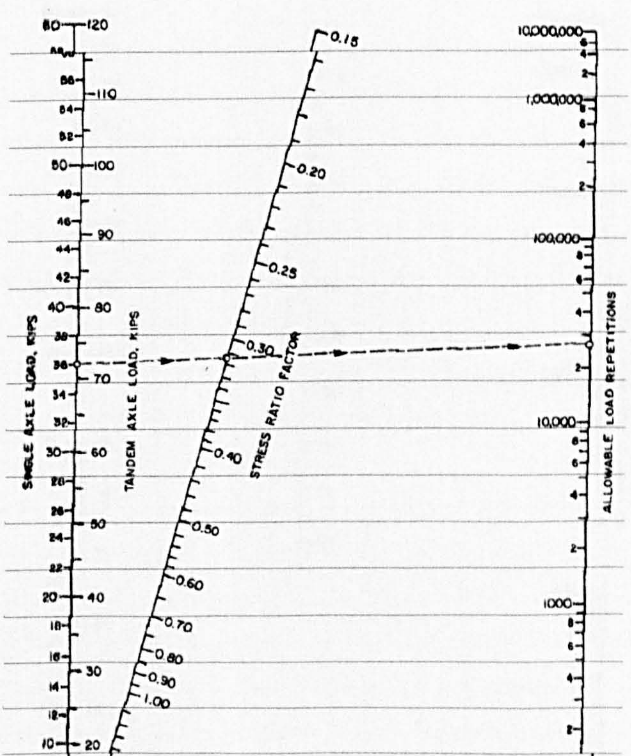

Figure B.2 – Fatigue analysis – allowable load repetitions based on stress ratio (with and without concrete shoulder).

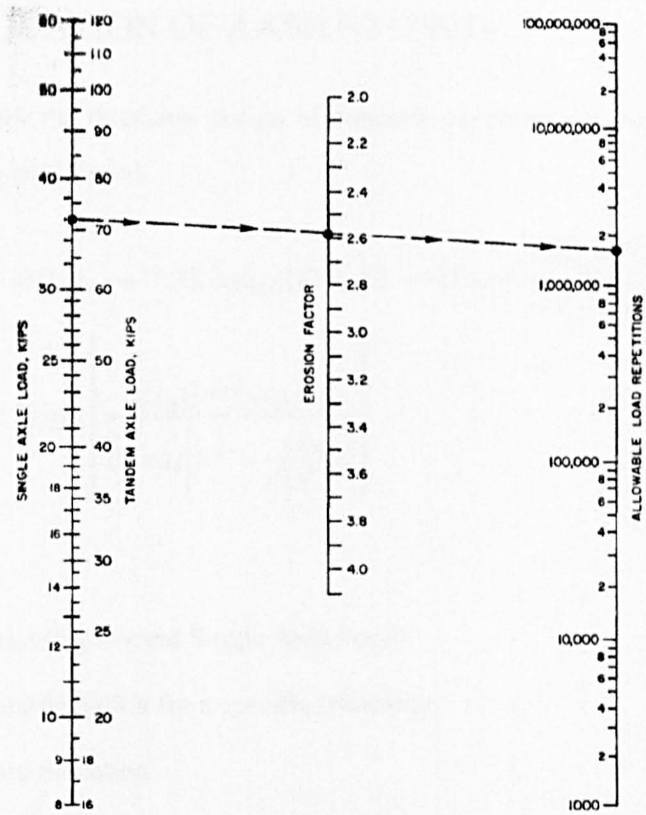

Figure B.3 – Erosion analysis – allowable load repetitions based on erosion factor (without concrete shoulder).

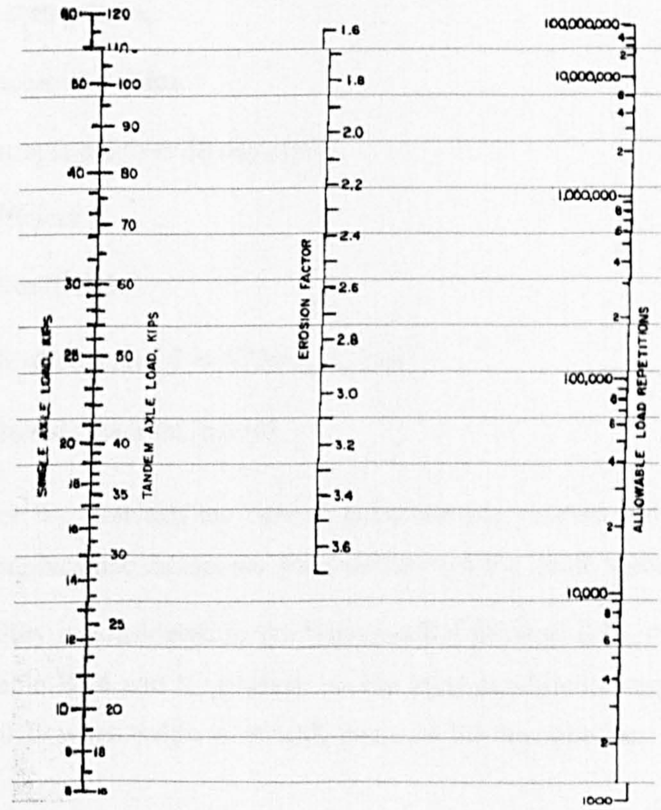

Figure B.4 – Erosion analysis –allowable load repetitions based on erosion factor (with concrete shoulder).

B.3 DESIGN EQUATION OF AASHTO (1993)

The main equation for the thickness design of concrete pavements, according to the guide, is shown below (in Imperial Units):

$$\log_{10} W_{18} = Z_R S_o + 7.35\log_{10}(D+1) - 0.06 + \frac{log_{10}\left[\frac{\Delta PSI}{4.5-1.5}\right]}{1+\frac{1.624\times10^7}{(D+1)^{8.46}}} + (4.22 - 0.32p_t) \times log_{10}\left[\frac{S_c' C_d\left[D^{0.75}-1.132\right]}{215.63J\left[D^{0.75}-\frac{18.42}{\left(\frac{E_c}{k}\right)^{0.25}}\right]}\right] \qquad \text{(B.4)}$$

Where:

W_{18} = traffic in ESALs (Equivalent Single Axle Load)

Z_R = normal standard deviation for a specific reliability

S_O = overall standard deviation

D = pavement thickness [in]

ΔPSI = change in the serviceability index $\Delta PSI = p_o - p_t$

p_o = initial serviceability index

p_t = terminal serviceability index

S'_c = concrete flexural strength at 28 days [psi]

C_d = drainage coefficient

J = load transfer coefficient

E_c = elastic module of concrete $E = 57000\sqrt{f_c'}$ [psi]

k = module of subgrade reaction [psi/in]

The traffic parameter W_{18} converts the various axles (simple, tandem and triple) to a standard axle of 80 kN. The equivalence factors are obtained through the guide specific tables.

The structure reliability is considered in the Equation B.4 through $Z_R S_O$ parameters. Z_R can be obtained through Table B.14 and S_O depends on the local conditions, varying from 0.3 to 0.4. The guide suggests 0.39 when traffic is variable and 0.34 for the opposite.

Table B.14 – Reliability and normal standard deviation Z_R [AASHTO, 1993].

Functional classification	Recommended level of reliability			
	Urban		Rural	
	Percentage	Z_R	Percentage	Z_R
Interstates and other freeways	85 – 99,9	-1.037 – -3.75	80 – 99,9	-0.841 – -3.75
Principal arterials	80 – 99	-0.841 – -2.327	75 – 95	-0.674 – -1.645
Collectors	80 – 95	-0.841 – -1.645	75 – 95	-0.674 – -1.645
Local	50 – 80	0 – -0.841	50 – 80	0 – -0.841

The initial and final PSI (present serviceability index) depends on how smooth the pavement can be constructed and on how long it takes for the pavement to be repaired, respectively. According to the AASHTO Guide (1993), p_o should be equal to 4.5 and p_t equal to 2.0, 2.5 and 3.0, which means that 85, 55 and 12% (respectively) of users consider the pavement as condemned.

Drainage coefficient varies from 0.7 to 1.2 (very poor to excellent), according to Table B.15. The load transfer factor varies from 2.3 to 4.4 and is influenced by the use of load transfer bars, asphalt or concrete hard shoulders and type of pavement used, as shown in Table B.16.

Table B.15 – Drainage coefficient C_d [AASHTO, 1993].

Drainage quality	Percentage of time exposed to moisture levels approaching saturation			
	<1%	1 – 5%	5 – 25%	>25%
Excellent	1.25 – 1.20	1.20 – 1.15	1.15 – 1.10	1.10
Good	1.20 – 1.15	1.15 – 1.10	1.10 – 1.00	1.00
Regular	1.15 – 1.10	1.10 – 1.00	1.00 – 0.90	0.90
Poor	1.10 – 1.00	1.00 – 0.90	0.90 – 0.80	0.80
Very poor	1.00 – 0.90	0.90 – 0.80	0.80 – 0.70	0.70

Table B.16 – Load transfer coefficient J according to the pavement type [source: AASHTO, 1993].

Pavement type	Hard shoulder			
	Asphalt		Concrete	
	Load transfer devices			
	Yes	No	Yes	No
JPCP. JRCP	3.2	3.8 – 4.4	2.5 – 3.1	3.6 – 4.2
CRCP	2.9 – 3.2	-	2.3 – 2.9	-

According to the guide, the modulus of resilience M_R is the main property that characterises the soil. However, concrete pavement design requires the module of subgrade reaction k, which can be correlated to M_R by equations and charts proposed by the guide.

B.4 HIGHWAYS AGENCY (2006) DESIGN CHART AND EQUATIONS

The method considers four classes of foundation stiffness and only the number 3 and 4 classes can be used for concrete pavements.

- Foundation class 1 $\geq$ 50 MPa
- Foundation class 2 $\geq$ 100 MPa
- Foundation class 3 $\geq$ 200 MPa
- Foundation class 4 $\geq$ 400 MPa

The method prefers the design of CRCP with an asphalt overlay of 30 mm; or the design of CRCB (continuously reinforced concrete base) with an asphalt overlay of 100 mm. JPCP and JRCP are also allowed subjected to approval by the regulation authority. Minimum concrete plate thickness should be 200 mm for CRCP and 150 mm for CRCB.

Life-cycle is estimated to 40 years for high and heavy traffic roads. The roads subjected to light traffic can be designed to resist to 20 years if allowed by the regulation authority.

The design thickness for CRCP and CRCB can be calculated according to Figure B.5, which is based on the flexural strength of concrete and on the number of standard axles (= 80 kN). Thickness value obtained is valid for pavement with concrete hard shoulder, otherwise 30 mm should be added to the concrete plate thickness.

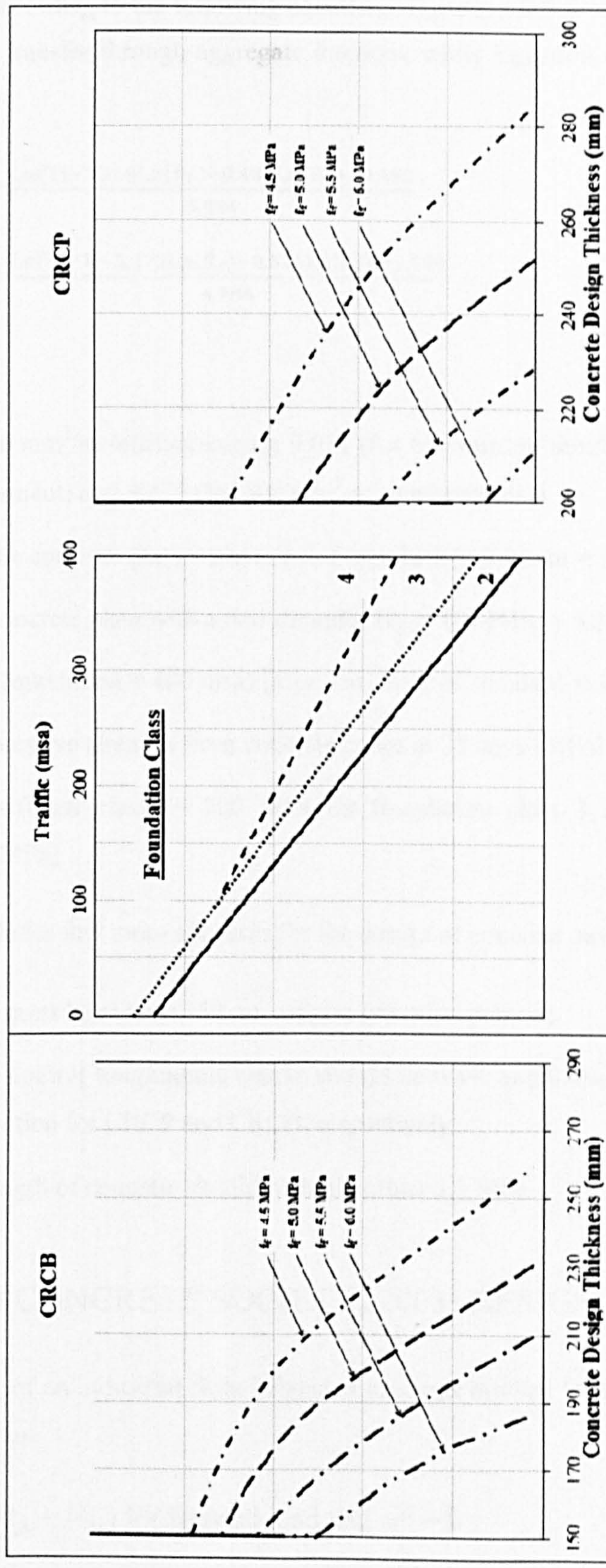

Figure B.5 – Design thickness for CRCP and CRCB.

JPCP are designed according to the following equations. Equation B.5 is used for plain concrete pavement with load transfer through aggregate interlock while Equation B.6 is used for JPCP with dowel bars.

$$\mathrm{Ln}(H_1) = \frac{\mathrm{Ln}(T) - 3.466\mathrm{Ln}(R_C) - 0.484\mathrm{Ln}(E) + 40.483}{5.094} \tag{B.5}$$

$$\mathrm{Ln}(H_1) = \frac{\mathrm{Ln}(T) - R - 3.171\mathrm{Ln}(R_C) - 0.326\mathrm{Ln}(E) + 45.150}{4.786} \tag{B.6}$$

Where:

R = 8.812 (for 500 mm^2/m reinforcement); 9.071 (for 600 mm^2/m reinforcement); 9.289 (for 700 mm^2/m reinforcement) and 9.479 (for 800 mm^2/m reinforcement)

H_1 = thickness of the concrete plate without a tied shoulder (minimum = 150 mm) [mm]

H_2 = thickness of concrete plate with a tied shoulder $H_2 = 0.934H_1 - 12.5$ [mm]

T = design traffic (maximum = 400 msa) [msa – millions of standard axles]

R_c = average compressive strength from concrete cubes at 28 days [MPa]

E = foundation stiffness class (= 200 MPa for foundation class 3 and = 400 MPa for foundation class 4) [MPa]

The method also includes few more concerns for the design of concrete pavements:

- Foundations must be at least 150 mm of non-granular material;
- Steel area to control longitudinal cracks should be 0.6% and 0.4% of the concrete plate transverse section for CRCP and CRCB, respectively;
- Flexural strength of concrete should be higher than 5.5 MPa.

B.5 TR 34 (THE CONCRETE SOCIETY, 2003) DESIGN EQUATIONS

The load capacity P_u of an industrial floor subjected to single applied loads can be obtained by the following equations:

$$P_u = 2\pi(M_p + M_n) \text{ for internal load and } \alpha/l = 0 \tag{B.7}$$

$$P_u = 4\pi(M_p + M_n)/\left(1 - \frac{\alpha}{3l}\right) \text{ for internal load and } \alpha/l \geq 0.2 \tag{B.8}$$

$$P_u = \left[\pi(M_p + M_n)/2\right] + 2M_n \text{ for edge load and } \alpha/l = 0 \tag{B.9}$$

$$P_u = \left[\pi\left(M_p + M_n\right) + 4M_n\right] / \left(1 - \frac{\alpha}{3l}\right) \text{ for edge load and } \alpha/l \geq 0.2 \tag{B.10}$$

$$P_u = 2M_n \text{ for corner load and } \alpha/l = 0 \tag{B.11}$$

$$P_u = 4M_n / \left[1 - \left(\frac{\alpha}{l}\right)\right] \text{ for corner load and } \alpha/l \geq 0.2 \tag{B.12}$$

Where:

l = radius of relative stiffness $l = \left[E_{cm}h^3/12(1-v^2)k\right]^{0.25}$

k = modulus of subgrade reaction [N/mm^3]

h = slab thickness [mm]

v = Poisson ratio

E_{cm} = Modulus of elasticity of concrete

α = equivalent contact radius of the load: $\alpha = \sqrt{\frac{P}{\pi G}}$ for circular loads and $\alpha = \sqrt{\frac{LW}{\pi}}$ for rectangular loads

P = wheel load [N]

G = tyre pressure [N/mm^2]

L = length of plate [mm]

W = widthof plate [mm]

The positive bending moment capacity M_p is obtained by Equation B.13 whilst the negative bending moment capacity M_n is described in Equation B.14.

$$M_p = \frac{f_{ctk,fl}}{\gamma_c}\left(R_{e,3}\right)\left(\frac{h^2}{6}\right) \tag{B.13}$$

$$M_p = \frac{f_{ctk,fl}}{\gamma_c}\left(\frac{h^2}{6}\right) \tag{B.14}$$

Where:

$f_{ctk,fl}$ = characteristic flexural strength of plain concrete

γ_c = partial factor for the strength of concrete

APPENDIX C

APPENDIX C. FLEXURAL BEHAVIOUR

C.1 CONTROL SPECIMENS – 28 DAYS

C.1.1 Flexural properties

C.1.1.1 f_{LOP} and f_{ult} [MPa]

Mix	f_{LOP} (visual)	f_{LOP} (BS EN 14651)	f_{LOP} (Che, 2010)	f_{ult}	Mix	f_{LOP} (visual)	f_{LOP} (BS EN 14651)	f_{LOP} (Che, 2010)	f_{ult}
W-CIP-0	2.69	4.60	3.59	4.60	R-CIP-0	3.67	5.74	4.80	5.74
	2.50	4.28	3.40	4.28		3.10	5.11	4.03	5.14
W-CIP-2I	3.26	5.66	4.87	7.48	R-CIP-2I	3.20	7.03	5.57	10.91
	2.69	5.71	4.21	8.13		3.11	6.24	4.63	8.37
W-CIP-2R	3.46	5.02	4.74	5.02	R-CIP-2R	2.80	4.38	3.56	4.43
	2.69	4.79	4.00	4.83		2.80	5.60	4.73	5.61
W-CIP-6R	3.84	7.17	6.18	8.45	R-CIP-6R	2.49	5.71	4.55	6.47
	3.84	6.13	4.91	7.09		2.66	5.71	3.41	6.86
W-LEC-0	2.69	4.57	4.08	4.57	R-LEC-0	4.03	7.69	6.82	7.69
	3.07	5.00	3.83	5.00		4.99	7.03	6.74	7.03
W-LEC-2I	3.46	6.22	5.55	6.22	R-LEC-2I	4.42	6.97	5.75	7.43
	2.88	6.89	5.75	8.49		3.65	7.54	6.08	7.54
W-LEC-2R	5.38	6.13	5.85	6.13	R-LEC-2R	5.38	7.14	6.69	7.14
	3.46	6.81	6.17	6.81		3.46	7.31	4.42	7.31
W-LEC-6R	4.61	7.29	6.77	7.29	R-LEC-6R	3.46	6.58	5.28	7.19
	4.80	6.92	6.68	6.92		4.42	6.67	5.86	6.94
R-CIP-6R pre-cracking before corrosion simulation (ambient temperature)	3.73	6.59	5.28	7.30	R-CIP-6R pre-cracking before corrosion simulation (40°C)	3.91	6.96	5.82	7.83
	3.85	6.56	4.42	7.03		3.37	6.07	4.96	6.64
	3.84	7.17	5.81	8.17		4.15	7.48	6.09	7.48
	3.85	7.66	6.31	8.59		4.03	7.04	5.74	7.74
	3.97	6.90	5.45	6.99		3.61	6.53	4.95	6.73
	3.91	6.51	5.59	7.05		4.69	6.94	6.25	7.02

C.1.1.2 $f_{R,i}$ [MPa] at 0.5 mm, 1.5 mm, 2.5 mm and 3.5 mm

Mix	$F_{R,0.5}$	$F_{R,1.5}$	$F_{R,2.5}$	$F_{R,3.5}$	Mix	$F_{R,0.5}$	$F_{R,1.5}$	$F_{R,2.5}$	$F_{R,3.5}$
W-CIP-0	0.96	-	-	-	R-CIP-0	1.75	-	-	-
	0.62	-	-	-		1.50	-	-	-
W-CIP-2I	7.37	4.22	3.10	2.95	R-CIP-2I	10.74	10.27	6.73	8.10
	7.02	4.79	2.73	2.85		7.96	7.49	6.71	6.30
W-CIP-2R	2.76	2.12	1.55	1.15	R-CIP-2R	3.21	2.19	1.75	2.08
	2.95	1.96	1.34	1.05		3.29	2.13	1.5	1.95
W-CIP-6R	7.43	5.84	4.22	2.90	R-CIP-6R	6.16	5.03	3.89	4.25
	6.58	5.65	4.34	3.27		6.51	5.17	3.95	4.71
W-LEC-0	0.5	-	-	-	R-LEC-0	1.32	-	-	-
	0.54	-	-	-		1.22	-	-	-
W-LEC-2I	6.02	5.61	3.06	2.44	R-LEC-2I	6.48	7.16	7.39	6.36
	7.96	7.07	4.95	3.15		5.71	5.74	5.94	5.60
W-LEC-2R	3.49	2.39	1.58	1.23	R-LEC-2R	2.57	1.67	1.28	1.89
	3.33	2.34	1.73	1.54		2.60	1.64	1.29	1.64
W-LEC-6R	5.86	3.81	2.63	1.86	R-LEC-6R	6.94	5.43	4.27	4.60
	5.25	3.38	2.35	1.77		6.20	4.38	3.46	4.02

C.1.1.3 f_{eq3} [MPa] and $R_{e,3}$

Mix	f_{eq3}	$R_{e,3}$	Mix	f_{eq3}	$R_{e,3}$
W-CIP-0	-	-	R-CIP-0	-	-
	-	-		-	-
W-CIP-2I	4.35	0.77	R-CIP-2I	8.10	1.15
	4.60	0.81		6.30	1.01
W-CIP-2R	1.87	0.37	R-CIP-2R	2.08	0.48
	1.85	0.39		1.95	0.35
W-CIP-6R	4.88	0.68	R-CIP-6R	4.25	0.75
	4.69	0.77		4.71	0.83
W-LEC-0	-	-	R-LEC-0	-	-
	-	-		-	-
W-LEC-2I	4.01	0.65	R-LEC-2I	6.36	0.91
	5.57	0.81		5.60	0.74
W-LEC-2R	2.25	0.37	R-LEC-2R	1.89	0.27
	2.33	0.34		1.64	0.22
W-LEC-6R	3.45	0.47	R-LEC-6R	4.60	0.70
	2.97	0.43		4.02	0.60

C.1.1.4 E [GPa]

Mix	E (Approach 1)	E (Approach 2)	Mix	E (1)	E (2)
W-CIP-0	30.5	32.5	R-CIP-0	37.2	40.1
	33.5	35.3		40.6	43.6
W-CIP-2I	35.8	37.3	R-CIP-2I	35.8	30.1
	33.7	34.0		36.0	37.2
W-CIP-2R	33.6	34.9	R-CIP-2R	30.3	33.1
	34.1	36.2		33.8	28.7
W-CIP-6R	32.8	34.0	R-CIP-6R	36.8	37.7
	37.4	40.5		56.9	60.3
W-LEC-0	35.3	31.4	R-LEC-0	40.3	41.4
	39.3	41.9		40.2	42.6
W-LEC-2I	40.6	43.4	R-LEC-2I	44.3	46.5
	44.8	45.3		41.2	42.1
W-LEC-2R	36.4	33.6	R-LEC-2R	38.2	40.1
	41.5	44.0		70.9	77.2
W-LEC-6R	39.2	41.6	R-LEC-6R	34.3	35.5
	36.4	37.5		35.3	37.2
R-CIP-6R pre-cracking before corrosion simulation (ambient temperature)	38.9	40.9	R-CIP-6R pre-cracking before corrosion simulation (40°C)	40.9	42.2
	43.4	48.7		44.0	46.1
	38.1	39.4		41.2	43.1
	42.0	43.0		36.7	37.9
	38.9	41.3		42.7	46.9
	37.5	38.2		38.9	40.8

C.1.2 Flexural Curves

C.1.2.1 W-CIP-0

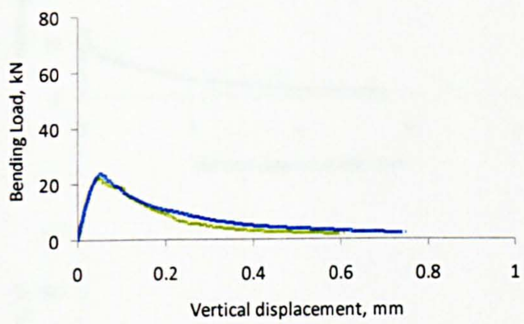

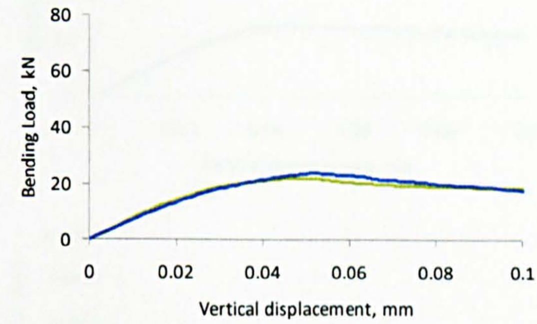

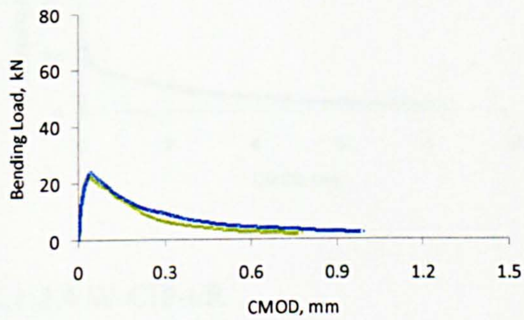

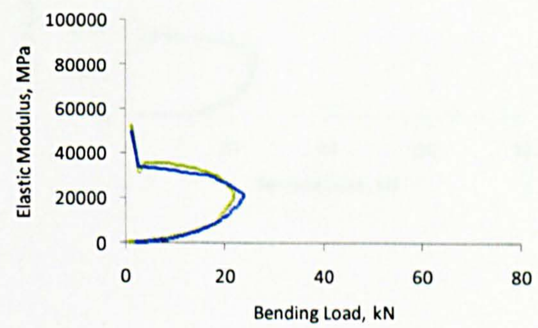

C.1.2.2 W-CIP-2I

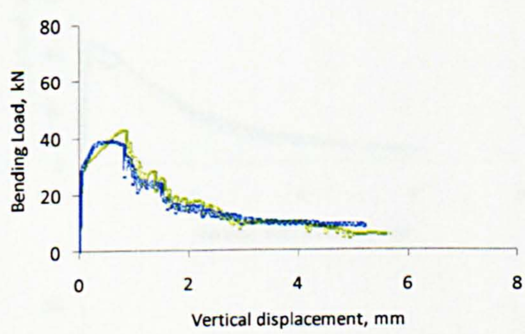

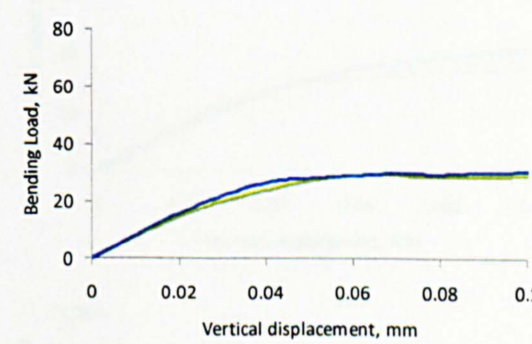

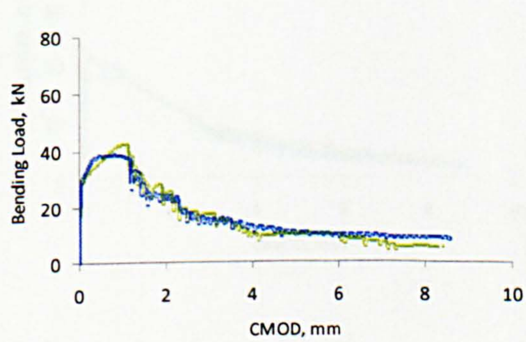

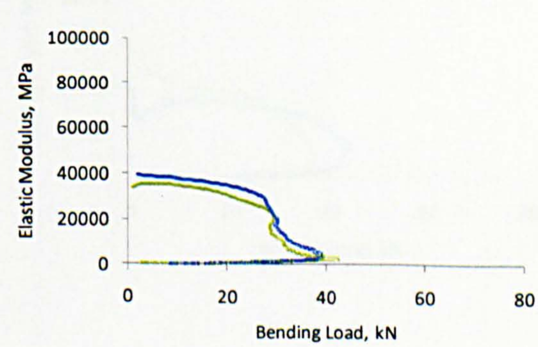

C.1.2.3 W-CIP-2R

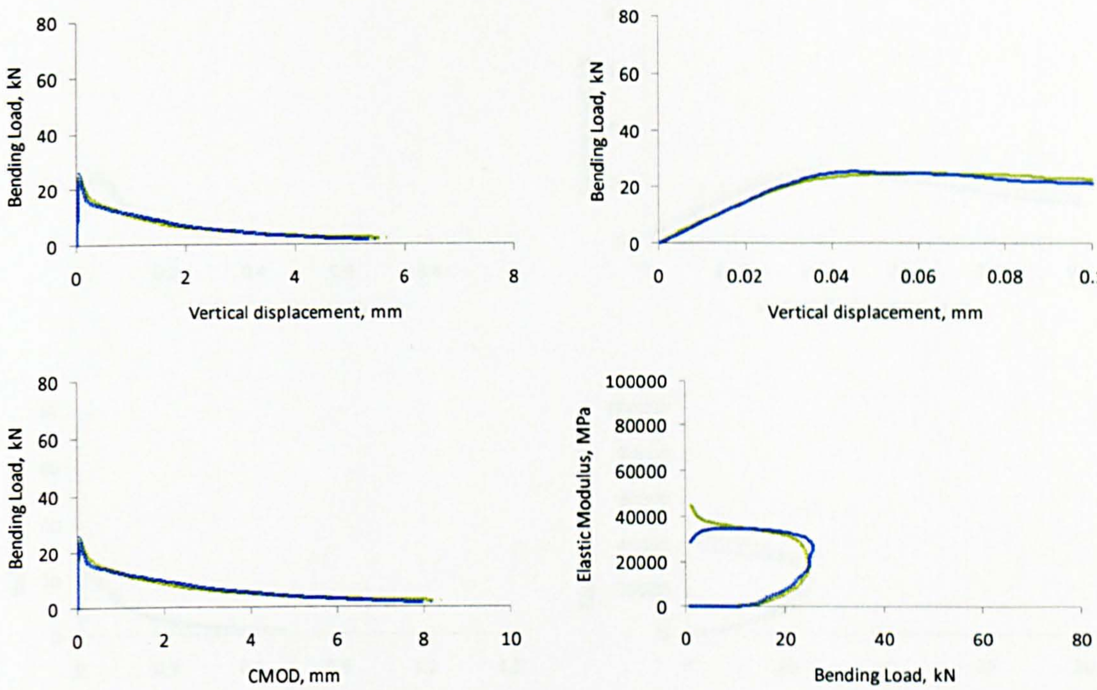

C.1.2.4 W-CIP-6R

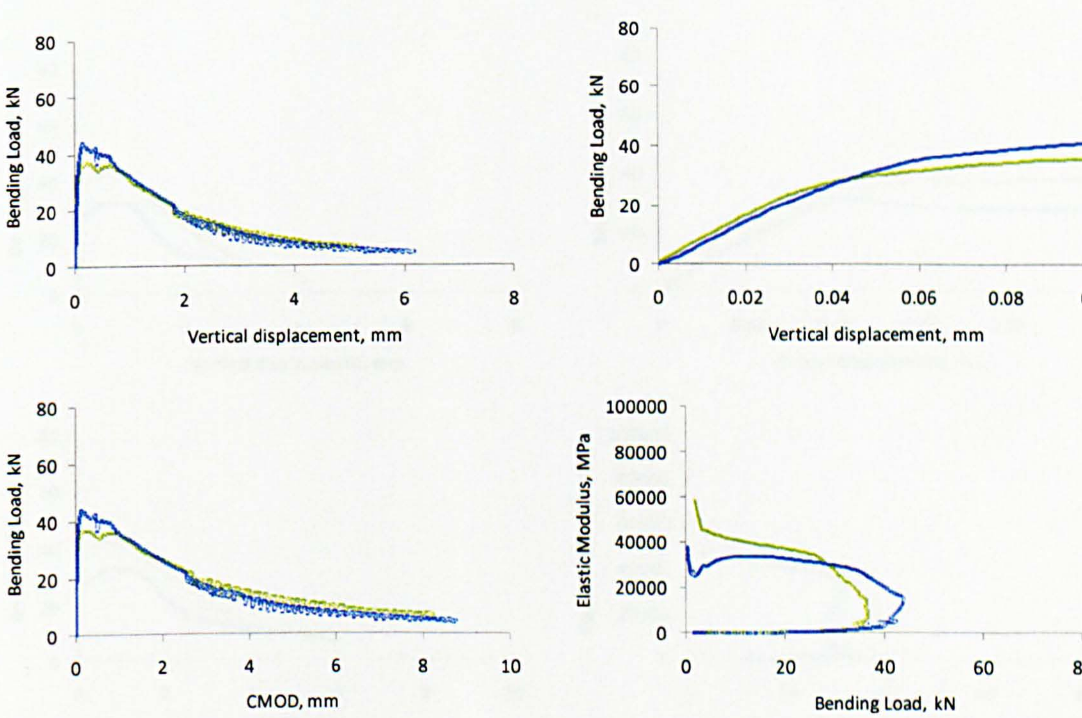

C.1.2.5 W-LEC-0

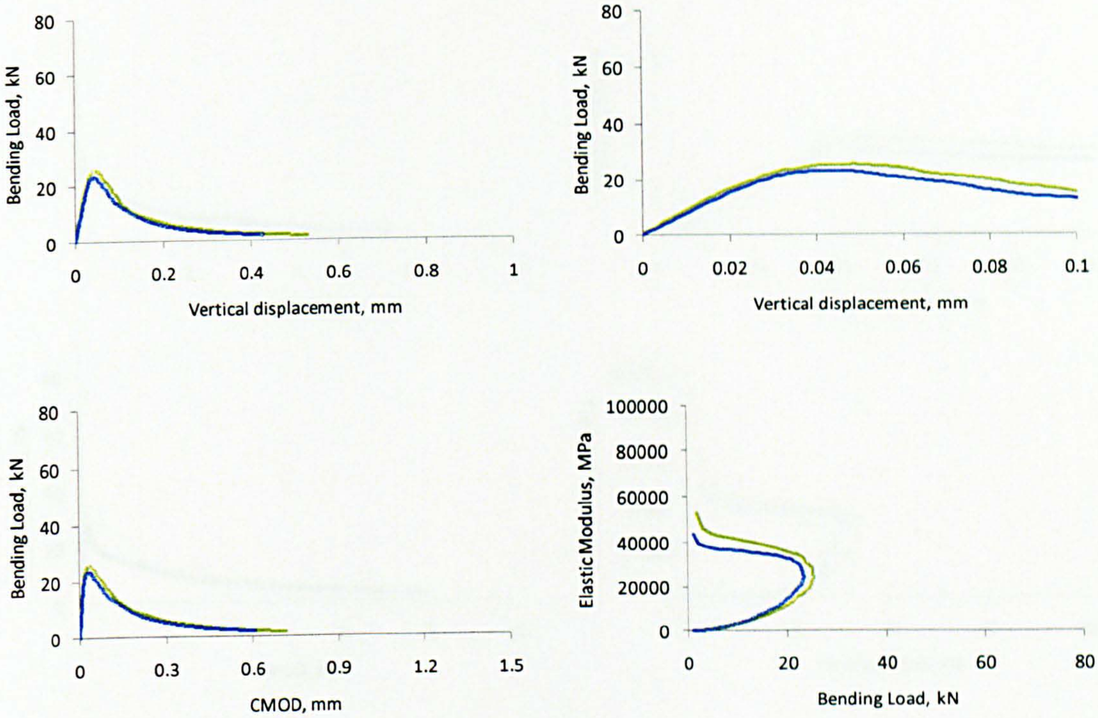

C.1.2.6 W-LEC-2I

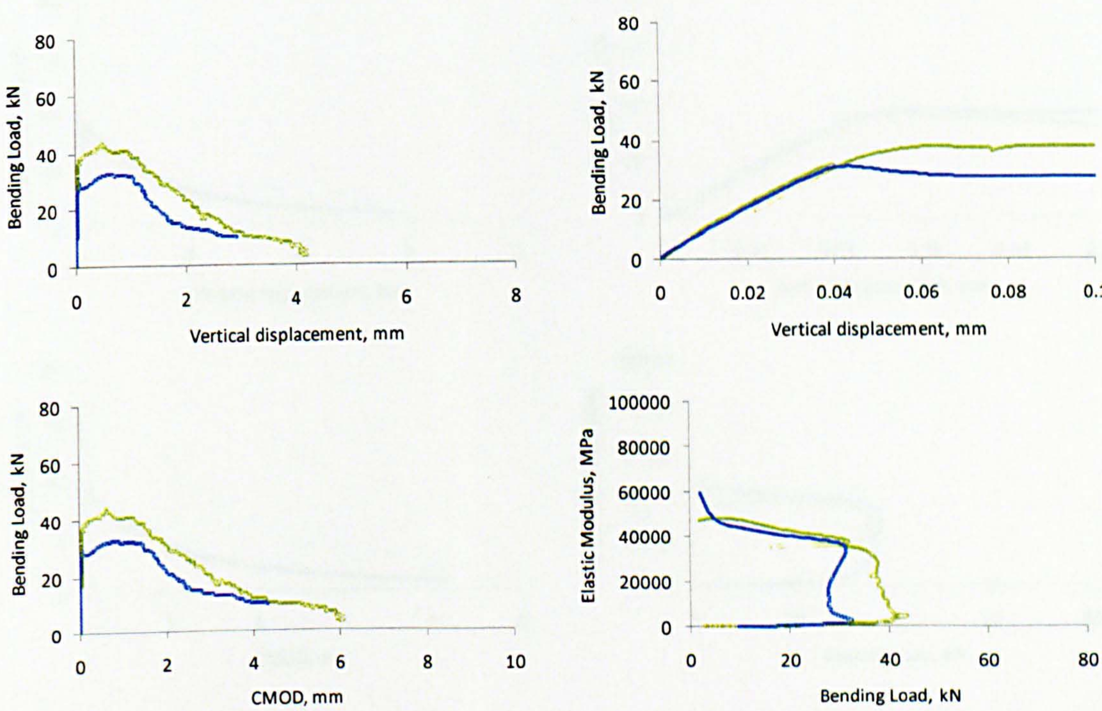

C.1.2.7 W-LEC-2R

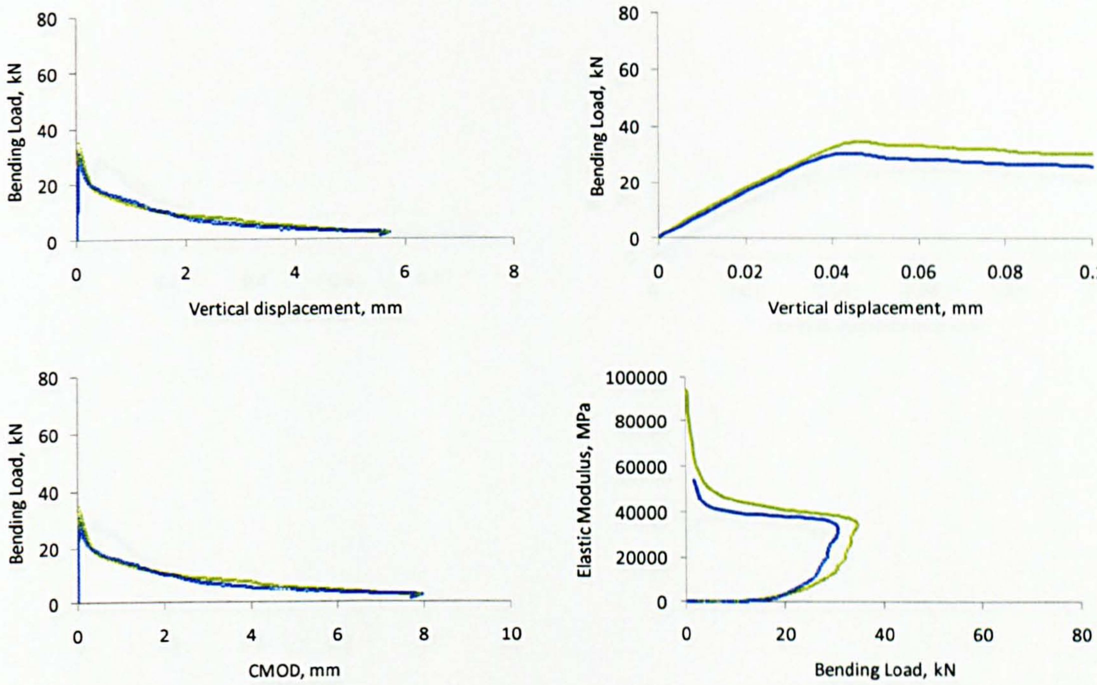

C.1.2.8 W-LEC-6R

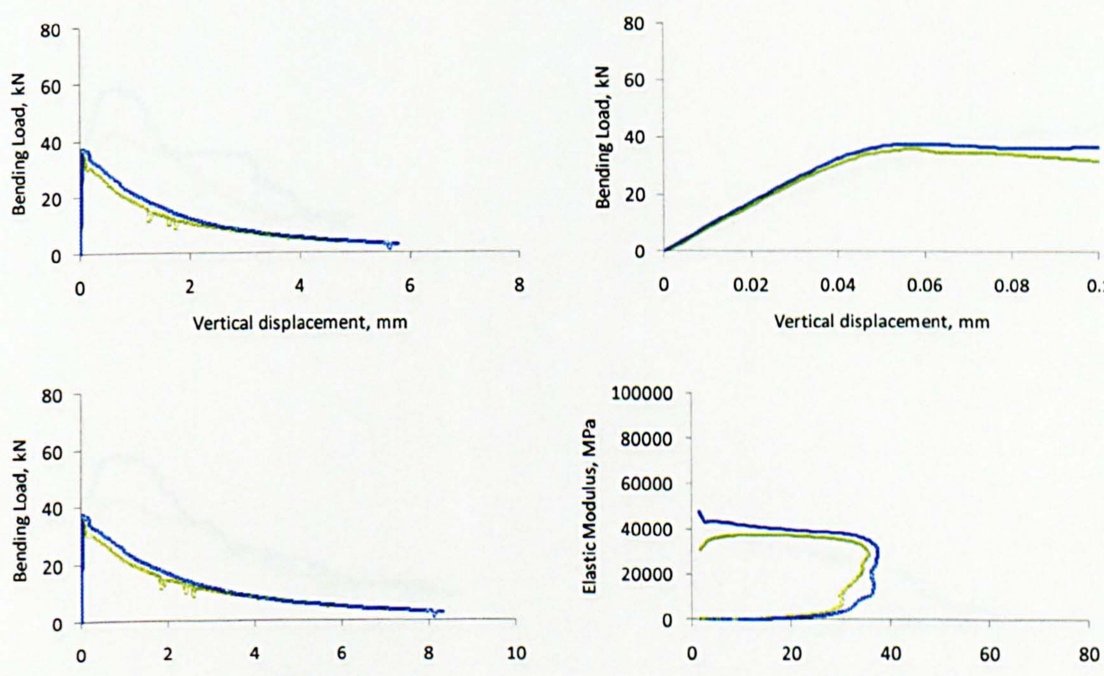

C.1.2.9 R-CIP-0

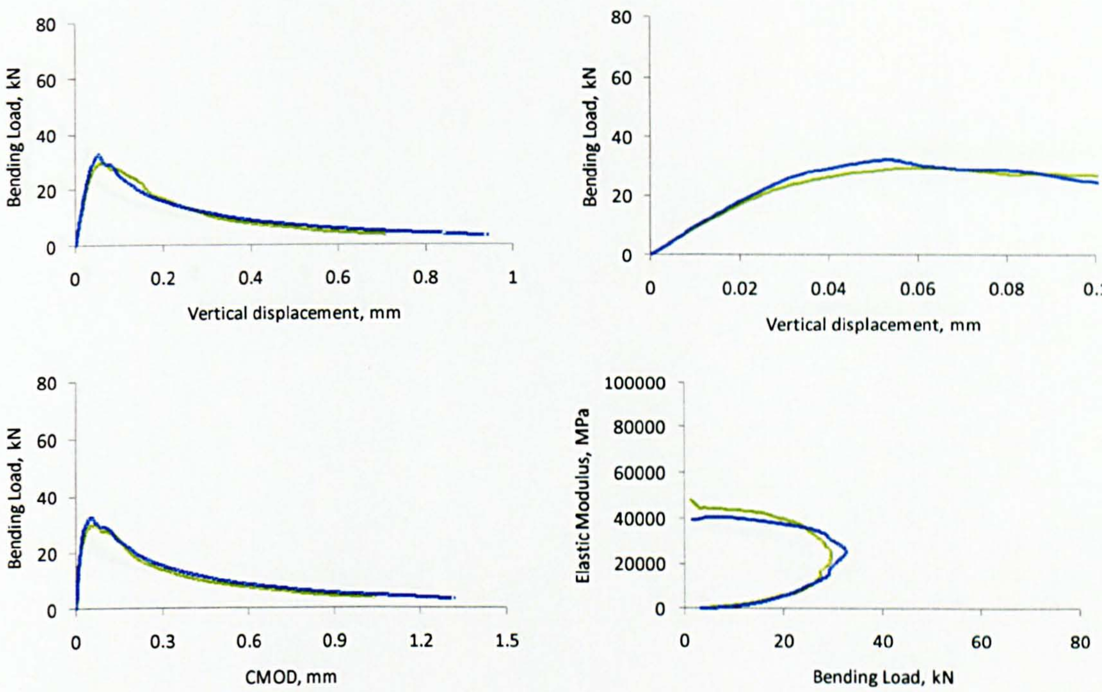

C.1.2.10 R-CIP-2I

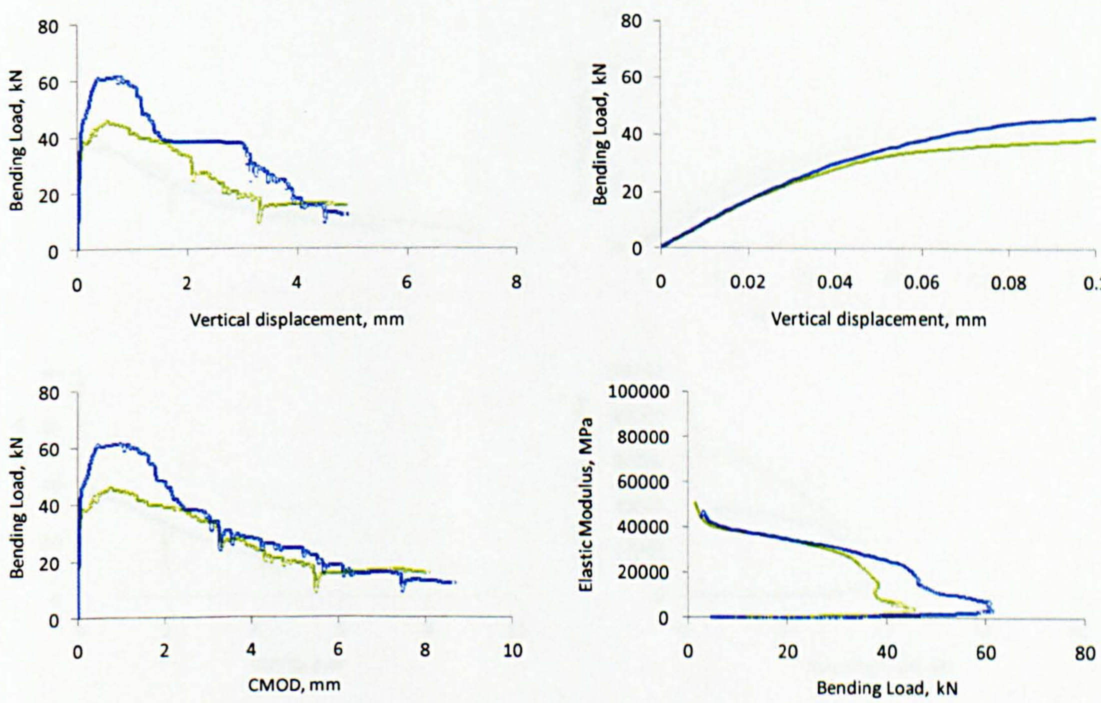

C.1.2.11 R-CIP-2R

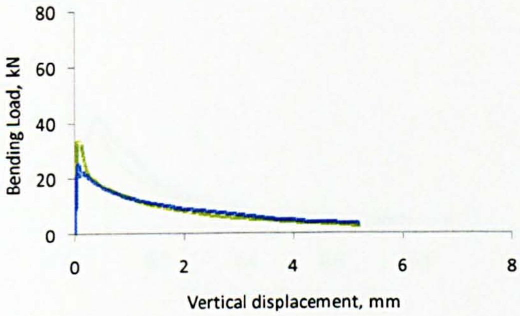

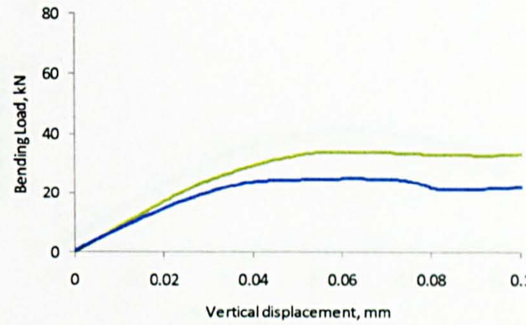

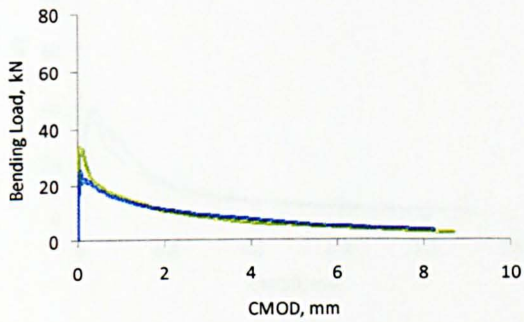

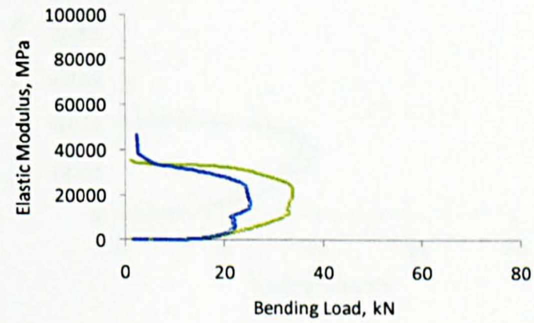

C.1.2.12 R-CIP-6R

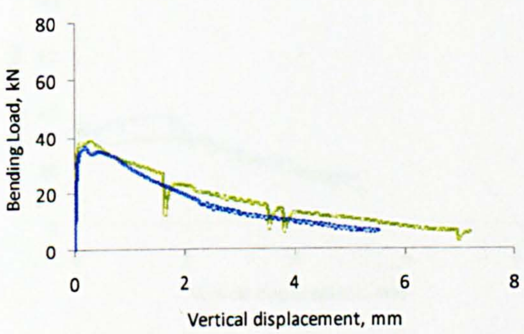

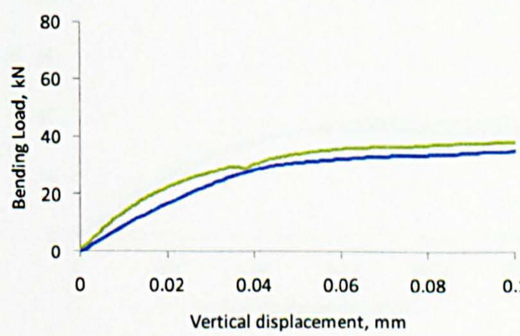

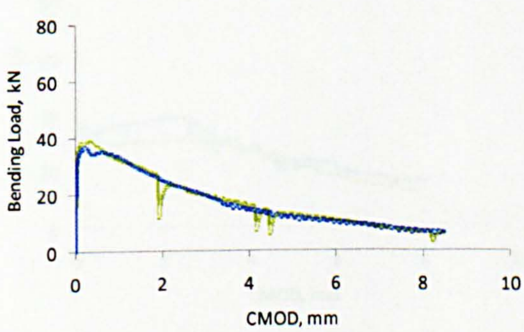

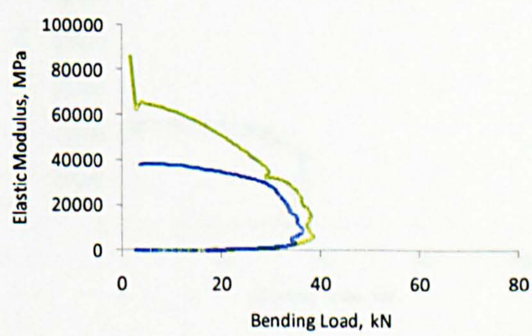

C.1.2.13 R-LEC-0

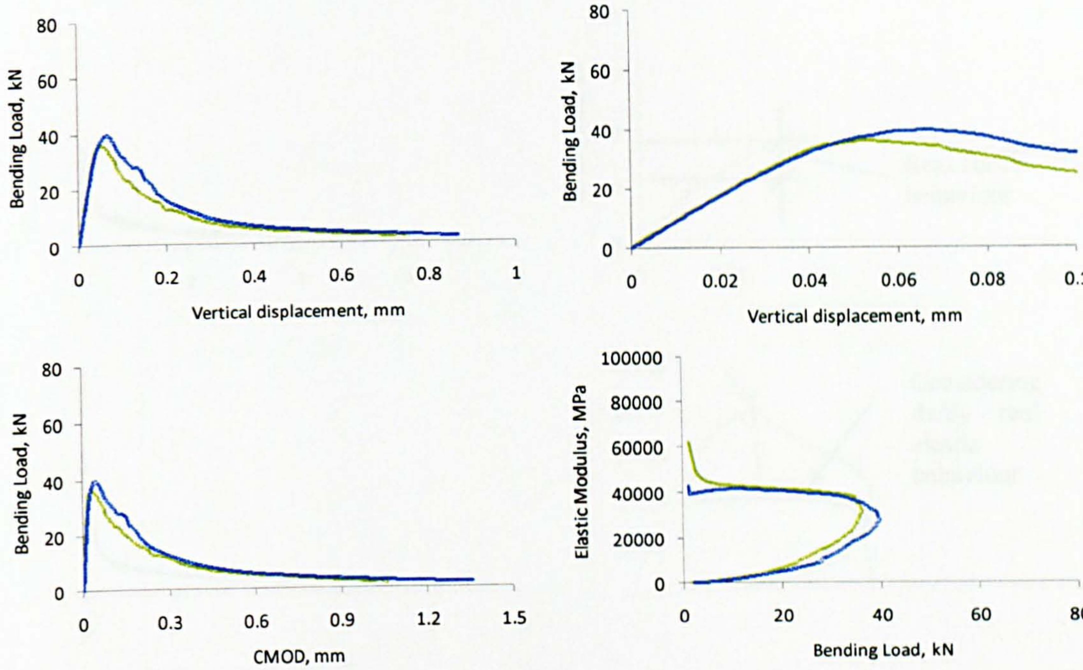

C.1.2.14 R-LEC-2I

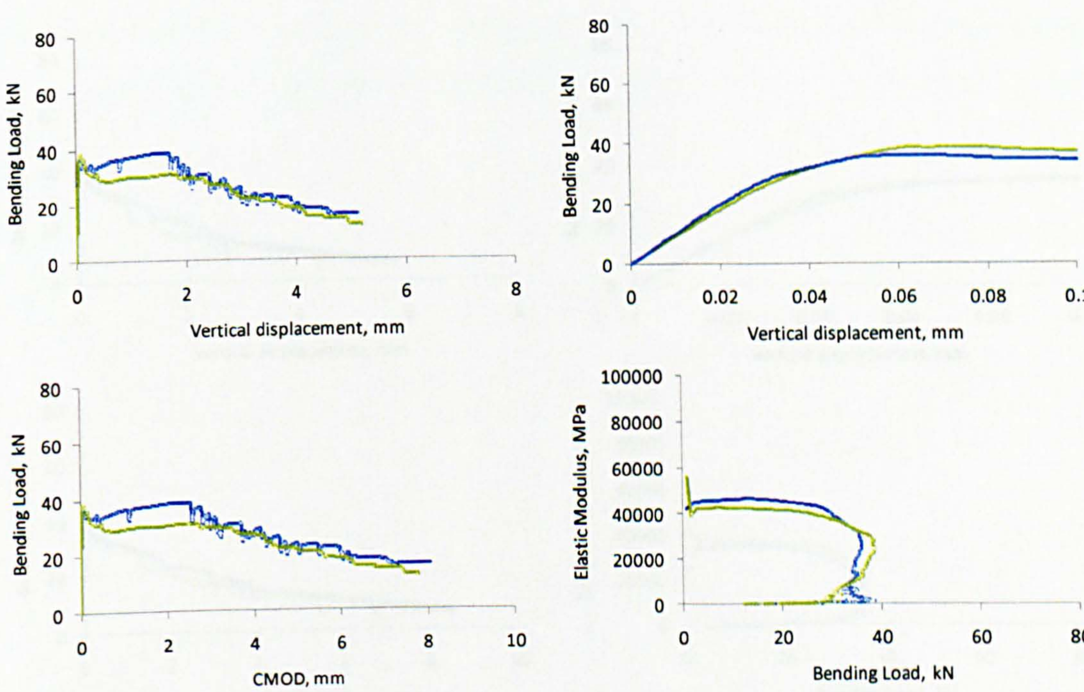

C.1.2.15 R-LEC-2R

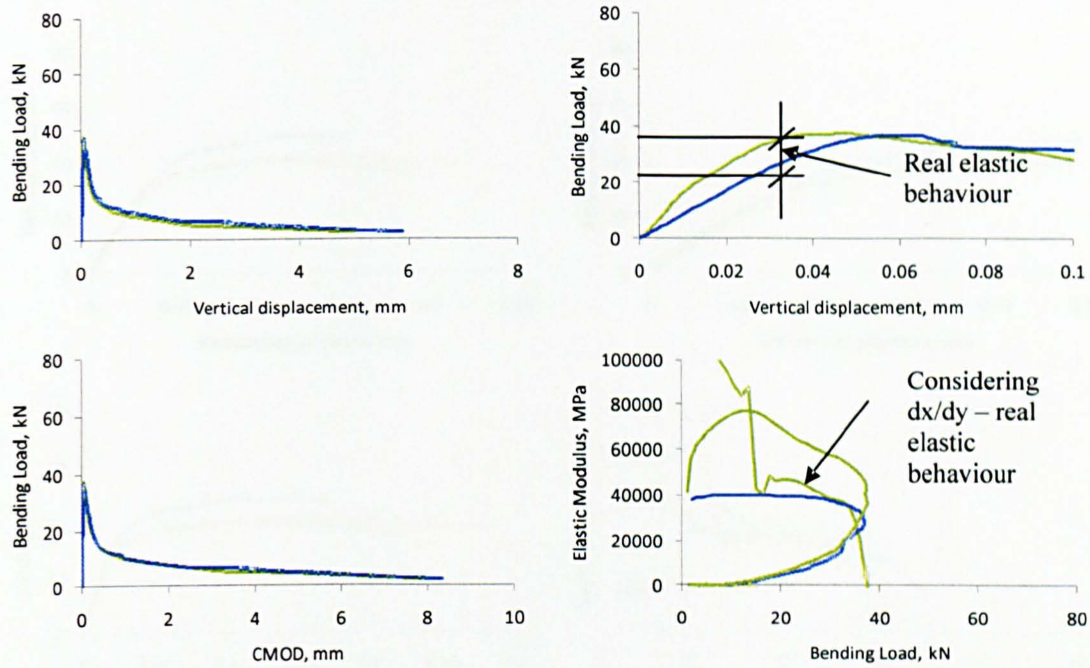

C.1.2.16 R-LEC-6R

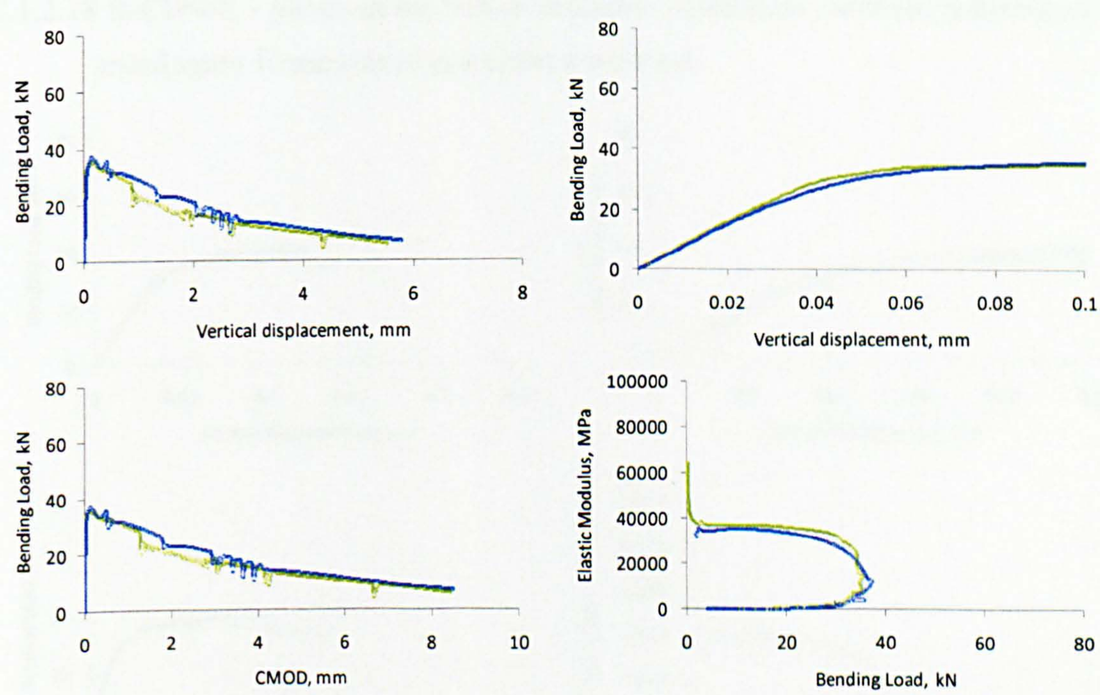

C.1.2.17 R-CIP-6R - pre-cracking before corrosion simulation (ambient temperature) – tested up to 5 months of corrosion simulation

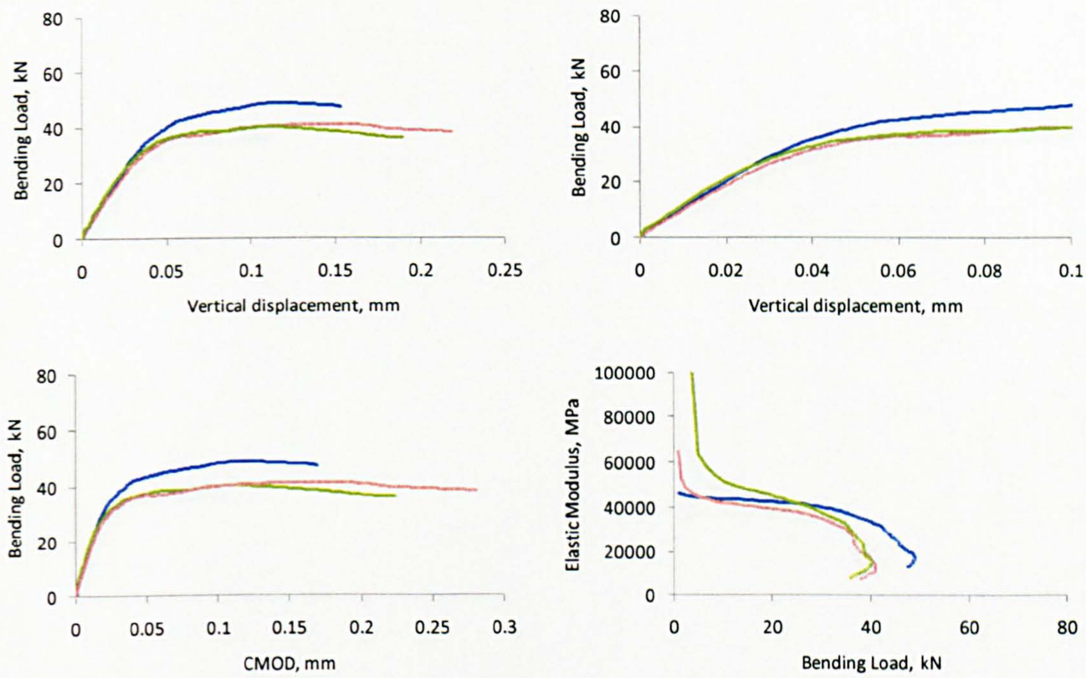

C.1.2.18 R-CIP-6R - pre-cracking before corrosion simulation (ambient temperature) – tested up to 10 months of corrosion simulation

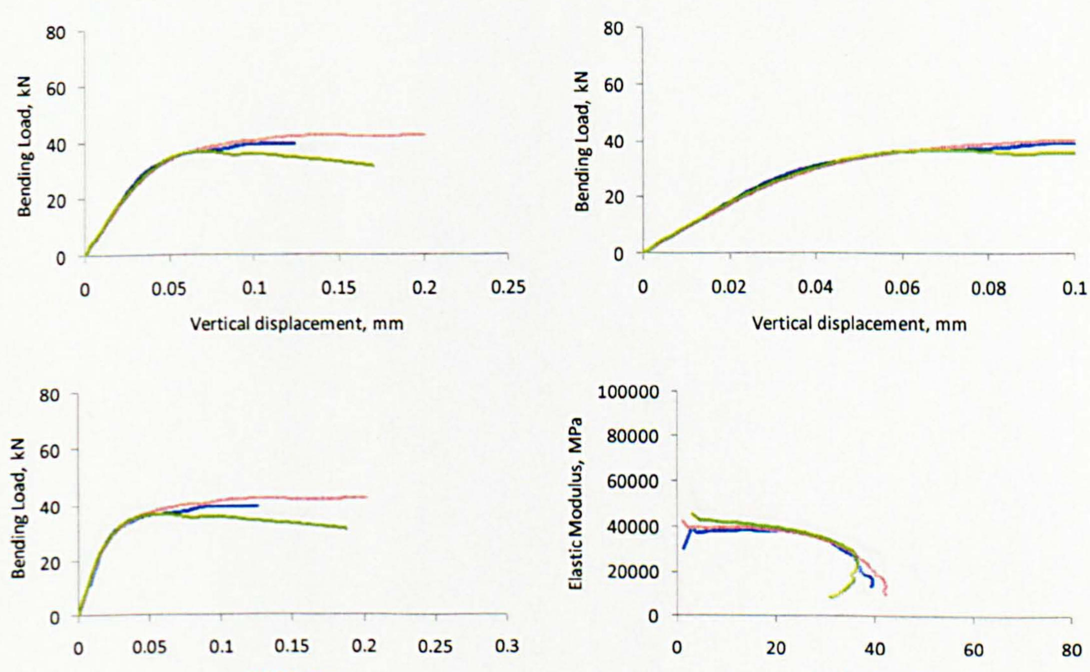

C.1.2.19 R-CIP-6R - pre-cracking before corrosion simulation (40°C) – tested up to 5 months of corrosion simulation

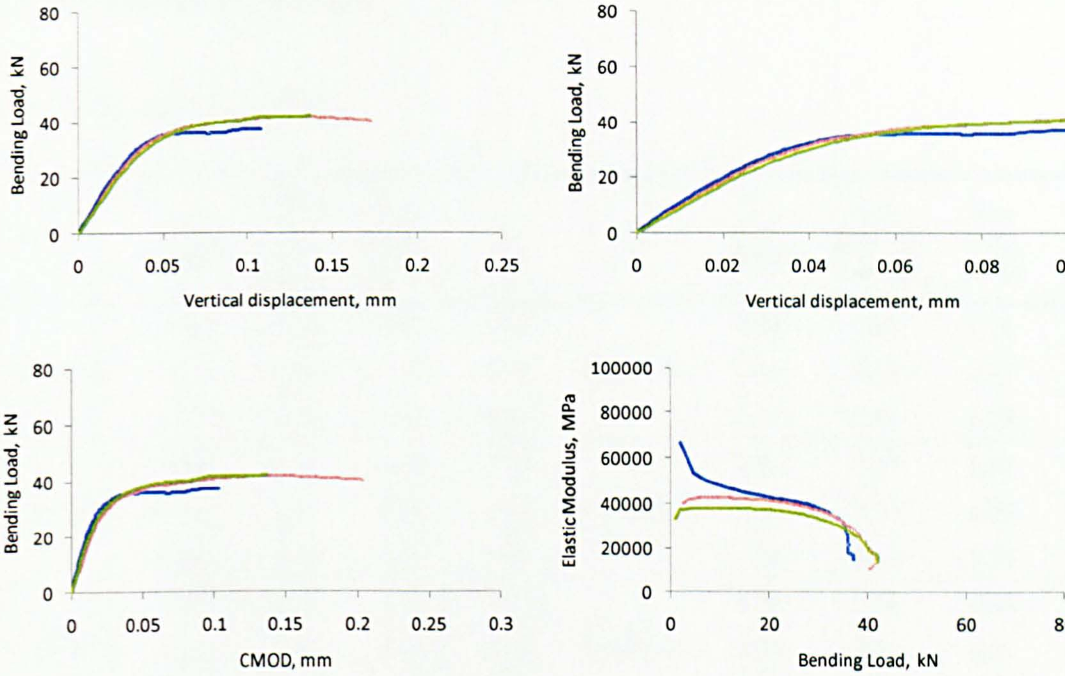

C.1.2.20 R-CIP-6R - pre-cracking before corrosion simulation (40°C) – tested up to 10 months of corrosion simulation

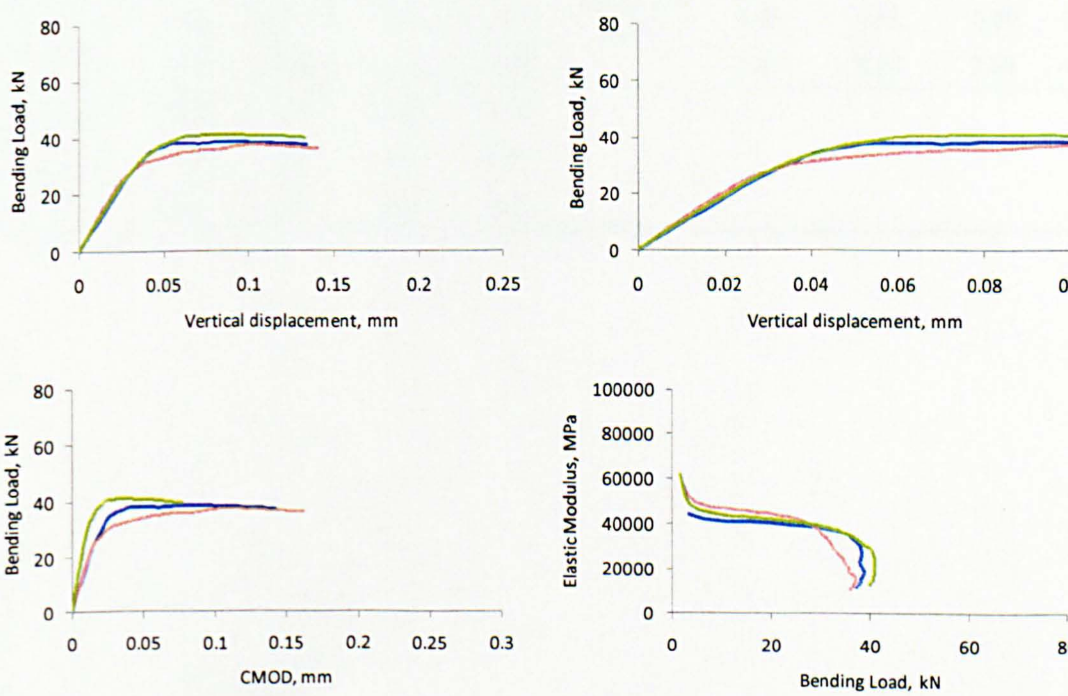

C.2 SPECIMENS EXPOSED TO WET-DRY CYCLES – 5 MONTHS

C.2.1 Flexural properties

C.2.1.1 f_{LOP} and f_{ult} [MPa]

Mix	f_{LOP} (visual)	f_{LOP} (BS EN 14651)	f_{LOP} (Che, 2010)	f_{ult}	Mix	f_{LOP} (visual)	f_{LOP} (BS EN 14651)	f_{LOP} (Che, 2010)	f_{ult}
W-CIP-2I	4.03	5.20	4.76	7.58	R-CIP-2I	4.76	7.87	6.10	9.43
	3.26	4.64	3.51	5.18		4.51	8.59	7.73	13.60
	3.46	6.07	4.62	9.24		4.79	7.70	6.28	9.68
W-CIP-6R	4.22	6.77	6.03	7.17	R-CIP-6R	4.16	7.27	5.62	9.58
	3.46	5.21	4.41	6.64		3.53	7.72	6.27	9.98
	2.88	6.50	4.87	7.02		2.70	6.54	5.22	8.92
W-LEC-2I	4.80	6.74	6.03	11.77	R-LEC-2I	4.03	7.76	6.66	10.40
	5.57	7.16	6.99	12.54		4.22	7.24	6.03	8.35
	4.22	7.02	6.10	14.20		3.21	6.18	4.96	6.55
W-LEC-6R	4.99	7.89	6.67	8.72	R-LEC-6R	4.28	6.13	5.75	7.17
	4.80	8.04	6.71	10.14		4.01	6.56	5.16	7.14
	3.65	7.01	5.86	8.78		3.79	6.91	5.30	7.53
R-CIP-6R pre-cracked	1.95	4.94	2.98	6.96	R-CIP-6R 40 °C	4.97	8.62	6.29	10.56
	1.42	3.73	2.76	6.86		5.48	9.43	7.96	11.36
	1.92	4.69	4.14	9.38		5.21	8.17	7.50	9.90
R-CIP-6R pre-cracked 40 °C	1.30	4.56	3.62	8.71	-				
	1.65	4.91	3.71	8.75					
	1.44	4.91	3.01	7.31					

C.2.1.2 $f_{R,i}$ [MPa] at 0.5 mm, 1.5 mm, 2.5 mm and 3.5 mm

Mix	$F_{R,0.5}$	$F_{R,1.5}$	$F_{R,2.5}$	$F_{R,3.5}$	Mix	$F_{R,0.5}$	$F_{R,1.5}$	$F_{R,2.5}$	$F_{R,3.5}$
W-CIP-2I	7.51	5.88	2.88	1.64	R-CIP-2I	9.12	5.76	4.12	3.01
	4.58	4.61	2.98	1.78		12.79	9.80	5.63	4.18
	9.22	7.24	4.91	3.57		9.40	8.44	5.82	2.93
W-CIP-6R	6.10	4.19	2.82	2.16	R-CIP-6R	9.14	7.47	5.83	4.53
	6.01	4.03	2.96	2.18		8.98	7.66	6.05	4.82
	5.97	3.78	2.57	1.95		8.90	6.26	4.79	3.77
W-LEC-2I	10.61	7.65	2.77	2.86	R-LEC-2I	10.14	10.39	8.87	8.47
	11.66	9.25	7.26	5.14		8.00	8.15	7.50	5.25
	13.34	9.75	3.72	3.80		5.30	6.18	6.05	4.84
W-LEC-6R	8.42	5.66	4.01	2.99	R-LEC-6R	6.44	4.48	2.93	2.00
	9.35	6.61	4.67	3.31		6.45	4.43	3.29	2.40
	8.45	5.36	3.44	2.46		6.72	4.86	3.30	2.32
R-CIP-6R pre-cracked	6.42	4.60	3.43	2.61	R-CIP-6R 40 °C	10.31	7.44	5.46	4.17
	6.72	4.02	2.96	2.17		9.91	8.52	6.45	4.88
	8.68	5.28	3.78	3.03		8.85	6.69	5.64	4.13
R-CIP-6R pre-cracked 40 °C	8.35	5.39	4.07	3.60					
	7.77	5.45	4.14	3.31			-		
	6.90	4.38	3.57	2.88					

C.2.1.3 f_{eq3} [MPa] and $R_{e,3}$

Mix	f_{eq3}	$R_{e,3}$	Mix	f_{eq3}	$R_{e,3}$
W-CIP-2I	4.18	0.81	R-CIP-2I	5.09	0.65
	3.19	0.69		7.46	0.87
	5.42	0.89		5.87	0.76
W-CIP-6R	3.70	0.55	R-CIP-6R	6.72	0.92
	3.38	0.65		6.70	0.87
	3.55	0.55		5.56	0.85
W-LEC-2I	5.56	0.83	R-LEC-2I	9.10	1.17
	7.64	1.07		6.71	0.93
	7.27	1.04		5.43	0.88
W-LEC-6R	4.80	0.61	R-LEC-6R	3.95	0.64
	5.47	0.68		3.92	0.60
	4.46	0.64		4.04	0.59
R-CIP-6R pre-cracked	3.01	0.61	R-CIP-6R 40 °C	7.01	0.81
	3.54	0.95		7.26	0.77
	4.56	0.97		6.10	0.75
R-CIP-6R pre-cracked 40 °C	4.93	1.08			
	4.91	1.00		-	
	4.18	0.85			

C.2.1.4 E [GPa]

Mix	E (1)	E (2)	Mix	E (1)	E (2)
W-CIP-2I	29.2	30.5	R-CIP-2I	41.3	45.1
	31.7	36.4		52.6	53.8
	33.4	34.6		43.6	46.3
W-CIP-6R	33.3	34.9	R-CIP-6R	33.0	34.9
	27.2	28.6		36.9	32.1
	36.3	37.3		32.3	32.3
W-LEC-2I	36.7	38.1	R-LEC-2I	35.4	36.1
	33.0	34.3		38.5	40.0
	39.2	39.2		34.2	35.6
W-LEC-6R	43.8	44.8	R-LEC-6R	26.5	27.0
	40.1	41.8		32.3	34.5
	36.4	37.6		33.8	35.5
R-CIP-6R pre-cracked	41.1	40.4	R-CIP-6R 40 °C	91.6	97.1
	27.0	23.4		41.7	43.1
	26.8	24.1		39.5	41.2
R-CIP-6R pre-cracked 40 °C	28.9	24.0	-		
	33.3	27.9			
	35.9	31.4			

C.2.2 Flexural Curves

C.2.2.1 W-CIP-2I

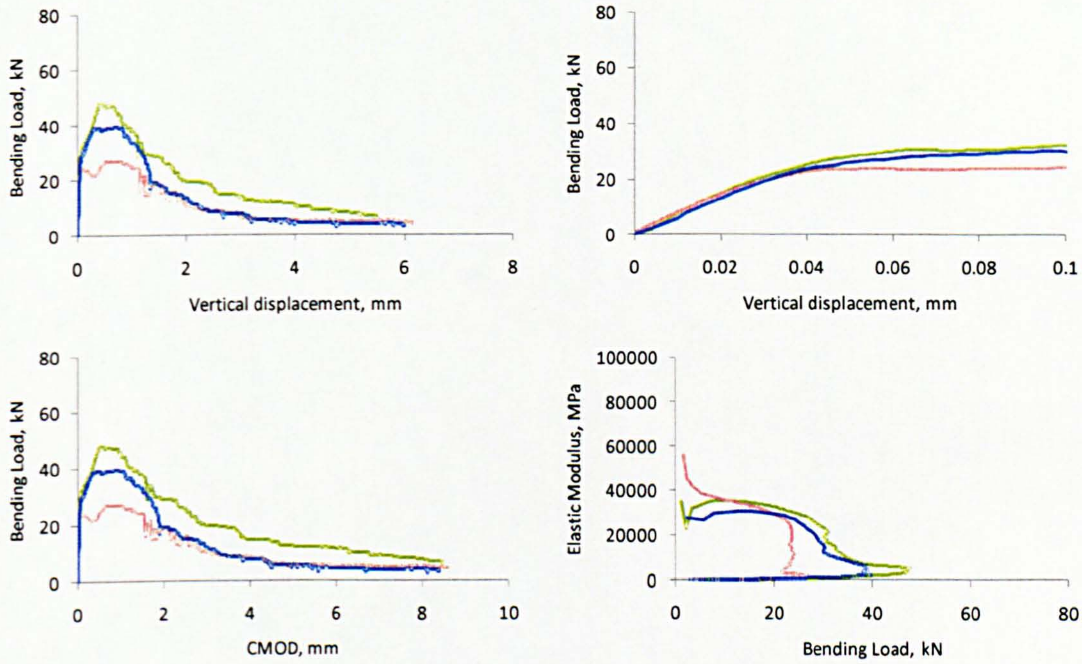

C.2.2.2 W-CIP-6R

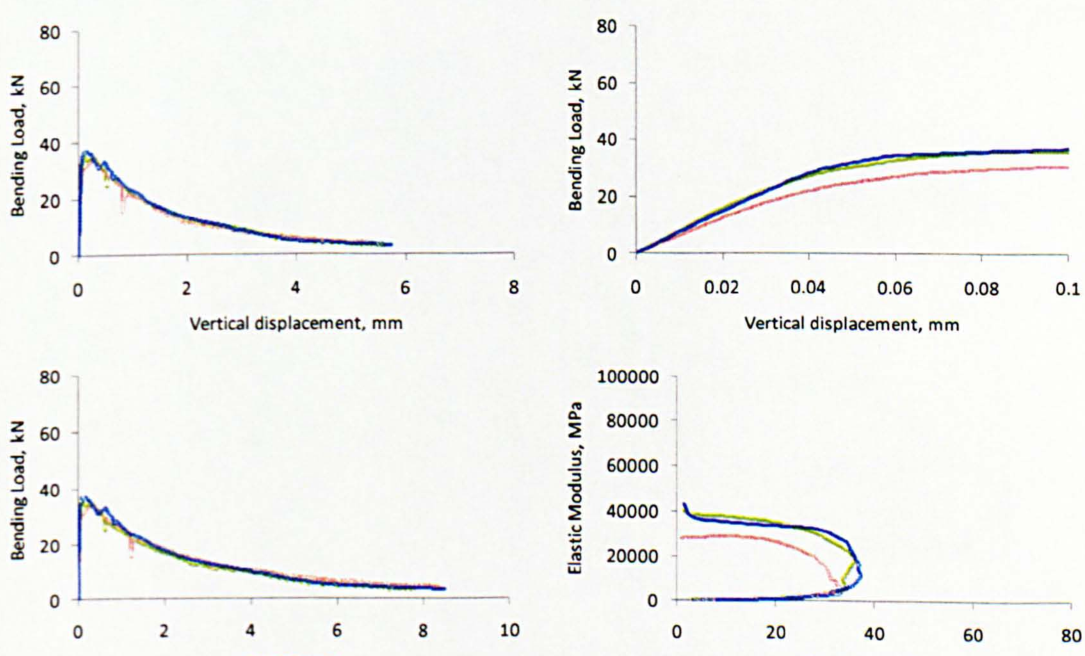

C.2.2.3 W-LEC-2I

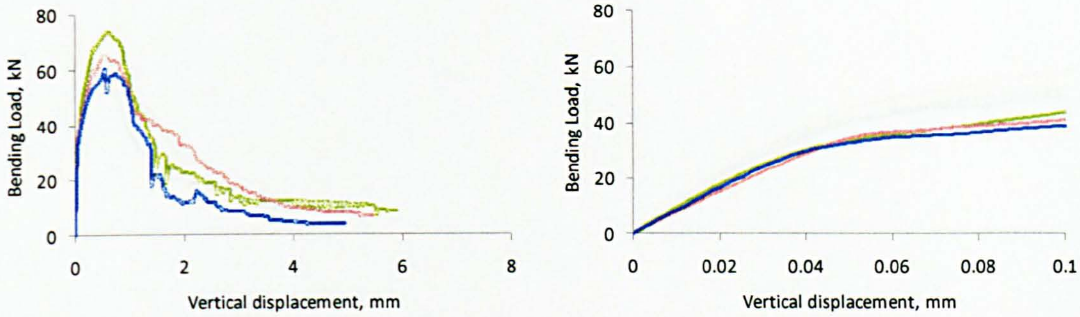

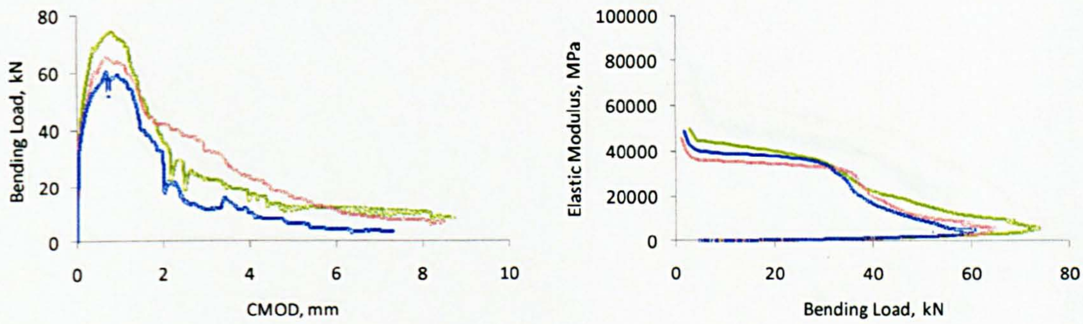

C.2.2.4 W-LEC-6R

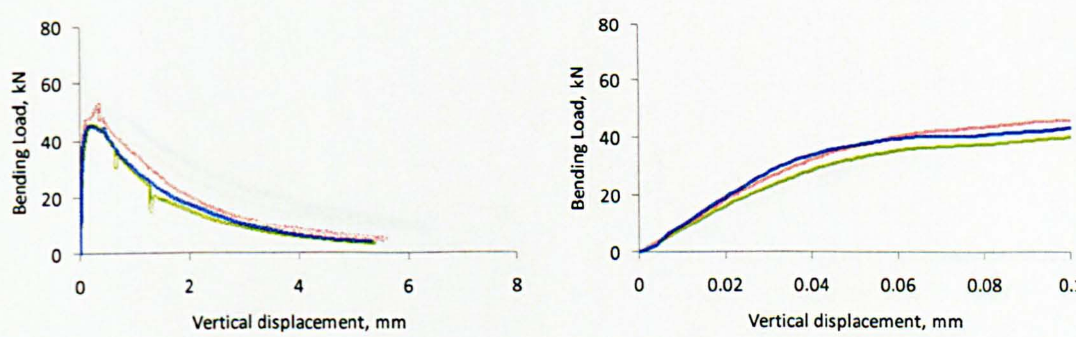

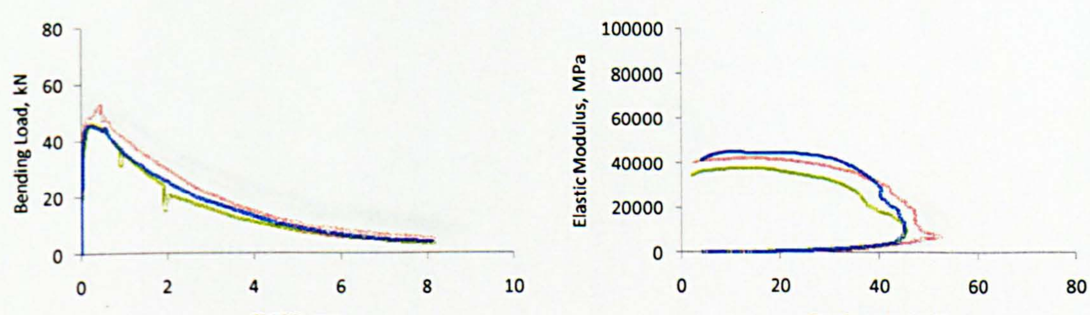

C.2.2.5 R-CIP-2I

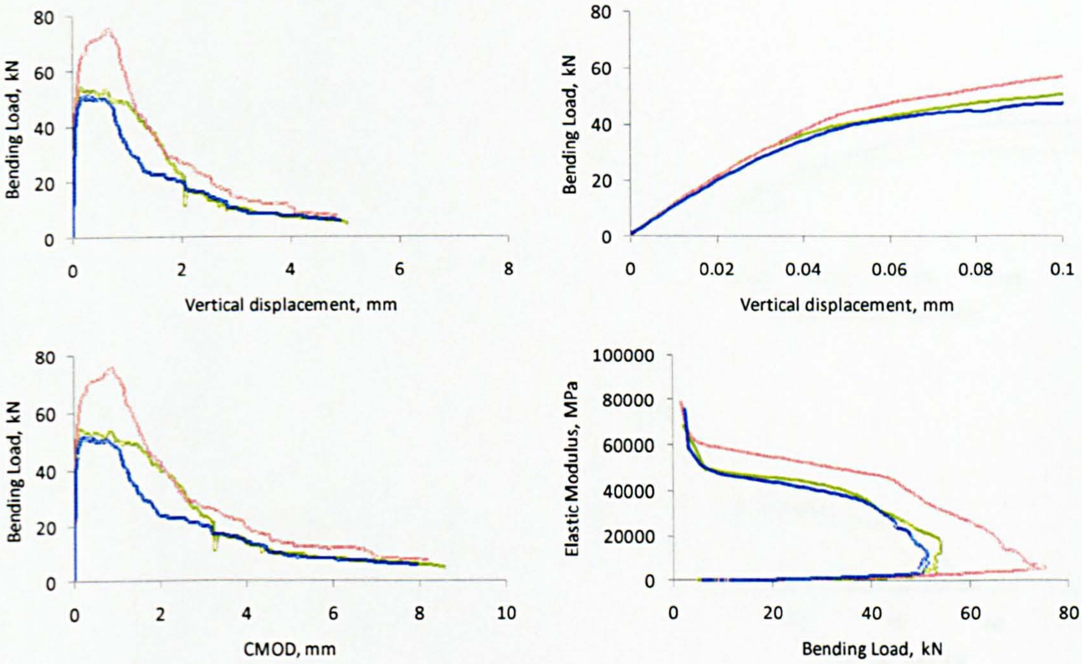

C.2.2.6 R-CIP-6R

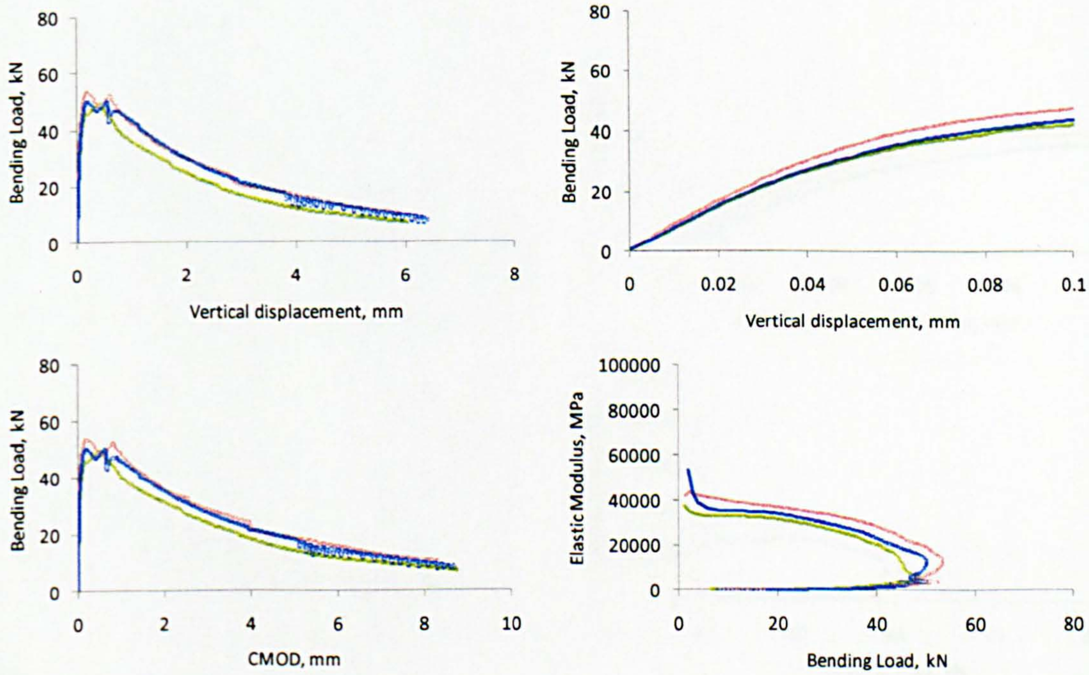

C.2.2.7 R-LEC-2I

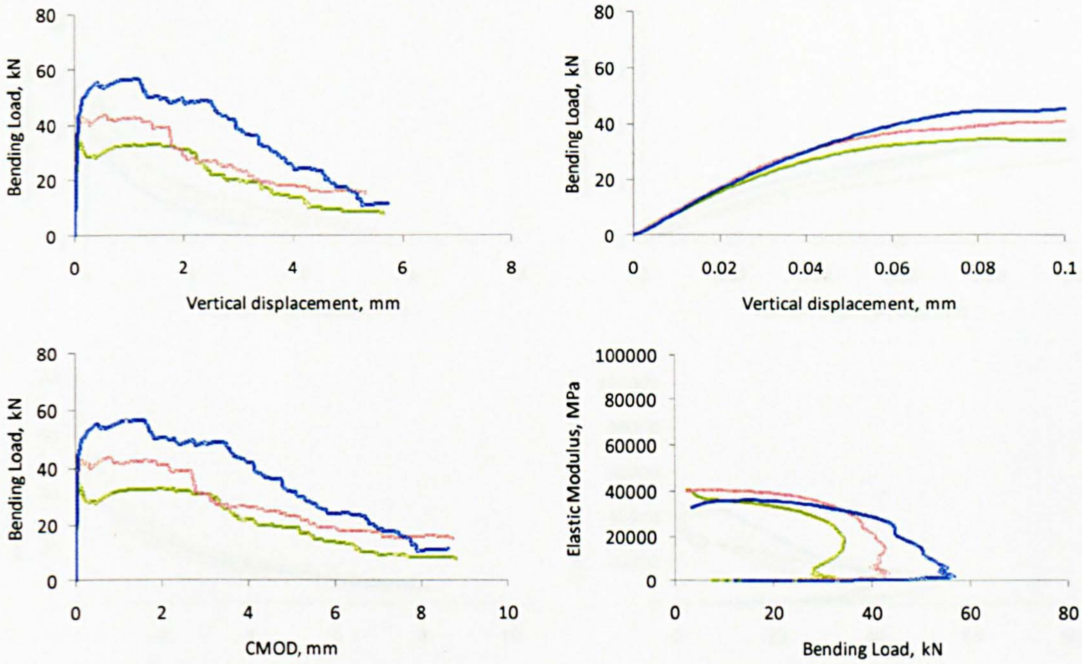

C.2.2.8 R-LEC-6R

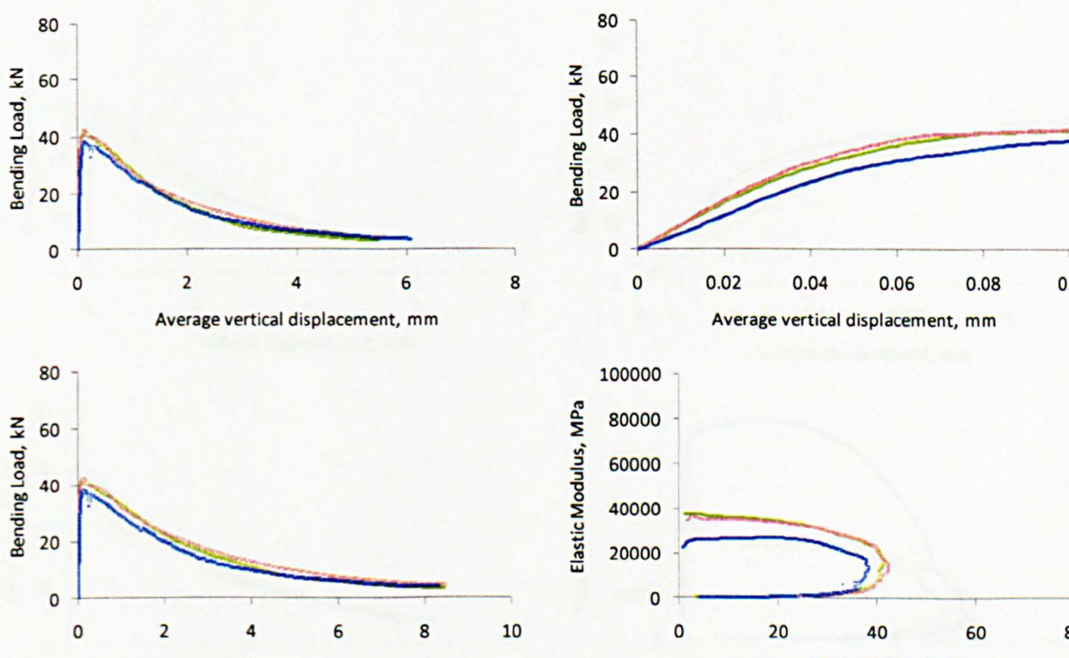

C.2.2.9 R-CIP-6R, PRE-CRACKED

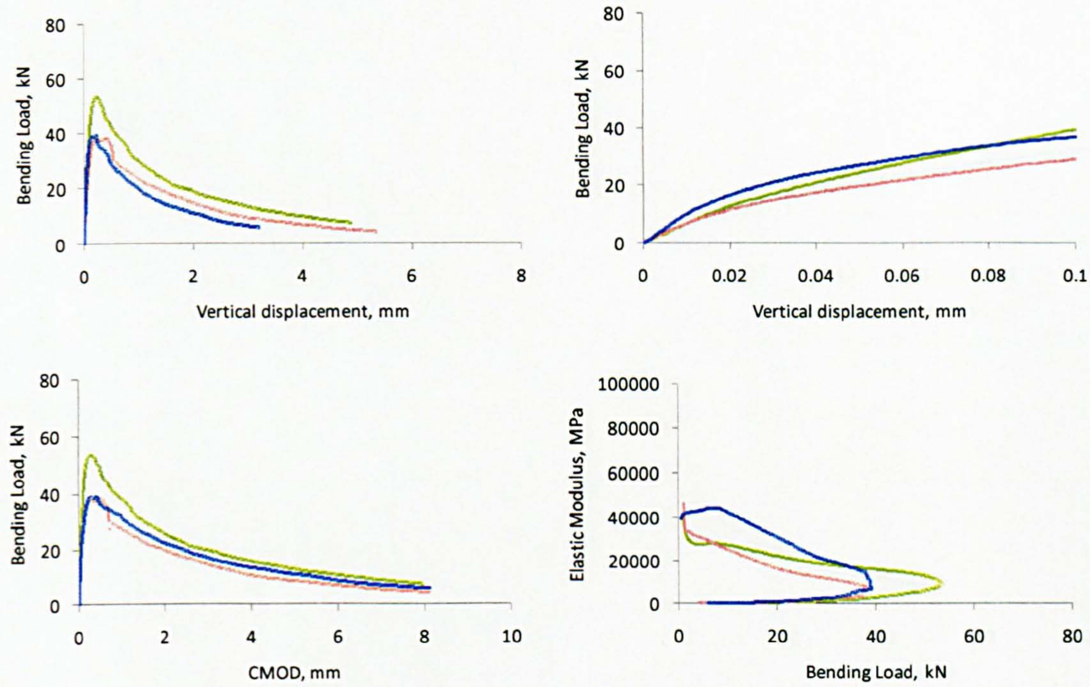

C.2.2.10 R-CIP-6R, 40°C

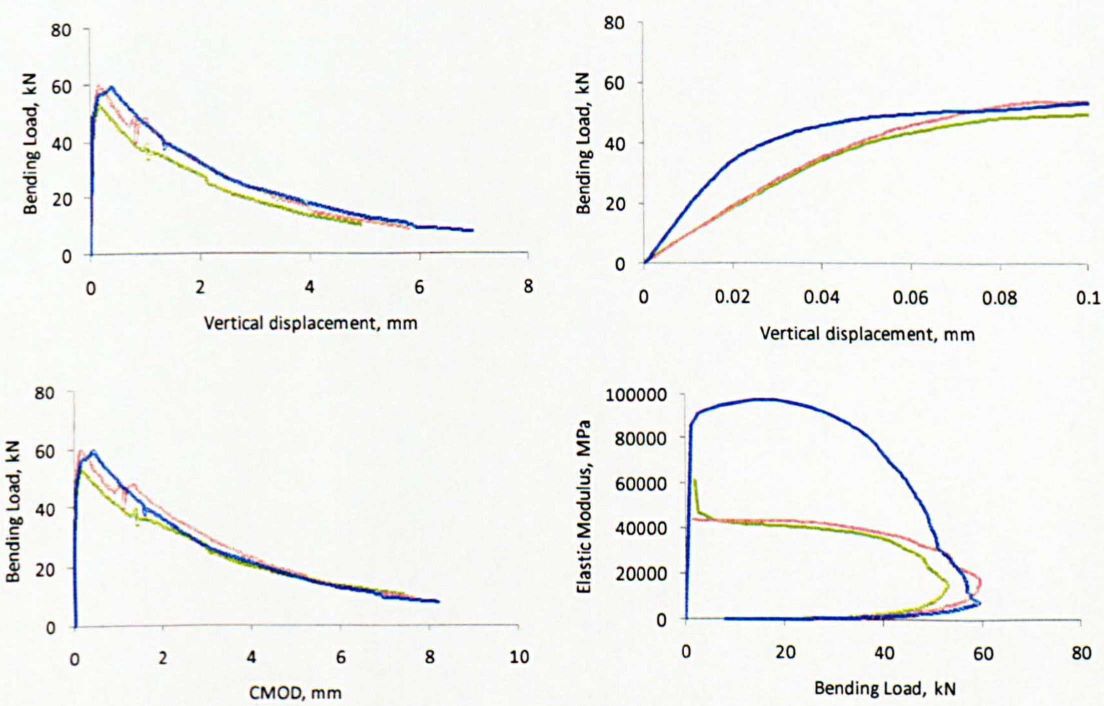

C.2.2.11 R-CIP-6R, PRE-CRACKED, 40ºC

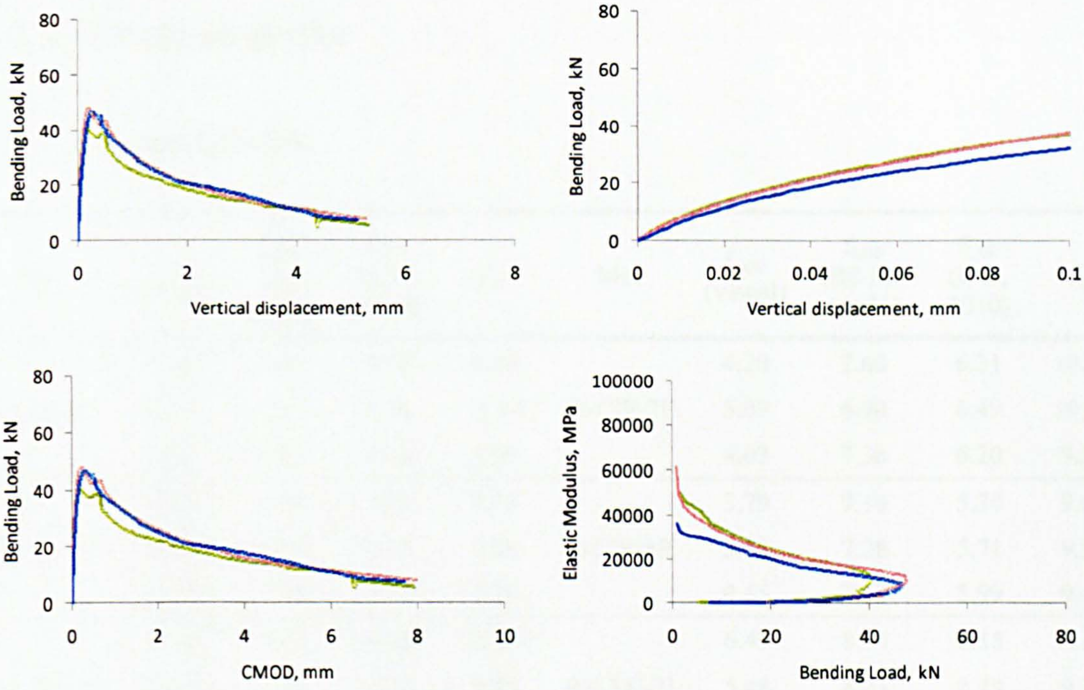

C.3 SPECIMENS EXPOSED TO WET-DRY CYCLES – 10 MONTHS

C.3.1 Flexural properties

C.3.1.1 f_{LOP} and f_{ult} [MPa]

Mix	f_{LOP} (visual)	f_{LOP} (BS EN 14651)	f_{LOP} (Che, 2010)	f_{ult}	Mix	f_{LOP} (visual)	f_{LOP} (BS EN 14651)	f_{LOP} (Che, 2010)	f_{ult}
W-CIP-2I	3.46	5.52	4.03	6.95	R-CIP-2I	4.20	7.60	6.31	10.43
	2.88	6.13	4.88	11.34		5.09	6.90	6.49	10.46
	3.26	5.41	4.18	8.09		4.07	7.36	6.20	9.30
W-CIP-6R	3.26	6.18	4.69	7.73	R-CIP-6R	3.79	7.19	5.30	9.67
	3.84	6.36	5.03	7.28		3.55	7.28	5.71	9.31
	4.22	7.08	5.72	7.70		4.65	7.30	5.99	9.46
W-LEC-2I	6.14	7.20	6.85	11.26	R-LEC-2I	6.49	8.94	8.15	11.03
	5.95	7.91	7.64	8.85		5.48	8.23	8.49	9.14
	6.53	8.21	7.89	9.00		6.44	7.87	7.07	8.75
W-LEC-6R	6.53	8.03	7.78	8.84	R-LEC-6R	4.79	7.06	6.62	7.58
	6.91	9.15	8.41	9.34		4.94	7.21	6.99	7.45
	5.76	9.00	8.35	10.43		5.58	7.44	6.75	8.17
R-CIP-6R pre-cracked	2.30	4.37	2.81	6.24	R-CIP-6R 40 °C	4.99	7.94	6.84	10.78
	1.89	3.99	2.62	6.20		3.95	7.27	6.42	9.15
	2.31	5.01	3.18	7.70		4.84	6.39	6.70	8.84
R-CIP-6R pre-cracked 40 °C	1.42	4.69	2.94	7.84					
	2.34	5.25	3.52	8.05			-		
	2.16	4.87	3.03	7.59					

C.3.1.2 $f_{R,i}$ [MPa] at 0.5 mm, 1.5 mm, 2.5 mm and 3.5 mm

Mix	$F_{R,0.5}$	$F_{R,1.5}$	$F_{R,2.5}$	$F_{R,3.5}$	Mix	$F_{R,0.5}$	$F_{R,1.5}$	$F_{R,2.5}$	$F_{R,3.5}$
W-CIP-2I	6.75	5.25	2.64	2.04	R-CIP-2I	9.01	6.21	5.04	3.46
	10.11	4.80	4.57	2.32		9.90	6.50	4.20	3.31
	7.82	5.76	3.49	1.44		8.23	5.87	3.57	2.62
W-CIP-6R	6.97	4.45	2.66	1.83	R-CIP-6R	9.35	6.77	4.69	3.89
	5.24	4.78	2.54	2.27		8.66	6.40	4.87	3.65
	6.92	4.07	2.93	2.19		8.51	6.74	5.03	3.80
W-LEC-2I	9.97	9.34	3.48	1.68	R-LEC-2I	10.53	9.88	7.80	7.63
	8.64	4.56	2.55	1.12		8.27	7.81	6.03	6.86
	8.81	6.24	2.99	1.51		8.50	7.86	5.84	4.45
W-LEC-6R	8.02	5.31	3.82	2.90	R-LEC-6R	6.27	4.44	3.17	2.41
	8.08	5.38	3.97	2.26		4.80	3.32	2.39	1.87
	10.37	6.92	3.91	3.92		5.84	3.75	2.70	1.88
R-CIP-6R pre-cracked	5.69	4.22	3.22	2.65	R-CIP-6R 40 °C	10.00	6.98	5.02	3.73
	5.47	3.91	2.89	2.16		8.51	6.07	4.64	3.11
	7.41	5.80	4.13	3.05		8.35	6.71	5.19	4.02
R-CIP-6R pre-cracked 40 °C	7.74	5.50	3.60	3.49					
	7.57	4.39	4.00	3.25			-		
	7.31	5.11	3.72	2.89					

C.3.1.3 f_{eq3} [MPa] and $R_{e,3}$

Mix	f_{eq3}	$R_{e,3}$	Mix	f_{eq3}	$R_{e,3}$
W-CIP-2I	3.22	0.58	R-CIP-2I	5.85	0.77
	4.94	0.81		5.40	0.78
	4.07	0.75		4.63	0.63
W-CIP-6R	3.58	0.58	R-CIP-6R	5.85	0.81
	3.90	0.61		5.79	0.80
	3.99	0.56		5.64	0.77
W-LEC-2I	5.62	0.71	R-LEC-2I	8.72	0.98
	4.13	0.52		7.38	0.90
	4.53	0.55		6.08	0.77
W-LEC-6R	4.95	0.62	R-LEC-6R	3.99	0.57
	4.87	0.53		2.93	0.41
	6.05	0.67		3.54	0.48
R-CIP-6R pre-cracked	3.90	0.89	R-CIP-6R 40 °C	6.19	0.78
	3.56	0.89		5.19	0.71
	4.79	0.96		5.91	0.93
R-CIP-6R pre-cracked 40 °C	4.69	1.00			
	4.57	0.87		-	
	4.47	0.92			

C.3.1.4 E [GPa]

Mix	E (Approach 1)	E (Approach 2)	Mix	E (Approach 1)	E (Approach 2)
W-CIP-2I	68.7	75.3	R-CIP-2I	40.0	41.5
	37.5	36.1		36.4	38.1
	33.0	29.6		37.8	39.6
W-CIP-6R	33.0	34.1	R-CIP-6R	39.0	39.4
	36.1	38.9		43.0	44.6
	34.2	36.6		37.2	39.1
W-LEC-2I	37.0	38.4	R-LEC-2I	39.2	42.3
	41.8	44.1		37.5	40.4
	42.0	43.7		33.6	36.2
W-LEC-6R	38.9	40.0	R-LEC-6R	36.3	39.0
	44.7	47.3		37.5	38.9
	45.8	48.6		32.5	33.4
R-CIP-6R pre-cracked	34.1	35.5	R-CIP-6R 40 °C	39.7	42.4
	30.5	30.5		37.0	38.6
	36.4	36.4		32.1	32.3
R-CIP-6R pre-cracked 40 °C	45.4	36.8			
	39.6	39.1		-	
	40.2	39.8			

C.3.2 Flexural Curves

C.3.2.1 W-CIP-2I

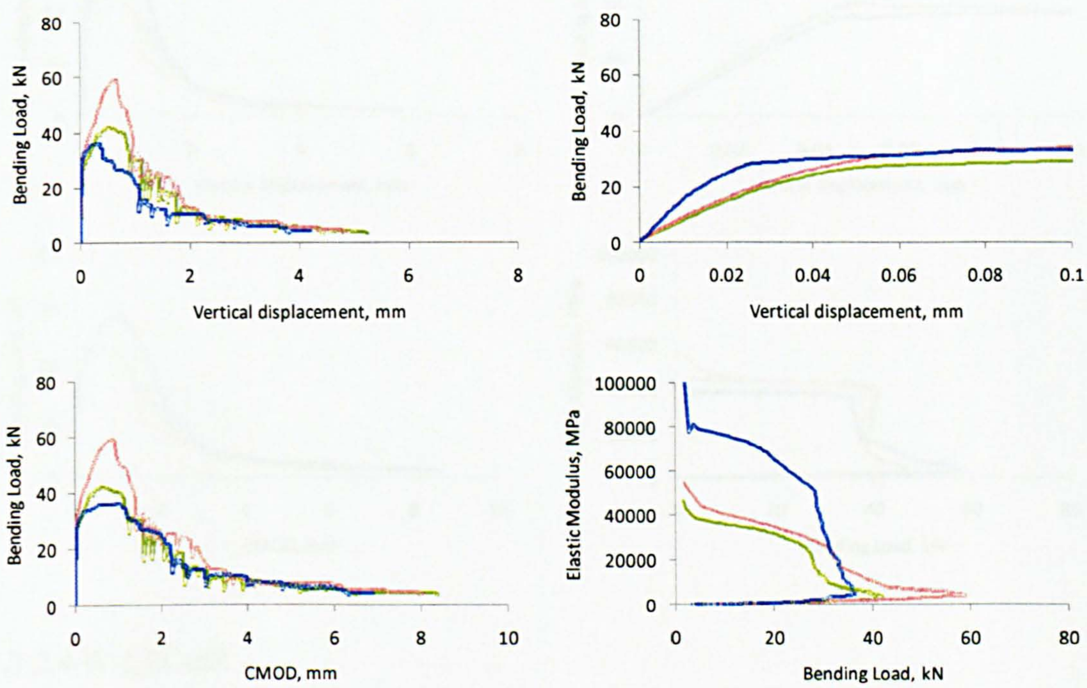

C.3.2.2 W-CIP-6R

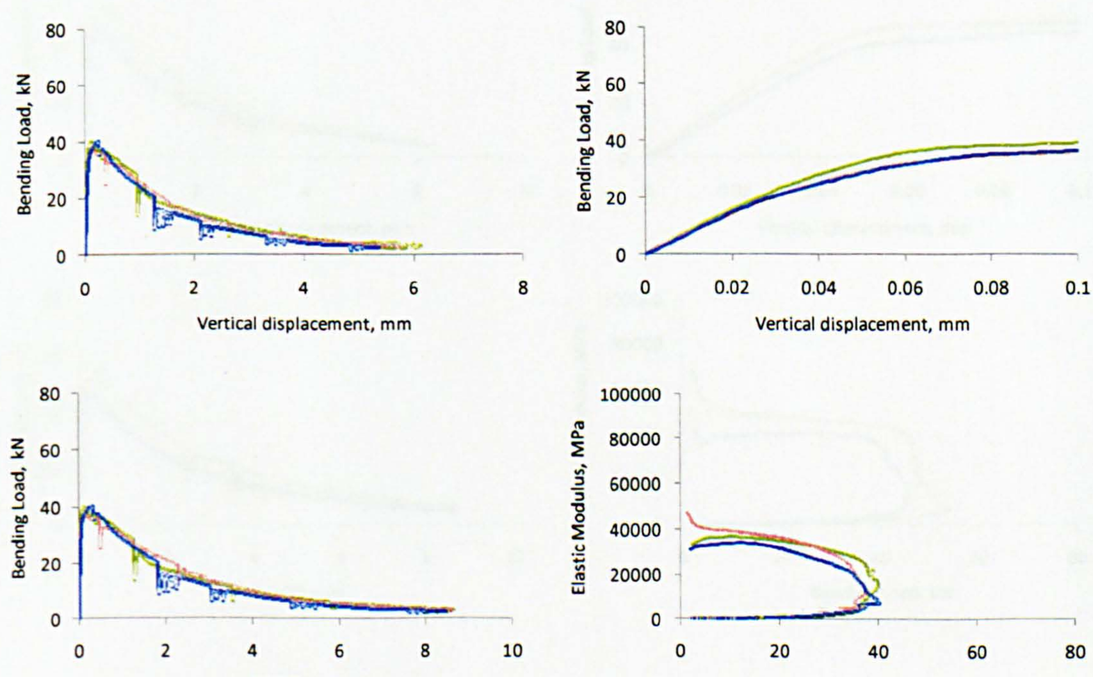

C.3.2.3 W-LEC-2I

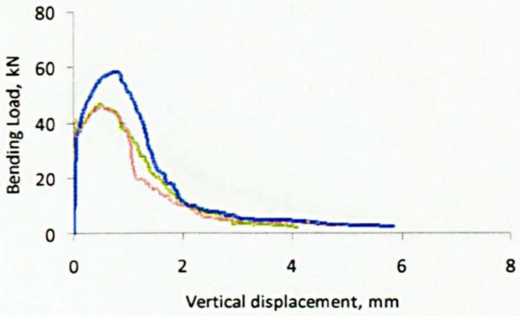

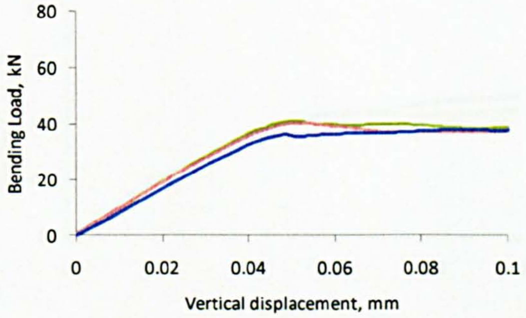

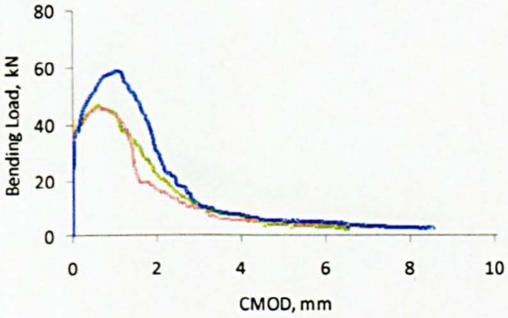

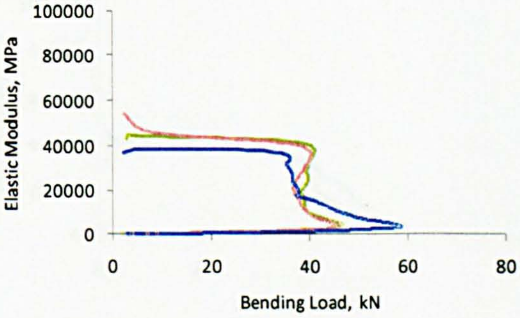

C.3.2.4 W-LEC-6R

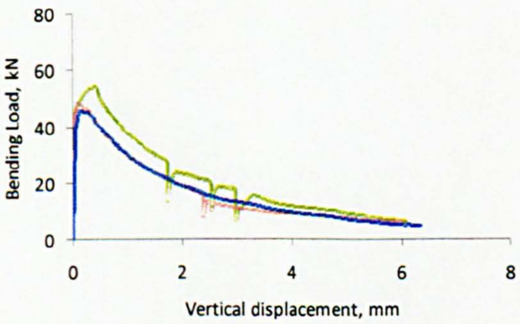

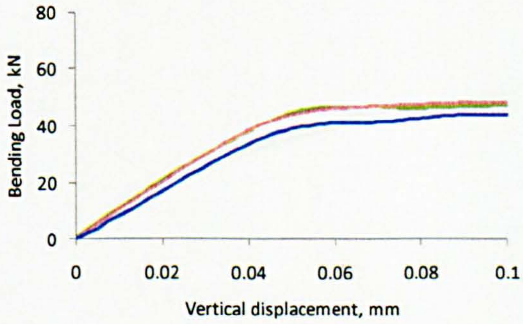

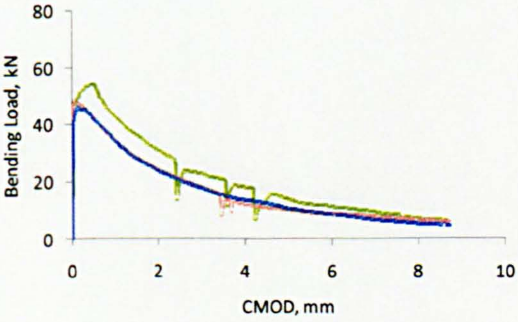

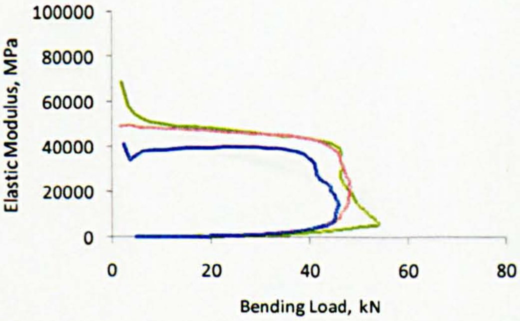

C.3.2.5 R-CIP-2I

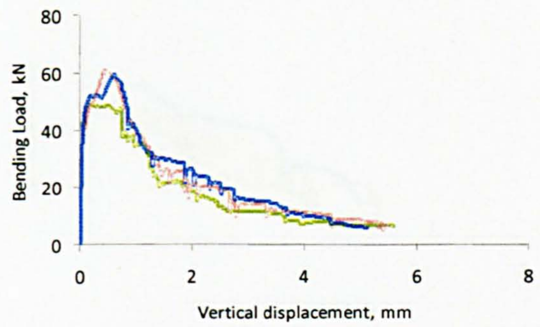

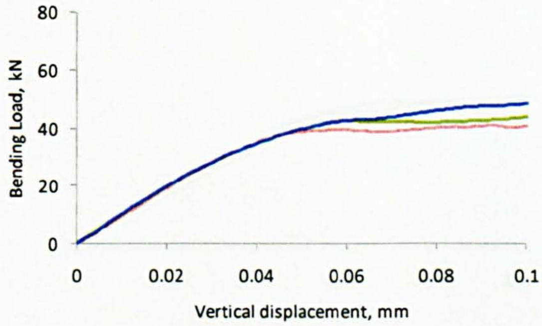

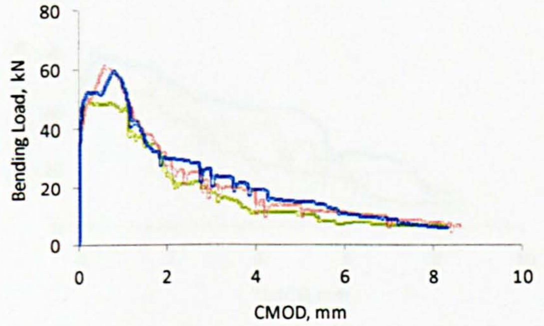

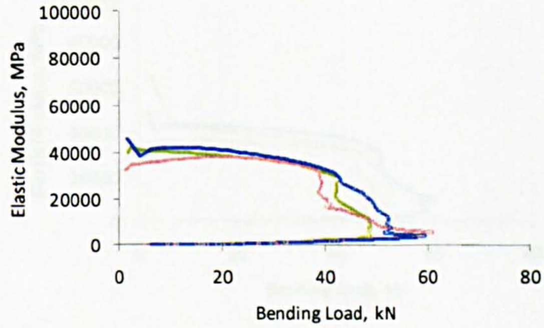

C.3.2.6 R-CIP-6R

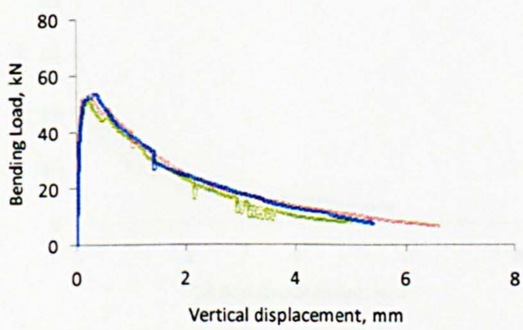

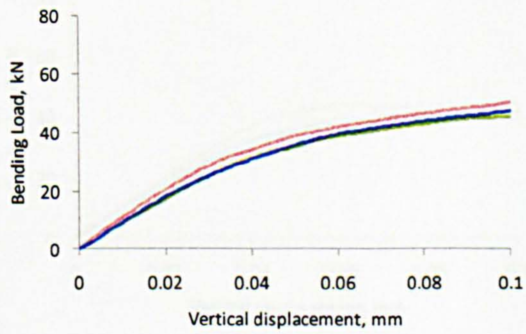

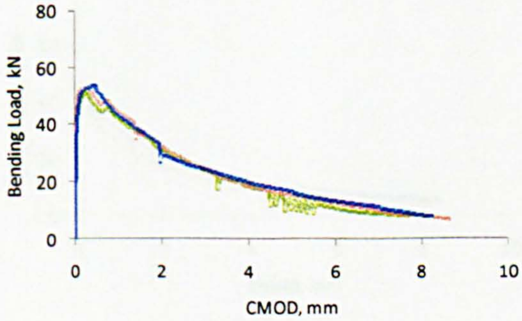

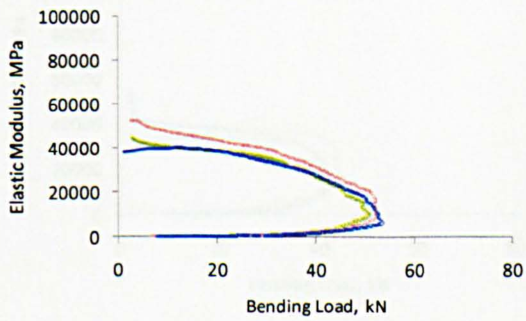

C.3.2.7 R-LEC-2I

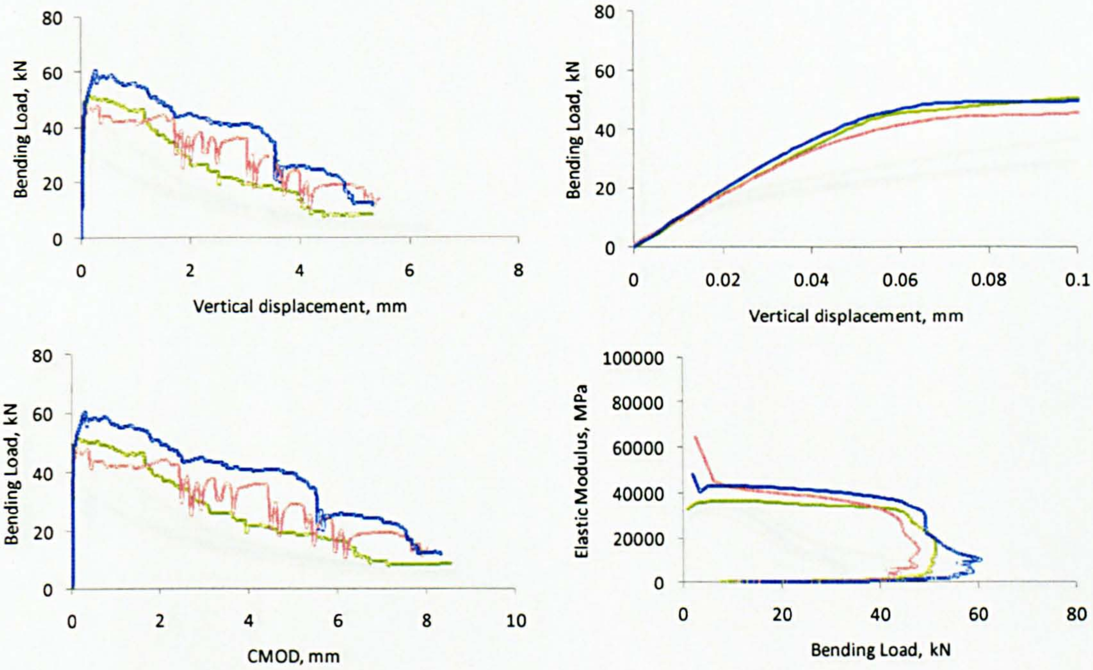

C.3.2.8 R-LEC-6R

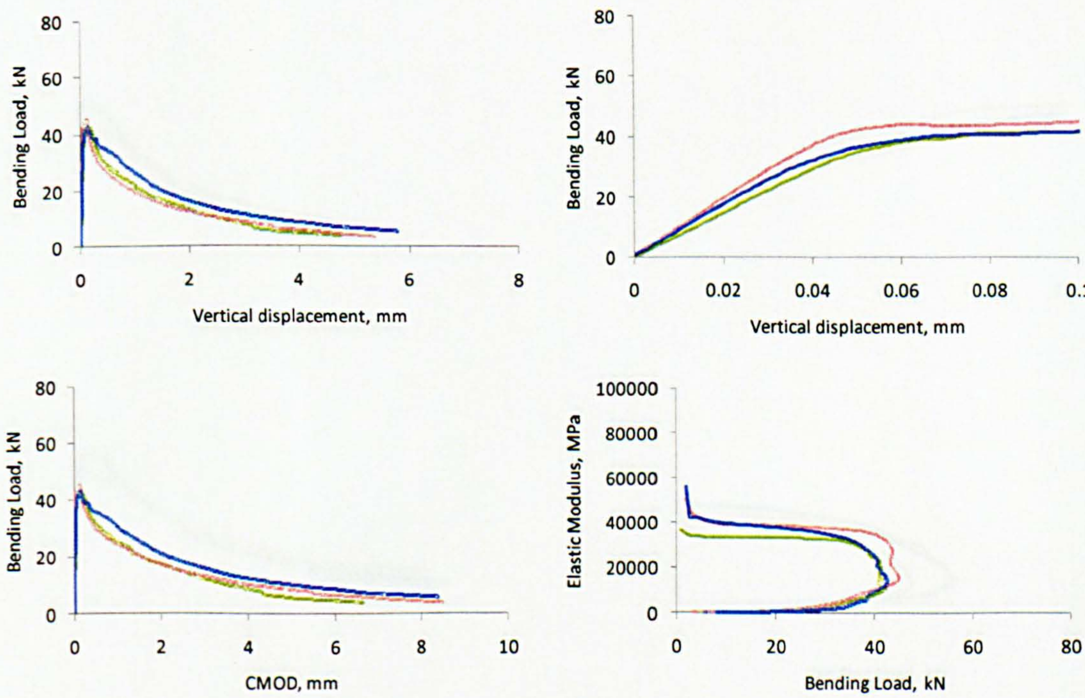

C.3.2.9 R-CIP-6R, PRE-CRACKED

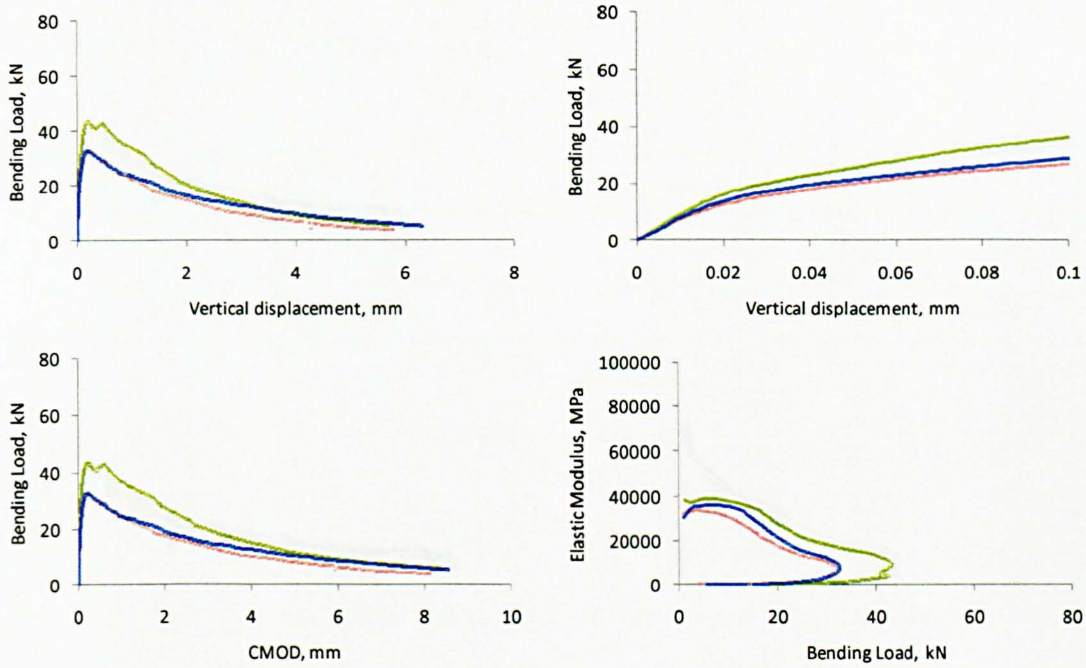

C.3.2.10 R-CIP-6R, 40°C

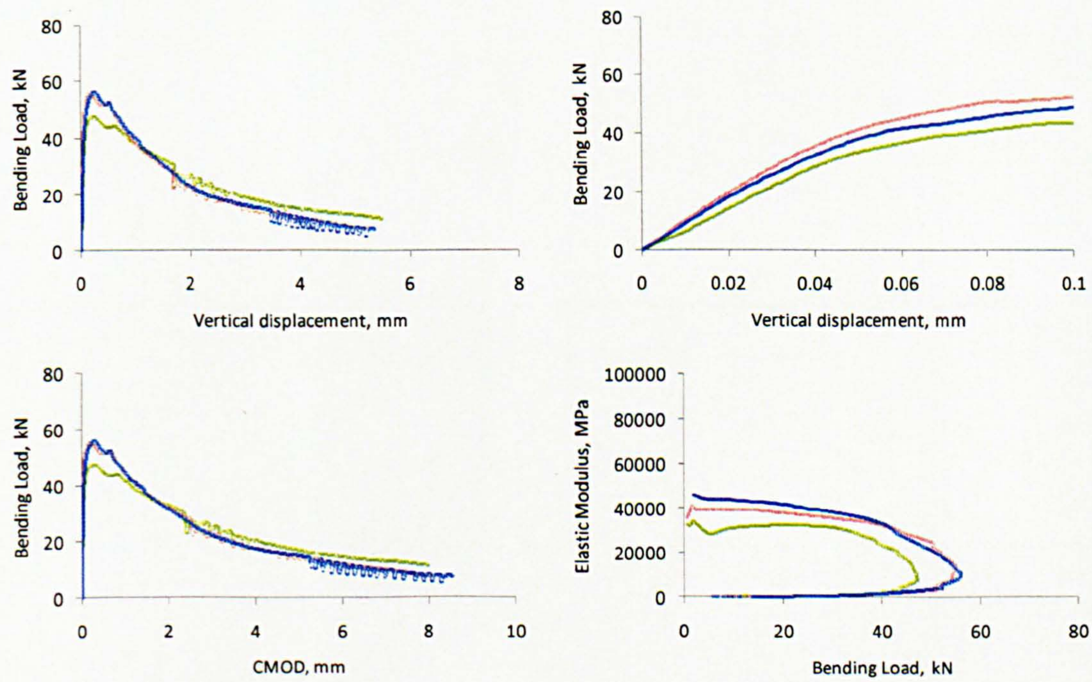

C.3.2.11 R-CIP-6R, PRE-CRACKED, 40ºC

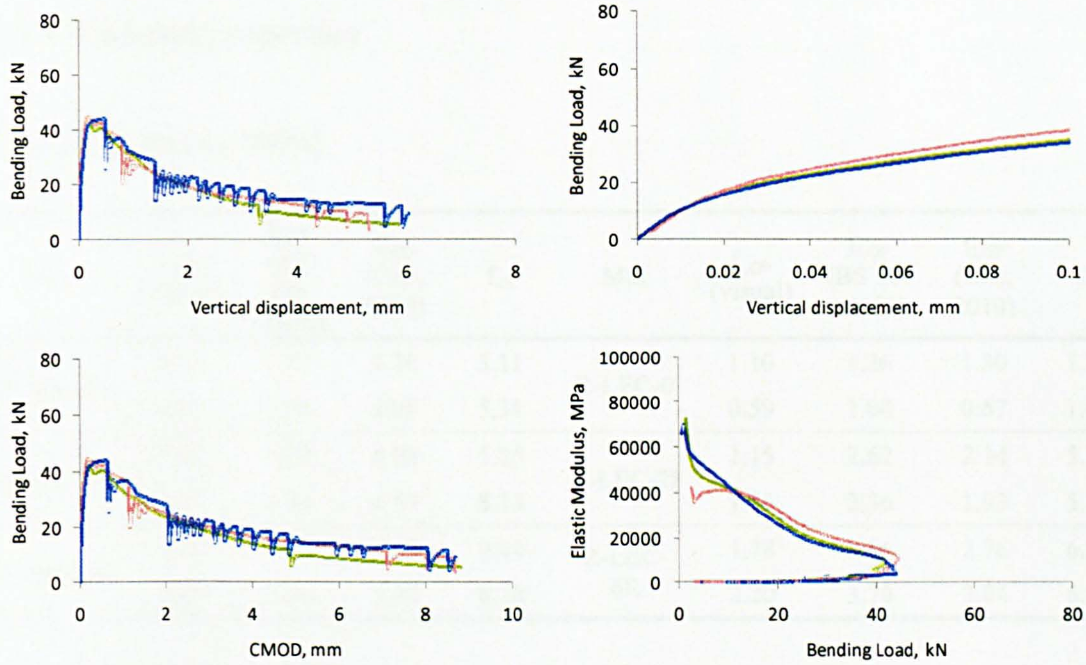

C.4 SPECIMENS EXPOSED TO FREEZE-THAW CYCLES

C.4.1 Flexural properties

C.4.1.1 f_{LOP} and f_{ult} [MPa]

Mix	f_{LOP} (visual)	f_{LOP} (BS EN 14651)	f_{LOP} (Che, 2010)	f_{ult}	Mix	f_{LOP} (visual)	f_{LOP} (BS EN 14651)	f_{LOP} (Che, 2010)	f_{ult}
W-LEC-0	4.03	5.11	4.36	5.11	R-LEC-0	1.10	1.26	1.30	1.74
	4.03	5.31	4.99	5.31		0.59	1.00	0.67	1.45
W-LEC-2I	3.84	5.25	4.98	5.25	R-LEC-2I	1.15	2.62	2.14	5.30
	4.61	5.44	4.57	8.15		1.15	2.36	1.93	5.13
W-LEC-6R	3.84	7.04	5.09	9.44	R-LEC-6R	1.78	3.66	2.76	6.24
	3.46	5.74	4.42	8.28		2.20	3.70	3.04	6.75

C.4.1.2 $f_{R,i}$ [MPa] at 0.5 mm, 1.5 mm, 2.5 mm and 3.5 mm

Mix	$F_{R,0.5}$	$F_{R,1.5}$	$F_{R,2.5}$	$F_{R,3.5}$	Mix	$F_{R,0.5}$	$F_{R,1.5}$	$F_{R,2.5}$	$F_{R,3.5}$
W-LEC-2I	3.82	2.09	1.12	0.85	R-LEC-2I	4.91	5.28	4.95	4.32
	7.45	3.45	1.29	1.40		4.74	4.51	4.67	4.13
W-LEC-6R	9.27	6.54	2.43	3.46	R-LEC-6R	6.14	5.21	4.01	3.20
	8.18	5.98	4.26	3.16		6.39	5.45	4.27	3.30

C.4.1.3 f_{eq3} [MPa] and $R_{e,3}$

Mix	f_{eq3}	$R_{e,3}$	Mix	f_{eq3}	$R_{e,3}$
W-LEC-2I	2.06	0.39	R-LEC-2I	4.51	1.73
	3.35	0.62		4.42	1.88
W-LEC-6R	5.60	0.80	R-LEC-6R	4.33	1.18
	5.09	0.89		4.69	1.27

C.4.1.4 E [GPa]

Mix	E (Approach 1)	E (Approach 2)	Mix	E (Approach 1)	E (Approach 2)
W-LEC-0	35.0	39.3	R-LEC-0	3.3	3.5
	37.2	39.7		6.4	7.0
W-LEC-2I	45.3	46.8	R-LEC-2I	16.3	14.2
	42.6	45.5		12.2	10.5
W-LEC-6R	37.2	38.9	R-LEC-6R	22.8	21.9
	33.9	36.1		20.2	20.3

C.4.2 Flexural Curves

C.4.2.1 W-LEC-0

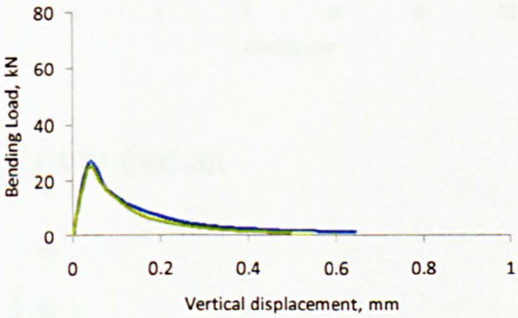

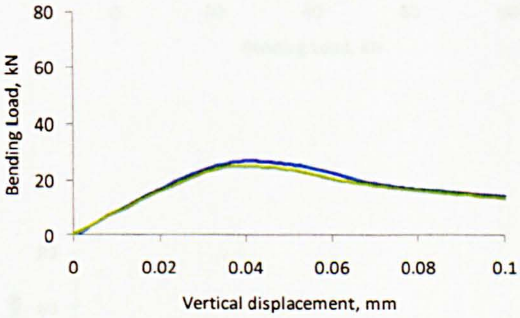

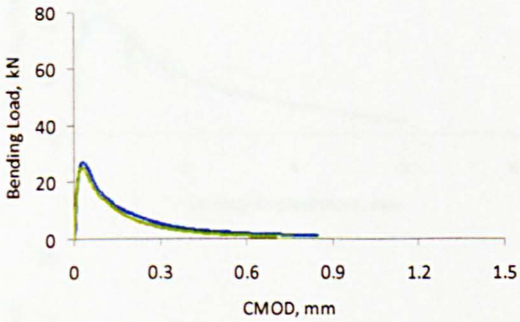

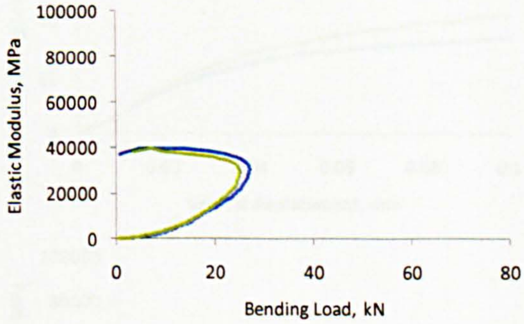

C.4.2.2 W-LEC-2I

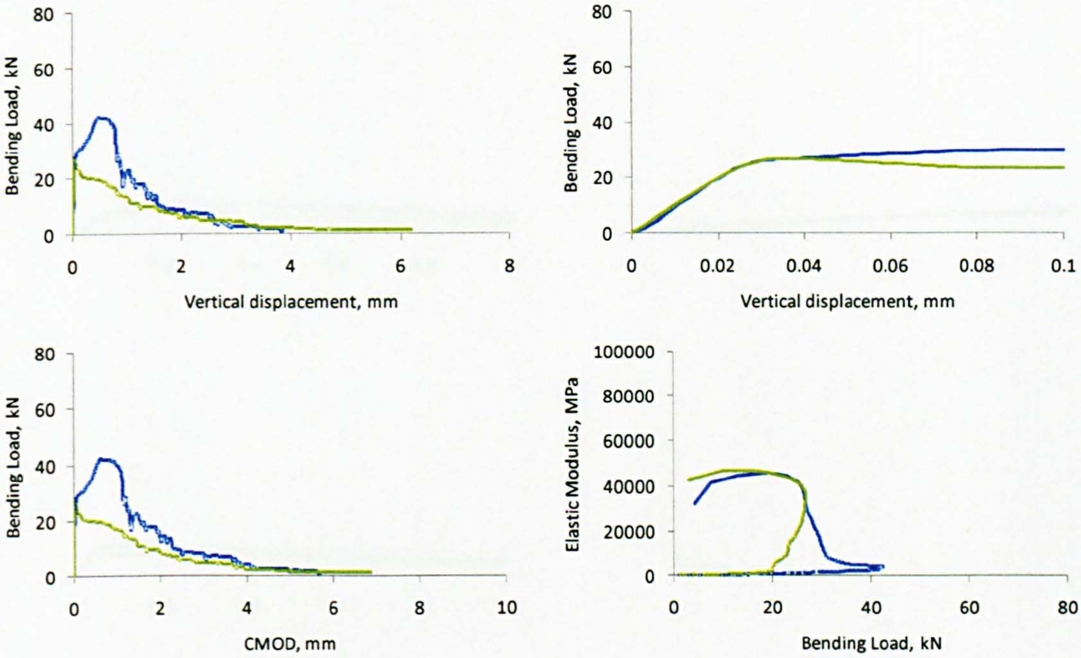

C.4.2.3 W-LEC-6R

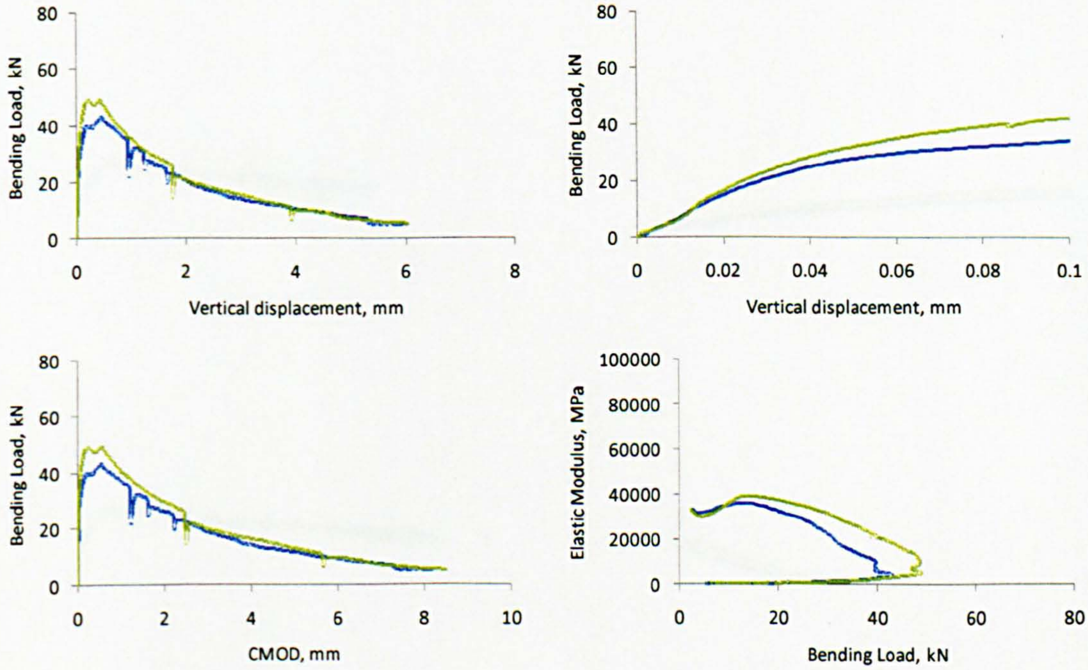

C.4.2.4 R-LEC-0

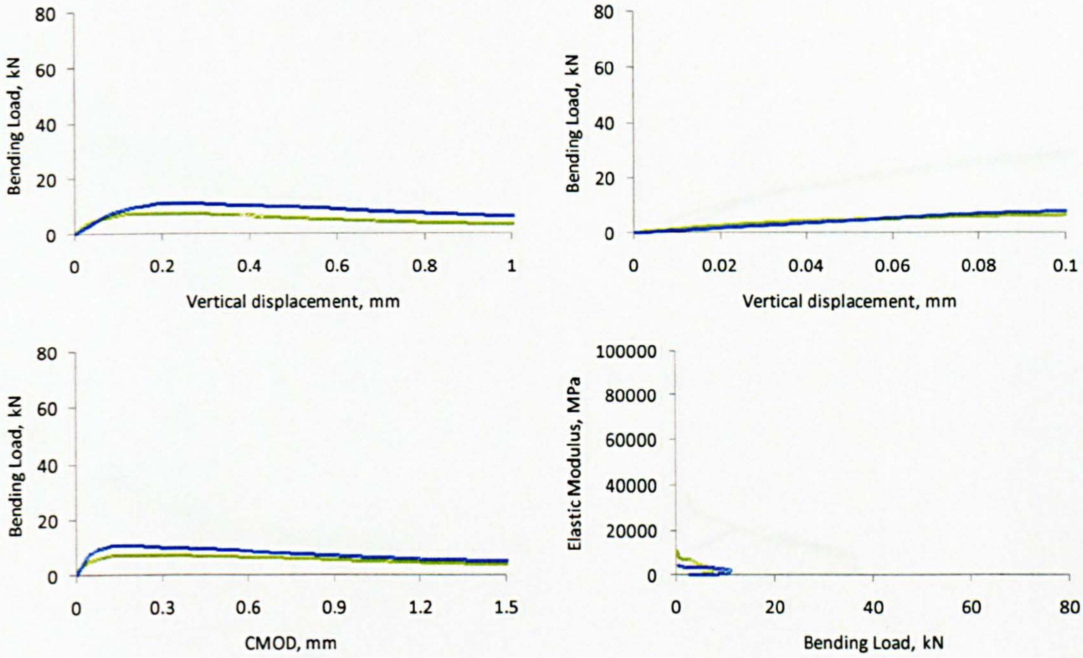

C.4.2.5 R-LEC-2I

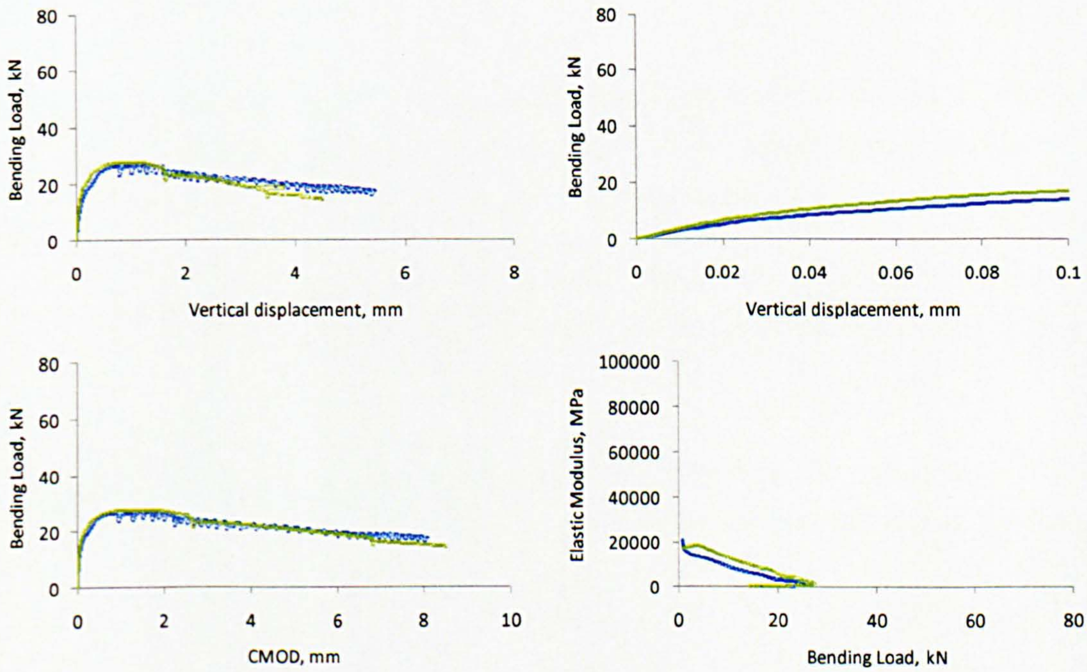

C.4.2.6 R-LEC-6R

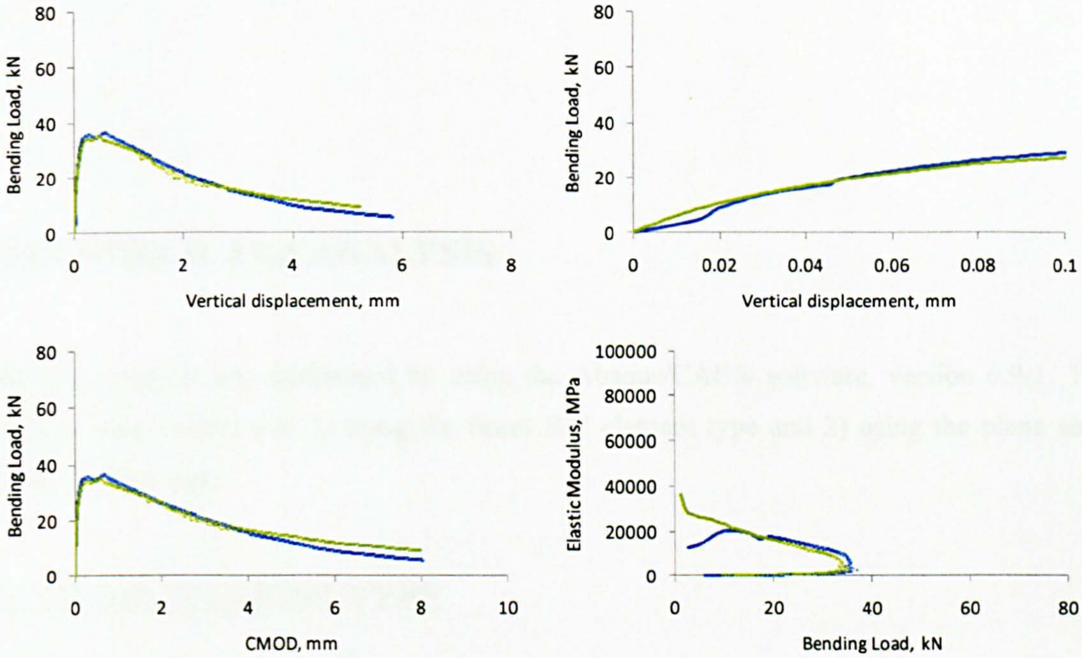
Bending Load, kN
Vertical displacement, mm
Bending Load, kN
Vertical displacement, mm
Bending Load, kN
CMOD, mm
Elastic Modulus, MPa
Bending Load, kN

APPENDIX D

APPENDIX D. FEA ANALYSIS

The FEA analysis was performed by using the Abaqus/CAE® software, version 6.9-1. Two analyses were carried out: 1) using the beam *B21* element type and 2) using the plane stress *CPS4I* element type.

D.1 BEAM ELEMENT TYPE

This analysis was carried out to first verify the accuracy of the results of the modulus of elasticity obtained from the elastic beam theory (Equation 19, Section 4.4.2.3). A deformable 2D planar wire-like element was created, with a cross section of 150 mm to 150 mm and length of 550 mm (span of 450 mm).

The element type used was the B21 – 2-noded linear beam in plane. The length of the finite elements was approximately 10 mm. Load was applied following the third-point load configuration as used in the experimental setup (Figure 64, Section 4.4.2.2).

The modulus of elasticity used was 32.5 GPa, the coefficient of poison was 0.18 and the total load applied to the system was 10 kN (divided into 2 concentrated loads of 5 kN). These parameters were obtained from mix W-CIP-0.

The vertical displacement contour graph is shown in Figure D.1. The vertical displacement at the mid-span of the beam was 0.01464 mm, which matches with the vertical displacement measured in the experiments.

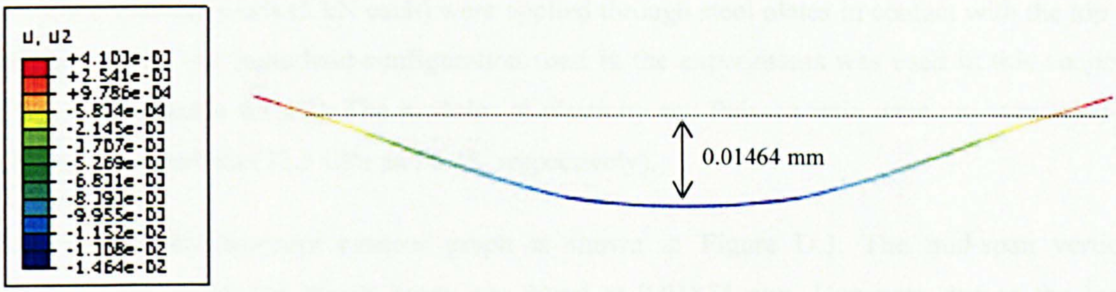

Figure D.1 – Vertical displacement contour graph for beam element type, considering concentrated loads.

Another analysis was carried out to consider the load-spreading effect. For that, the concentrated loads were substituted by pressure loads following the load configuration shown in Figure 99, Section 5.3.4. The magnitude of the total vertical load applied to the system remained the same as in the previous analysis (10 kN).

The vertical displacement contour graph obtained considering the pressure load is shown in Figure D.2. The vertical displacement in the mid-span is now reduced to 0.01439 mm (a 2% reduction compared to the analysis with concentrated loads).

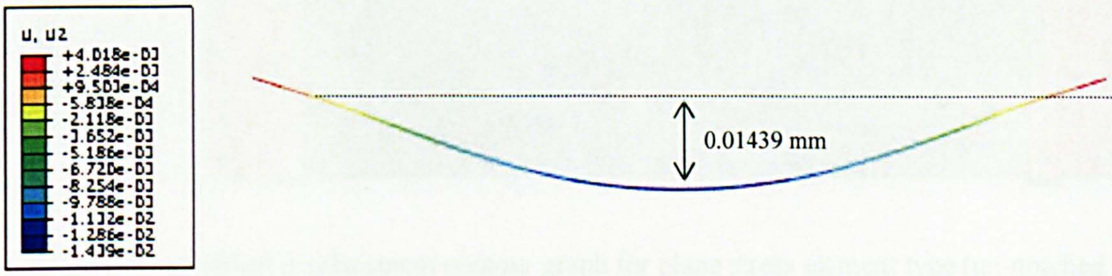

Figure D.2 - Vertical displacement contour graph for beam element type, considering the load-spreading effect.

D.2 PLANE STRESS ELEMENT TYPE

This analysis was carried to account for the load-spreading and other effects that may influence the modulus of elasticity of the material. A deformable 2D planar shell-like element was used for the model. The model dimension was 550 mm in length 150 mm in depth, with a span of 450 mm. The thickness of the element was considered to be 150 mm.

The element type used for the analysis was the CPS4I – 4-noded bilinear plane stress quadrilateral, incompatible modes. The size of the finite elements was approximately 10 mm.

Two concentrated loads (5 kN each) were applied through steel plates in contact with the top of the specimen. The same load-configuration used in the experiments was used in this analysis (Figure 64, Section 4.4.2.2). The modulus of elasticity and Poisson ratio were the same used in the previous analysis (32.5 GPa and 0.18, respectively).

The vertical displacement contour graph is shown in Figure D.3. The mid-span vertical displacement in the top of the beam was equal to 0.01853 mm. However, due to the local deformation in the regions next to the supports (equal to 0.004149 mm), the real mid-span vertical displacement should be 0.01853 mm – 0.004149 mm = 0.01438 mm. This value is basically the same as the displacement obtained considering the load-spreading effect in the previous analysis (0.01439 mm). Hence, it is reasonable to assume that deep elements, such as the prism used in the experimental programme of this thesis (550 mm x 150 mm x 150 mm), is affected by the load-spreading effect. However, the reduction in the displacements caused by the load-spreading effect (approximately 2%) does not cause any significant change (also approximately 2%) in the modulus of elasticity of the material.

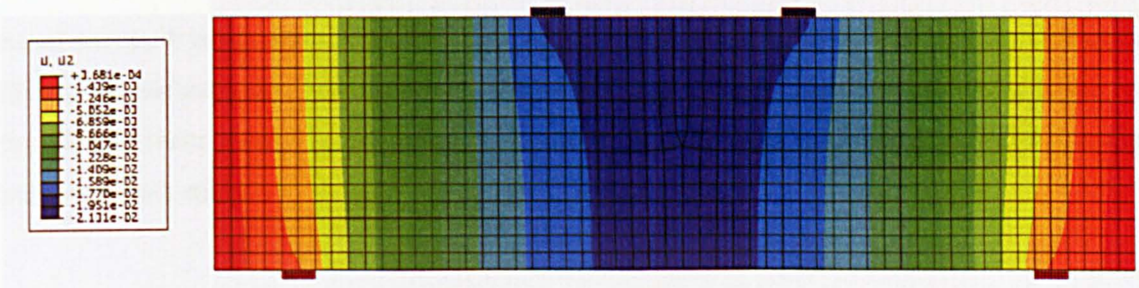

Figure D.3 – Vertical displacement contour graph for plane stress element type (un-notched beam).

Finally, the effect of the notch was also investigated through FEA. A similar model as the previous one was used, with the inclusion of the notch in the bottom mid-span on the prism. The notch was 3 mm wide and 25 mm deep, following the same conditions used in the experiments.

Figure D.4 shows the vertical displacement contour graph for the notched beam. The mid-span vertical displacement in the top of the beam was equal to 0.02143 mm. Considering the effect of the local deformation near the supports, this displacement drops to 0.01690 mm.

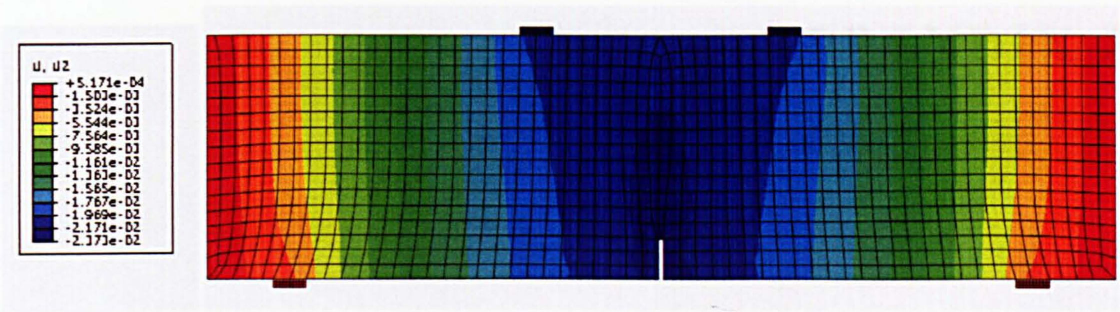

Figure D.4 - Vertical displacement contour graph for plane stress element type (notched beam).

If the effect of the notch is taken into account, there is a 17% increase in the displacements compared to the un-notched prism. However, as previously mentioned in section D.1 of this appendix, the experimental displacements were similar to the results of the FEA for the un-notched prism. Since the displacements obtained from the notched prism FEA analysis were higher than the experimental results (both analyses considered the same modulus of elasticity), the FEA analysis should consider a higher modulus of elasticity (of 17%) for the displacements to comply with the experimental results.

Nevertheless, it is not realistic to have even higher values of modulus of elasticity than the ones obtained experimentally. For this reason, the values of modulus of elasticity calculated based on the elastic beam theory (considering un-notched prisms) were considered as valid for the purpose of this study.

APPENDIX E

APPENDIX E. TABLE OF RESULTS – DENSITY, POROSITY AND FREE-SHRINKAGE

E.1 DENSITY AND POROSITY – 105°C

Mix	Saturated density [kg/m³]	Dry density [kg/m³]	Porosity P [% mass of concrete]
W-CIP-0	2263.32	2170.98	9.25
	2232.78	2143.35	8.96
W-CIP-2I	2263.24	2157.41	10.60
	2274.53	2168.79	10.60
W-CIP-2R	2311.02	2192.09	11.92
	2307.63	2214.94	9.29
W-CIP-6R	2415.95	2304.00	11.22
	2409.60	2304.73	10.51
W-LEC-0	2375.91	2244.96	13.12
	2347.79	2232.35	11.57
W-LEC-2I	2408.40	2322.35	8.62
	2408.32	2300.68	10.79
W-LEC-2R	2387.92	2271.19	11.70
	2393.29	2273.30	12.02
W-LEC-6R	2457.85	2368.34	8.97
	2460.87	2378.56	8.25
R-CIP-0	2520.45	2407.63	11.30
	2539.32	2442.09	9.74
R-CIP-2I	2551.53	2440.15	11.16
	2541.55	2439.76	10.20
R-CIP-2R	2568.31	2464.36	10.42
	2505.49	2364.18	14.16
R-CIP-6R	2518.92	2362.38	15.69
	2557.61	2405.66	15.23
R-LEC-0	2501.69	2356.25	14.57
	2507.33	2365.30	14.23
R-LEC-2R	2501.93	2344.50	15.77
	2542.93	2403.70	13.95
R-LEC-2I	2531.88	2386.71	14.55
	2542.40	2398.99	14.37
R-LEC-6R	2529.73	2349.70	18.04
	2491.88	2302.86	18.94

E.2 DENSITY AND POROSITY – 80°C

Mix	Saturated density [kg/m^3]	Dry density [kg/m^3]	Porosity P [% mass of concrete]
W-CIP-0	2337.49	2280.65	5.70
	2327.10	2266.27	6.10
W-CIP-2I	2328.23	2266.04	6.23
	2378.24	2329.10	4.92
W-CIP-2R	2390.87	2335.66	5.53
	2348.86	2293.18	5.58
W-CIP-6R	2408.61	2357.08	5.16
	2429.94	2378.20	5.18
W-LEC-0	2400.60	2315.81	8.50
	2419.27	2351.95	6.75
W-LEC-2I	2401.09	2313.80	8.75
	2415.22	2338.76	7.66
W-LEC-2R	2463.65	2407.78	5.60
	2407.12	2331.01	7.63
W-LEC-6R	2476.82	2414.26	6.27
	2473.25	2407.95	6.54
R-CIP-0	2554.85	2466.32	8.87
	2544.45	2459.29	8.53
R-CIP-2I	2537.69	2420.26	11.77
	2560.79	2447.85	11.32
R-CIP-2R	2561.38	2449.52	11.21
	2563.25	2451.89	11.16
R-CIP-6R	2503.25	2341.00	16.26
	2499.74	2335.96	16.41
R-LEC-0	2517.60	2393.58	12.43
	2522.17	2399.44	12.30
R-LEC-2R	2543.67	2416.90	12.70
	2544.48	2422.31	12.24
R-LEC-2I	2566.30	2452.44	11.41
	2543.36	2416.24	12.74
R-LEC-6R	2569.27	2433.83	13.57
	2547.86	2395.88	15.23

E.3 DENSITY AND POROSITY – 50°C

Mix	Saturated density [kg/m^3]	Dry density [kg/m^3]	Porosity P [% mass of concrete]
W-CIP-0	2301.79	2280.68	2.12
	2308.82	2286.70	2.22
W-CIP-2I	2328.70	2296.68	3.21
	2337.27	2301.64	3.57
W-CIP-2R	2333.20	2307.79	2.55
	2342.63	2317.30	2.54
W-CIP-6R	2408.02	2371.14	3.70
	2414.79	2381.48	3.34
W-LEC-0	2385.21	2338.85	4.65
	2378.17	2344.20	3.40
W-LEC-2I	2414.33	2366.95	4.75
	2430.00	2380.00	2.91
W-LEC-2R	2455.00	2388.27	2.79
	2460.26	2400.00	2.48
W-LEC-6R	2479.30	2446.08	3.33
	2471.23	2442.53	2.88
R-CIP-0	2558.53	2499.41	5.92
	2555.87	2498.61	5.74
R-CIP-2I	2547.59	2491.14	5.66
	2551.72	2487.67	6.42
R-CIP-2R	2539.48	2477.43	6.22
	2558.89	2504.80	5.42
R-CIP-6R	2564.04	2450.92	11.33
	2564.27	2441.20	12.33
R-LEC-0	2527.93	2472.97	5.51
	2541.46	2493.64	4.79
R-LEC-2R	2553.65	2496.47	5.73
	2553.93	2503.65	5.04
R-LEC-2I	2555.32	2505.98	4.94
	2564.56	2516.14	4.85
R-LEC-6R	2544.74	2455.50	8.94
	2582.77	2500.09	8.28

E.4 FREE-SHRINKAGE

Mix	1 day [mm/m]	3 days [mm/m]	5 days [mm/m]	7 days [mm/m]	14 days [mm/m]	28 days [mm/m]	56 days [mm/m]	112 days [mm/m]
	-0.045	-0.115	-0.118	-0.135	-0.264	-0.316	-0.446	-0.471
W-LEC-0	-0.035	-0.095	-0.138	-0.115	-0.243	-0.305	-0.462	-0.483
	-0.025	-0.090	-0.117	-0.111	-0.237	-0.282	-0.442	-0.466
	-0.074	-0.140	-0.157	-0.156	-0.276	-0.333	-0.480	-0.505
W-LEC-2I	-0.092	-0.179	-0.190	-0.174	-0.313	-0.364	-0.503	-0.515
	-0.075	-0.163	-0.171	-0.157	-0.291	-0.333	-0.517	-0.526
	-0.050	-0.128	-0.141	-0.146	-0.263	-0.334	-0.468	-0.491
W-LEC-2R	-0.063	-0.117	-0.130	-0.129	-0.252	-0.309	-0.543	-0.476
	-0.073	-0.123	-0.139	-0.137	-0.259	-0.325	-0.480	-0.497
	-0.055	-0.158	-0.143	-0.201	-0.350	-0.413	-0.568	-0.586
W-LEC-6R	-0.057	-0.124	-0.143	-0.140	-0.281	-0.348	-0.492	-0.506
	-0.034	-0.103	-0.143	-0.143	-0.266	-0.339	-0.480	-0.505
	-0.125	[b]	-0.329	-0.359	-0.342	-0.470	-0.584	-0.614
R-LEC-0	-0.098	[b]	-0.291	-0.320	-0.319	-0.425	-0.567	-0.598
	-0.095	[b]	-0.290	-0.316	-0.299	-0.425	-0.552	-0.584
	[a]	[b]	[a]	[a]	[a]	[a]	[a]	[a]
R-LEC-2R	-0.104	[b]	-0.298	-0.339	-0.339	-0.455	-0.572	-0.599
	-0.103	[b]	-0.283	-0.323	-0.329	-0.423	-0.579	-0.592
	-0.146	[b]	-0.404	-0.450	-0.458	-0.585	-0.719	-0.749
R-LEC-2I	-0.182	[b]	-0.386	-0.449	-0.469	-0.587	-0.733	-0.768
	-0.159	[b]	-0.414	-0.461	-0.483	-0.594	-0.756	-0.793
	-0.226	[b]	-0.497	-0.542	-0.547	-0.677	-0.801	-0.836
R-LEC-6R	-0.191	[b]	-0.475	-0.515	-0.520	-0.639	-0.775	-0.815
	-0.199	[b]	-0.466	-0.521	-0.508	-0.628	-0.773	-0.807

[a] no measurements due to damaged stud

[b] no measurements – compensated by measurement at 5 days.

APPENDIX F

APPENDIX F. RESULTS – PERMEABILITY, SORPTIVITY AND CHLORIDE CONTENT

F.1 PERMEABILITY (m²) – 50 °C, 80 °C AND 105 °C (RCC MIXES)

Mix	50 °C	80 °C	105 °C
R-CIP-0	0.36E-16	0.53E-16	1.09E-16
	0.27E-16	0.42E-16	0.72E-16
	0.25E-16	0.37E-16	
	0.29E-16	0.51E-16	
	0.28E-16	0.66E-16	
R-CIP-2I	0.34E-16	b	0.74E-16
	0.33E-16	b	0.84E-16
	0.23E-16	b	
	0.39E-16	b	
	0.32E-16	b	
R-CIP-2R	0.60E-16	2.84E-16	0.76E-16
	0.39E-16	0.78E-16	0.56E-16
	0.25E-16	1.11E-16	
	0.46E-16	1.44E-16	
	0.30E-16	1.00E-16	
R-CIP-6R[a]	-	-	-
R-LEC-0	1.40E-16	17.2E-16	25.7E-16
	0.86E-16	11.4E-16	34.3E-16
	1.49E-16	24.3E-16	
	1.39E-16	20.2E-16	
	1.77E-16	24.0E-16	
R-LEC-2I	4.08E-16	20.1E-16	64.4E-16
	4.97E-16	24.6E-16	45.0E-16
	2.10E-16	27.9E-16	
	2.97E-16	25.7E-16	
	6.89E-16	21.1E-16	
R-LEC-2R	6.72E-16	9.98E-16	13.7E-16
	7.56E-16	14.4E-16	13.8E-16
	6.80E-16	17.1E-16	
	8.30E-16	11.7E-16	
	8.41E-16	12.1E-16	
R-LEC-6R[a]	-	-	-

[a] results not recorded due to high permeability of mix
[b] specimen with compaction problem – permeability not measured

F.2 PERMEABILITY (m^2) – 50 °C, 80 °C AND 105 °C (WET MIXES)

Mix	50 °C	80 °C	105 °C
W-CIP-0	0.10E-16	0.26E-16	0.82E-16
	0.15E-16	0.32E-16	0.88E-16
	0.09E-16	0.23E-16	
	0.14E-16	0.27E-16	
	0.21E-16	0.29E-16	
W-CIP-2I	0.18E-16	0.38E-16	0.98E-16
	0.13E-16	0.39E-16	0.98E-16
	0.18E-16	0.31E-16	
	0.12E-16	0.28E-16	
	0.11E-16	0.31E-16	
W-CIP-2R	0.25E-16	0.22E-16	1.01E-16
	0.23E-16	0.17E-16	0.83E-16
	0.27E-16	0.19E-16	
	0.41E-16	0.23E-16	
	0.35E-16	0.25E-16	
W-CIP-6R	0.28E-16	0.19E-16	0.76E-16
	0.18E-16	0.17E-16	0.76E-16
	0.26E-16	0.17E-16	
	0.13E-16	0.20E-16	
	0.31E-16	0.23E-16	
W-LEC-0	0.24E-16	0.61E-16	1.21E-16
	0.30E-16	0.60E-16	1.05E-16
	0.16E-16	0.63E-16	
	0.31E-16	0.54E-16	
	0.17E-16	0.63E-16	
W-LEC-2I	0.20E-16	0.67E-16	0.65E-16
	0.17E-16	0.50E-16	0.94E-16
	0.31E-16	0.57E-16	
	0.14E-16	0.47E-16	
	0.16E-16	0.61E-16	
W-LEC-2R	0.30E-16	0.42E-16	1.16E-16
	0.25E-16	0.42E-16	1.21E-16
	0.49E-16	0.45E-16	
	0.54E-16	0.45E-16	
	0.44E-16	0.50E-16	
W-LEC-6R	0.10E-16	0.24E-16	0.66E-16
	0.08E-16	0.43E-16	0.59E-16
	0.07E-16	0.29E-16	
	0.10E-16	0.32E-16	
	0.13E-16	0.32E-16	

F.3 SORPTIVITY ($kg/m^2h^{0.5}$) – TABLE OF RESULTS – 50°C AND 80°C

Mix	50 °C	80 °C
W-CIP-0	0.152	0.250
	0.134	0.288
	0.140	0.265
W-CIP-2I	0.147	0.263
	0.149	0.284
	0.137	0.290
W-CIP-2R	0.135	0.258
	0.139	0.250
	0.168	0.253
W-CIP-6R	0.153	0.219
	0.146	0.223
	0.131	0.240
W-LEC-0	0.155	0.313
	0.201	0.293
	0.178	0.294
W-LEC-2I	0.130	0.271
	0.159	0.285
	0.155	0.276
W-LEC-2R	0.161	0.250
	0.137	0.271
	0.148	0.275
W-LEC-6R	0.136	0.232
	0.138	0.272
	0.141	0.247
R-CIP-0	0.240	0.716
	0.241	0.814
	0.316	0.694
R-CIP-2I	0.321	0.697
	0.347	0.795
	0.310	0.722
R-CIP-2R	0.293	0.753
	0.333	0.808
	0.312	0.738
R-CIP-6R	0.448	0.758
	0.476	0.699
	0.401	0.780
R-LEC-0	0.272	0.690
	0.305	0.798
	0.292	0.777
R-LEC-2R	0.278	0.862
	0.267	0.905
	0.329	0.759
R-LEC-2I	0.349	0.629
	0.196	0.647
	0.278	0.687
R-LEC-6R	0.489	1.045
	0.544	1.077
	0.398	0.986

F.4 SORPTIVITY – GRAPHS OF SLOPE – 50 °C

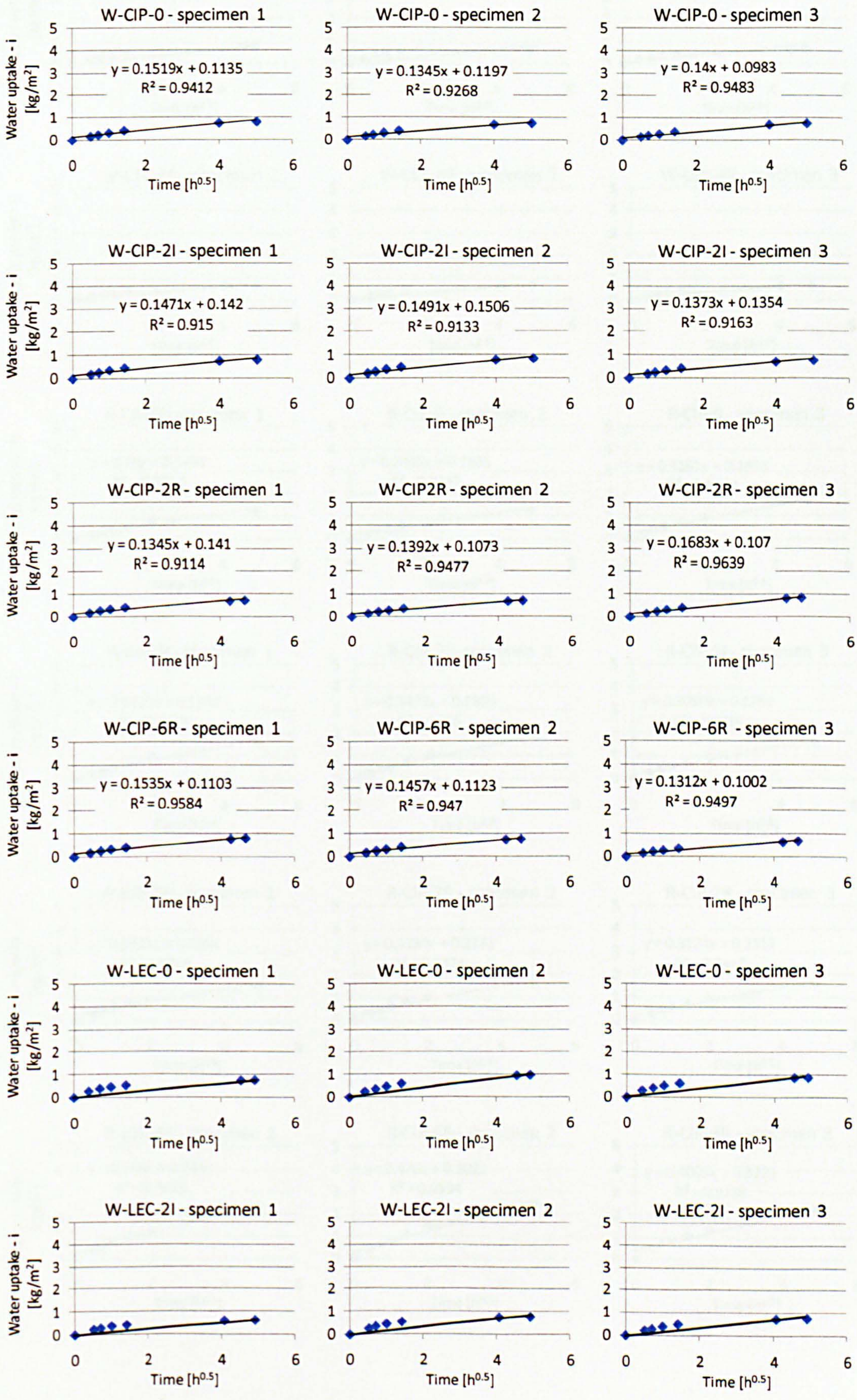

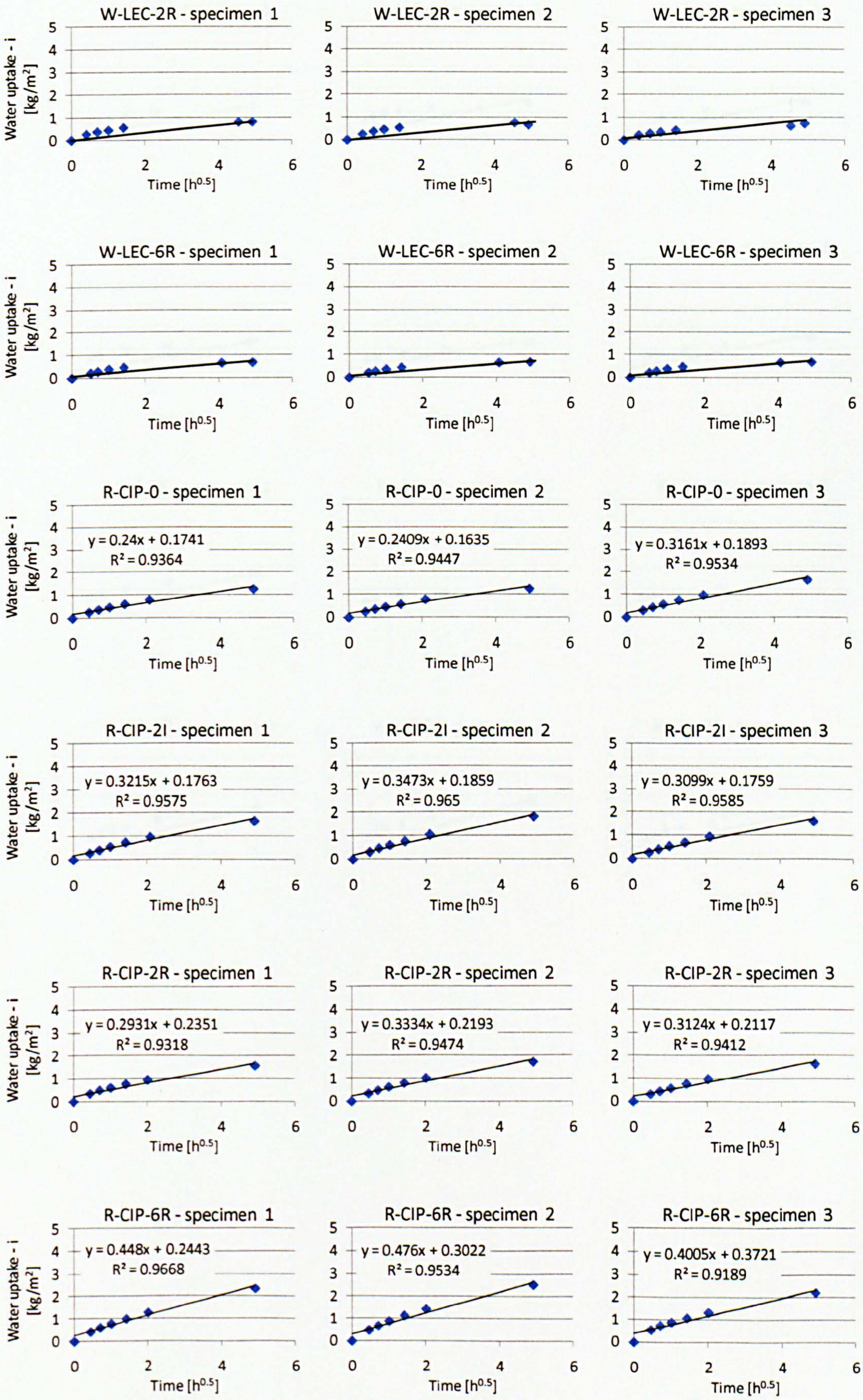
W-LEC-2R - specimen 1
W-LEC-2R - specimen 2
W-LEC-2R - specimen 3
W-LEC-6R - specimen 1
W-LEC-6R - specimen 2
W-LEC-6R - specimen 3
R-CIP-0 - specimen 1
y = 0.24x + 0.1741
R² = 0.9364
R-CIP-0 - specimen 2
y = 0.2409x + 0.1635
R² = 0.9447
R-CIP-0 - specimen 3
y = 0.3161x + 0.1893
R² = 0.9534
R-CIP-2I - specimen 1
y = 0.3215x + 0.1763
R² = 0.9575
R-CIP-2I - specimen 2
y = 0.3473x + 0.1859
R² = 0.965
R-CIP-2I - specimen 3
y = 0.3099x + 0.1759
R² = 0.9585
R-CIP-2R - specimen 1
y = 0.2931x + 0.2351
R² = 0.9318
R-CIP-2R - specimen 2
y = 0.3334x + 0.2193
R² = 0.9474
R-CIP-2R - specimen 3
y = 0.3124x + 0.2117
R² = 0.9412
R-CIP-6R - specimen 1
y = 0.448x + 0.2443
R² = 0.9668
R-CIP-6R - specimen 2
y = 0.476x + 0.3022
R² = 0.9534
R-CIP-6R - specimen 3
y = 0.4005x + 0.3721
R² = 0.9189
Water uptake - i [kg/m²]
Time [h^0.5]

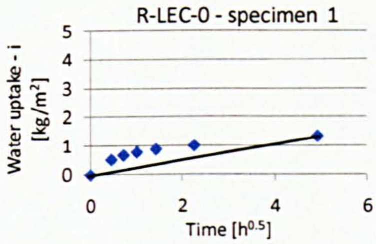
R-LEC-0 - specimen 1
Water uptake - i [kg/m²]
Time [h^0.5]

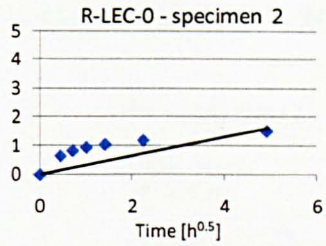
R-LEC-0 - specimen 2
Time [h^0.5]

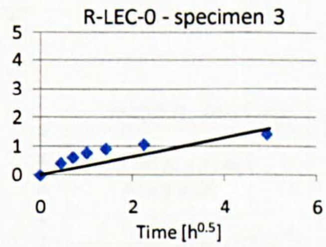
R-LEC-0 - specimen 3
Time [h^0.5]

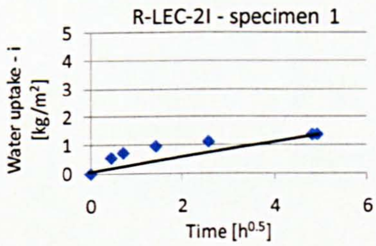
R-LEC-2I - specimen 1
Water uptake - i [kg/m²]
Time [h^0.5]

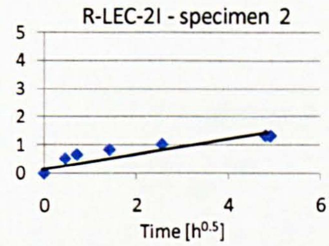
R-LEC-2I - specimen 2
Time [h^0.5]

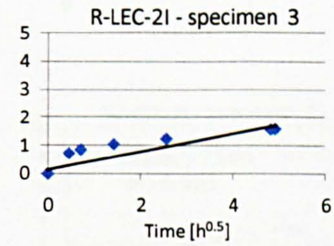
R-LEC-2I - specimen 3
Time [h^0.5]

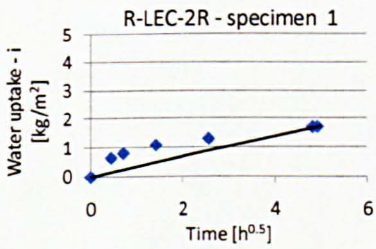
R-LEC-2R - specimen 1
Water uptake - i [kg/m²]
Time [h^0.5]

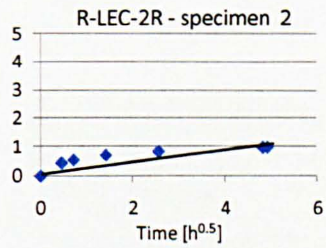
R-LEC-2R - specimen 2
Time [h^0.5]

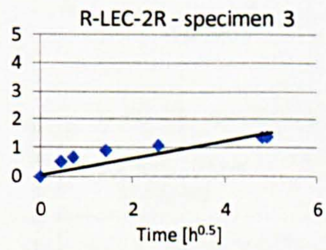
R-LEC-2R - specimen 3
Time [h^0.5]

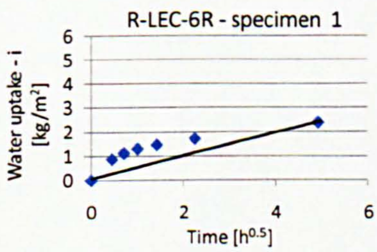
R-LEC-6R - specimen 1
Water uptake - i [kg/m²]
Time [h^0.5]

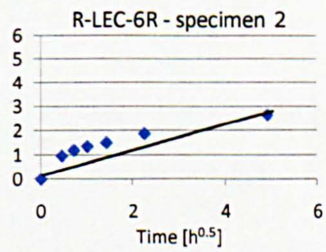
R-LEC-6R - specimen 2
Time [h^0.5]

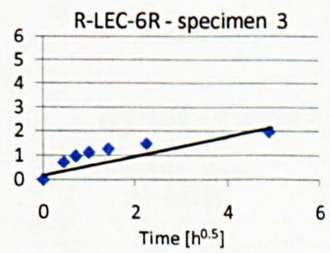
R-LEC-6R - specimen 3
Time [h^0.5]

F.5 SORPTIVITY – GRAPHS OF SLOPE – 80 °C

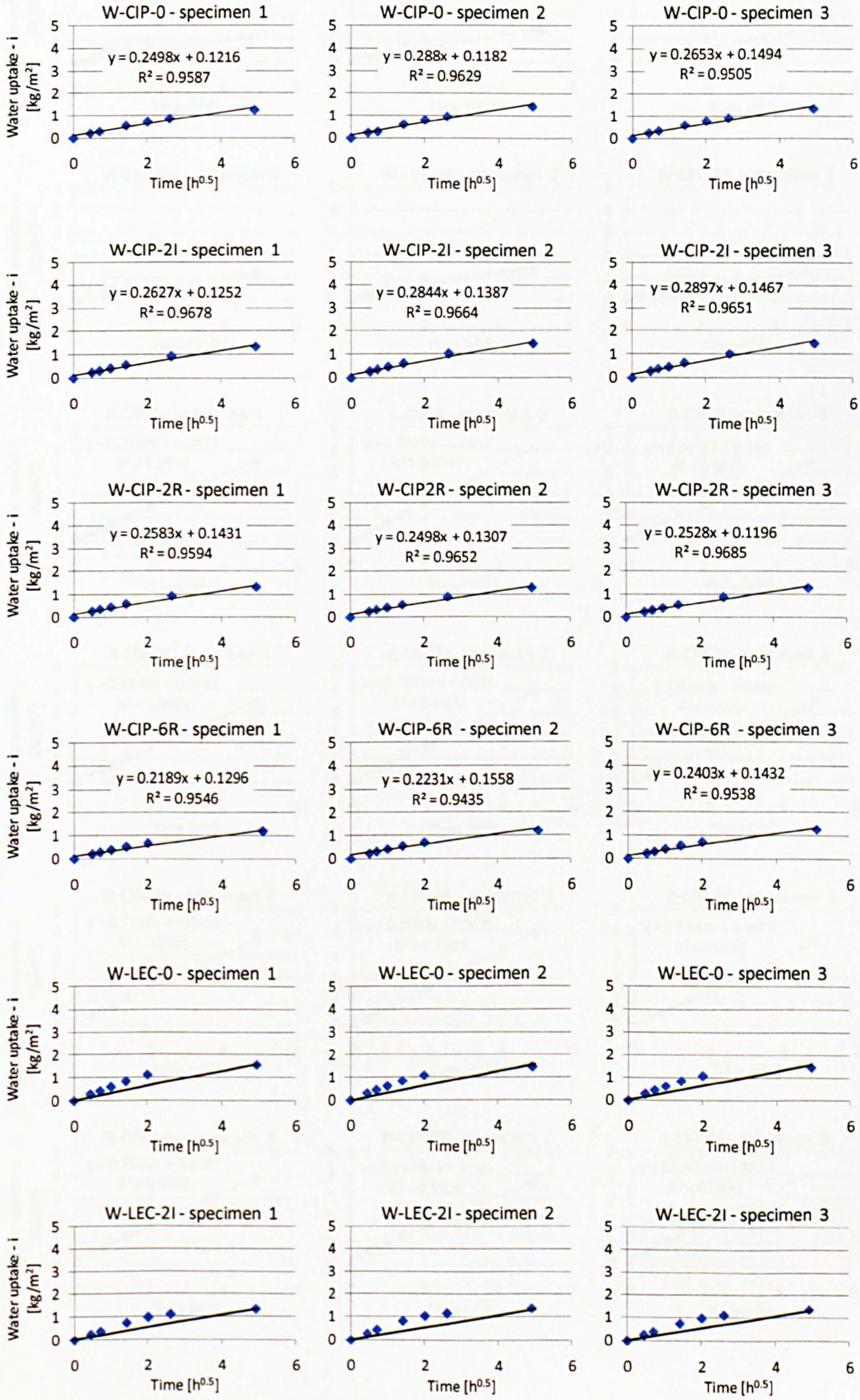

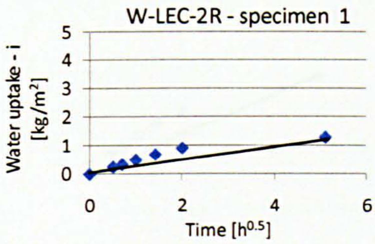
W-LEC-2R - specimen 1
Water uptake - i [kg/m²]
Time [h^0.5]

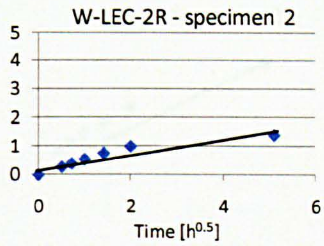
W-LEC-2R - specimen 2
Time [h^0.5]

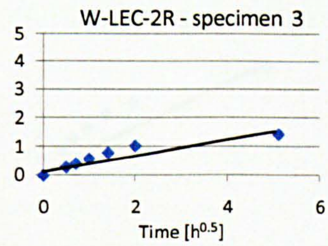
W-LEC-2R - specimen 3
Time [h^0.5]

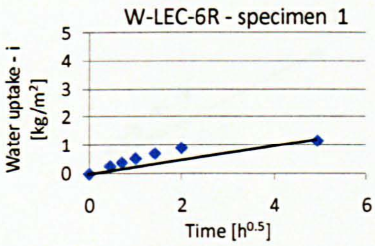
W-LEC-6R - specimen 1
Water uptake - i [kg/m²]
Time [h^0.5]

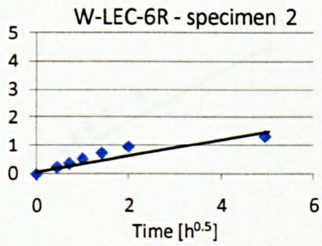
W-LEC-6R - specimen 2
Time [h^0.5]

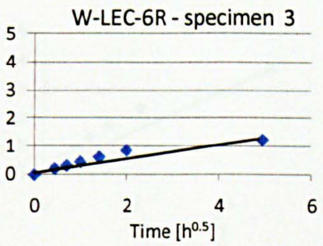
W-LEC-6R - specimen 3
Time [h^0.5]

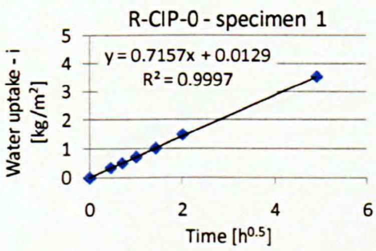
R-CIP-0 - specimen 1
y = 0.7157x + 0.0129
R² = 0.9997
Water uptake - i [kg/m²]
Time [h^0.5]

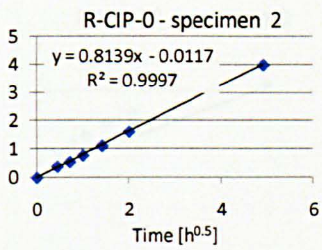
R-CIP-0 - specimen 2
y = 0.8139x - 0.0117
R² = 0.9997
Time [h^0.5]

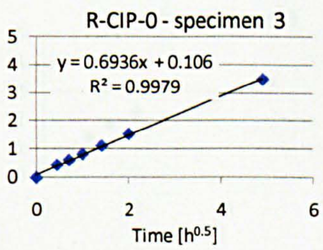
R-CIP-0 - specimen 3
y = 0.6936x + 0.106
R² = 0.9979
Time [h^0.5]

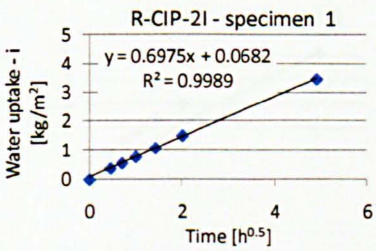
R-CIP-2I - specimen 1
y = 0.6975x + 0.0682
R² = 0.9989
Water uptake - i [kg/m²]
Time [h^0.5]

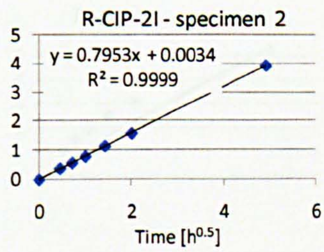
R-CIP-2I - specimen 2
y = 0.7953x + 0.0034
R² = 0.9999
Time [h^0.5]

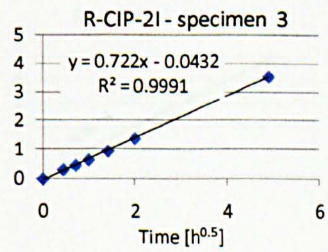
R-CIP-2I - specimen 3
y = 0.722x - 0.0432
R² = 0.9991
Time [h^0.5]

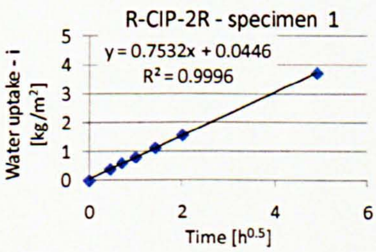
R-CIP-2R - specimen 1
y = 0.7532x + 0.0446
R² = 0.9996
Water uptake - i [kg/m²]
Time [h^0.5]

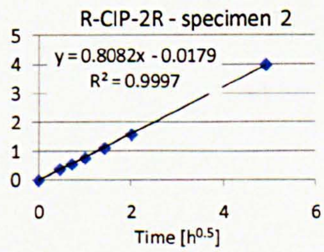
R-CIP-2R - specimen 2
y = 0.8082x - 0.0179
R² = 0.9997
Time [h^0.5]

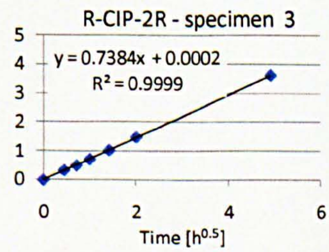
R-CIP-2R - specimen 3
y = 0.7384x + 0.0002
R² = 0.9999
Time [h^0.5]

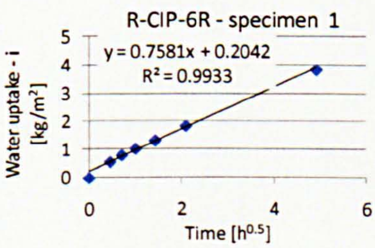
R-CIP-6R - specimen 1
y = 0.7581x + 0.2042
R² = 0.9933
Water uptake - i [kg/m²]
Time [h^0.5]

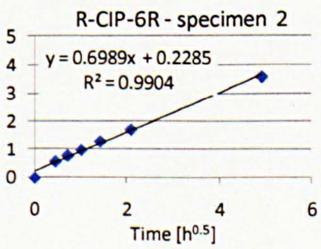
R-CIP-6R - specimen 2
y = 0.6989x + 0.2285
R² = 0.9904
Time [h^0.5]

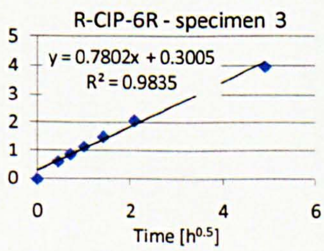
R-CIP-6R - specimen 3
y = 0.7802x + 0.3005
R² = 0.9835
Time [h^0.5]

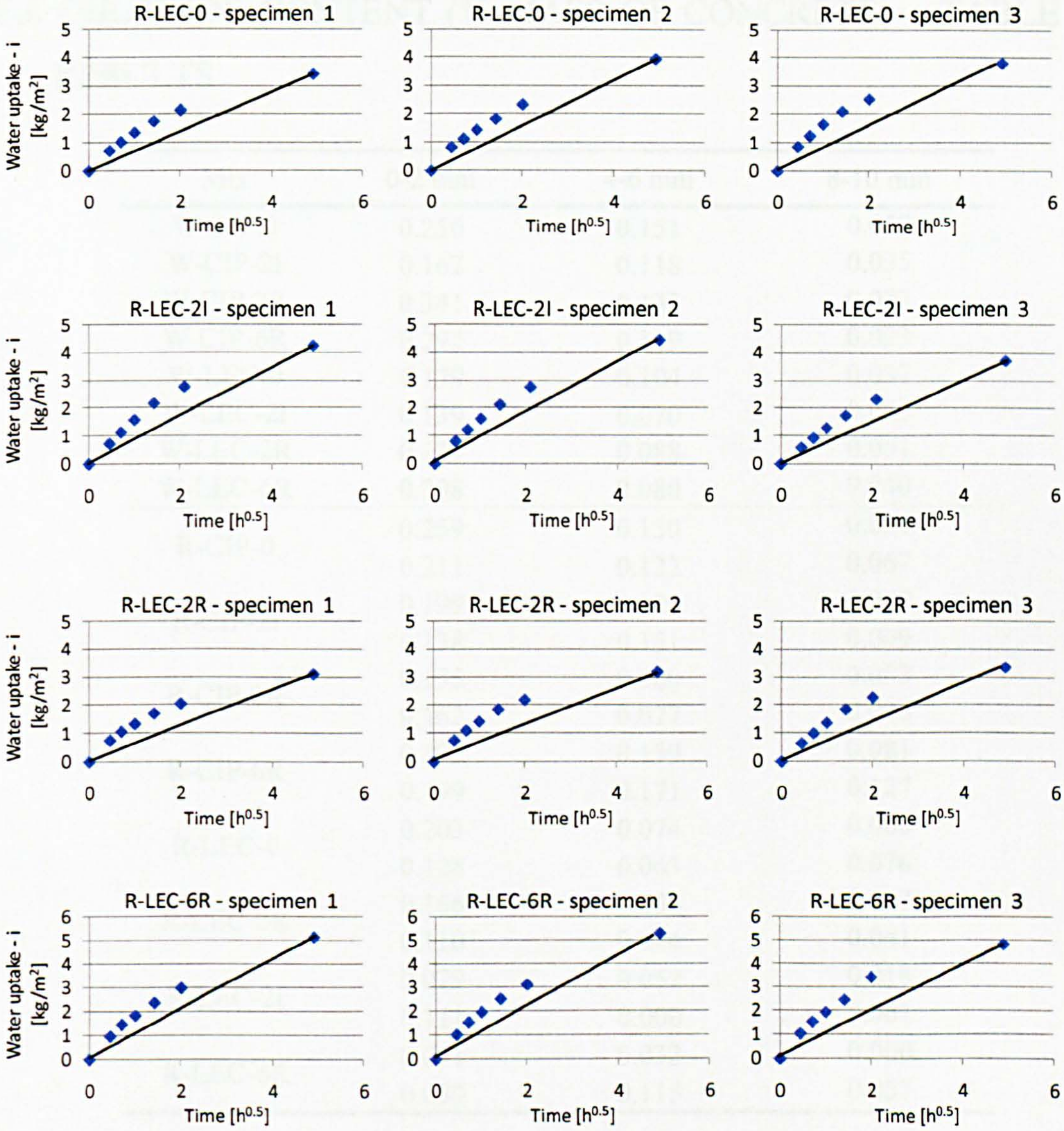
R-LEC-0 - specimen 1
R-LEC-0 - specimen 2
R-LEC-0 - specimen 3
R-LEC-2I - specimen 1
R-LEC-2I - specimen 2
R-LEC-2I - specimen 3
R-LEC-2R - specimen 1
R-LEC-2R - specimen 2
R-LEC-2R - specimen 3
R-LEC-6R - specimen 1
R-LEC-6R - specimen 2
R-LEC-6R - specimen 3
Water uptake - i [kg/m^2]
Time [h$^{0.5}$]

F.6 CHLORIDE CONTENT (% MASS OF CONCRETE) - TABLE OF RESULTS

Mix	0-2 mm	4-6 mm	8-10 mm
W-CIP-0	0.250	0.151	0.057
W-CIP-2I	0.162	0.118	0.035
W-CIP-2R	0.341	0.133	0.032
W-CIP-6R	0.292	0.119	0.023
W-LEC-0	0.179	0.104	0.037
W-LEC-2I	0.139	0.070	0.035
W-LEC-2R	0.139	0.088	0.051
W-LEC-6R	0.208	0.080	0.040
R-CIP-0	0.259	0.150	0.054
	0.211	0.122	0.067
R-CIP-2I	0.199	0.120	0.043
	0.138	0.151	0.049
R-CIP-2R	0.135	0.080	0.053
	0.162	0.077	0.045
R-CIP-6R	0.193	0.139	0.081
	0.199	0.171	0.127
R-LEC-0	0.203	0.074	0.000
	0.128	0.063	0.076
R-LEC-2R	0.166	0.080	0.057
	0.110	0.044	0.041
R-LEC-2I	0.079	0.052	0.018
	0.111	0.000	0.061
R-LEC-6R	0.071	0.032	0.000
	0.059	0.115	0.057

F.7 CHLORIDE CONTENT – GRAPHS OF CONDUCTIVITY

x axis – silver nitrate volume
y axis – change in conductivity

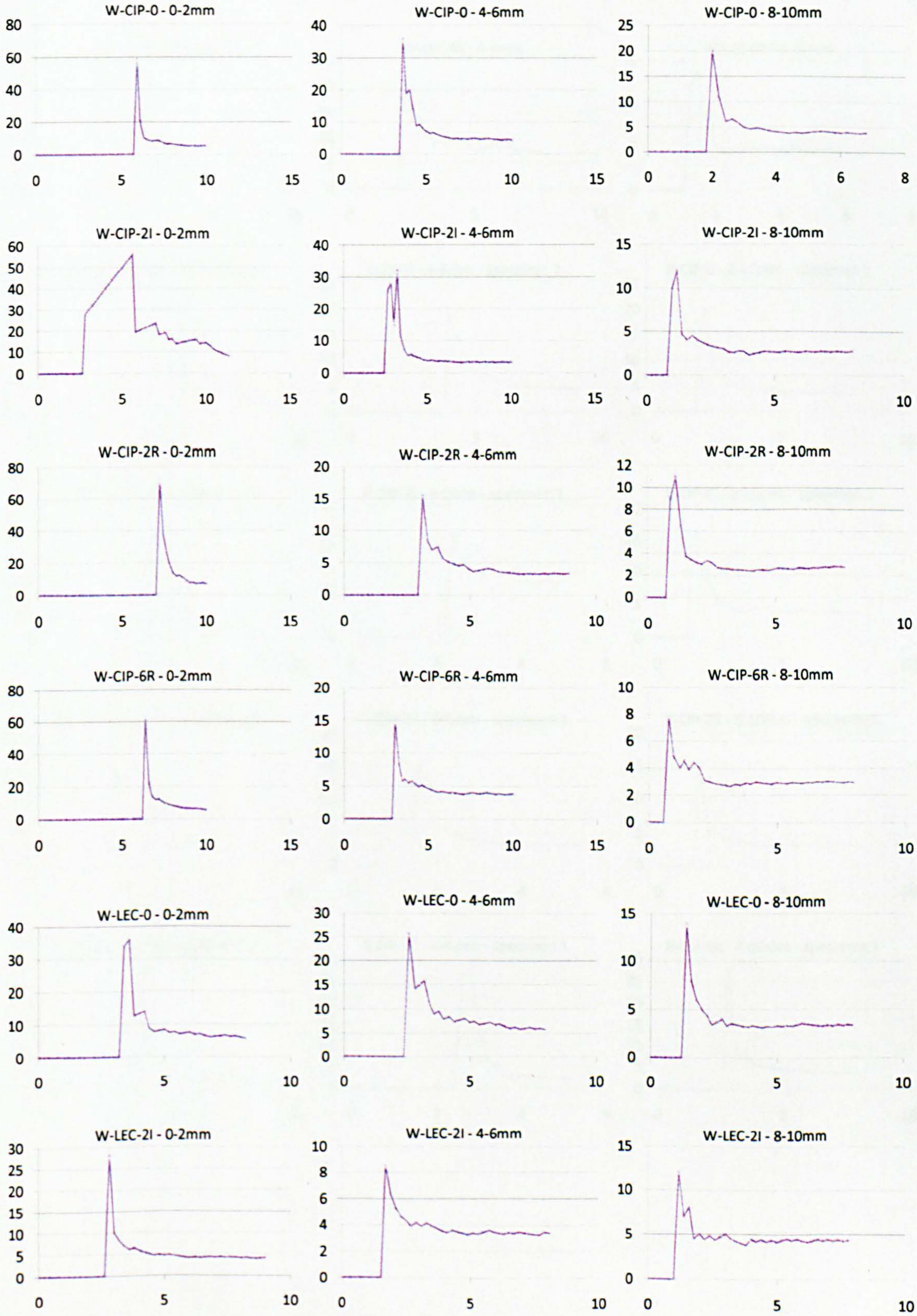

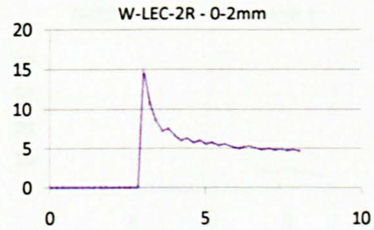
W-LEC-2R - 0-2mm
0 5 10 15 20
0 5 10

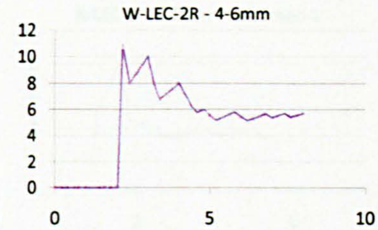
W-LEC-2R - 4-6mm
0 2 4 6 8 10 12
0 5 10

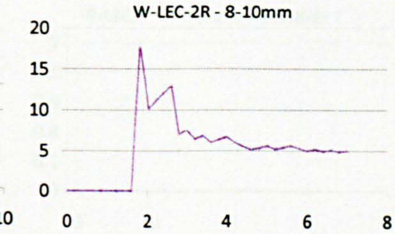
W-LEC-2R - 8-10mm
0 5 10 15 20
0 2 4 6 8

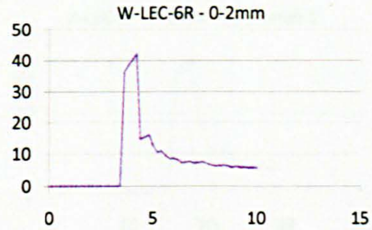
W-LEC-6R - 0-2mm
0 10 20 30 40 50
0 5 10 15

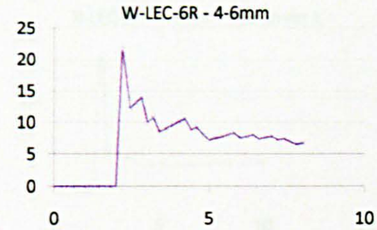
W-LEC-6R - 4-6mm
0 5 10 15 20 25
0 5 10

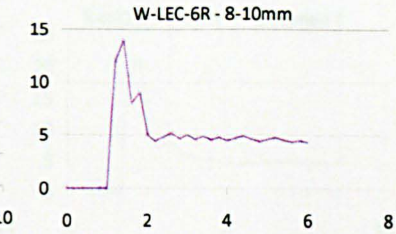
W-LEC-6R - 8-10mm
0 5 10 15
0 2 4 6 8

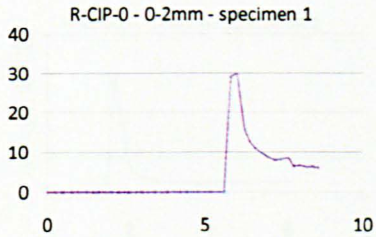
R-CIP-0 - 0-2mm - specimen 1
0 10 20 30 40
0 5 10

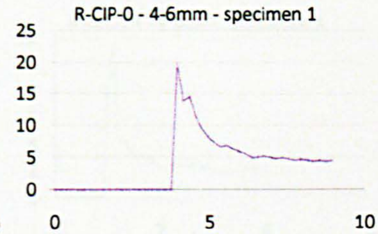
R-CIP-0 - 4-6mm - specimen 1
0 5 10 15 20 25
0 5 10

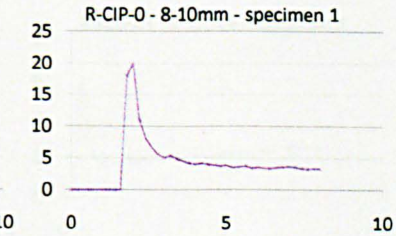
R-CIP-0 - 8-10mm - specimen 1
0 5 10 15 20 25
0 5 10

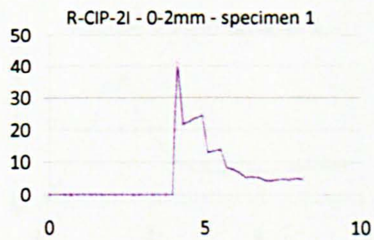
R-CIP-2I - 0-2mm - specimen 1
0 10 20 30 40 50
0 5 10

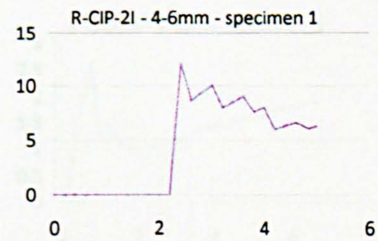
R-CIP-2I - 4-6mm - specimen 1
0 5 10 15
0 2 4 6

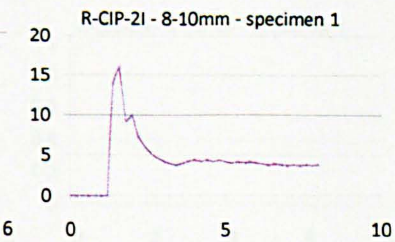
R-CIP-2I - 8-10mm - specimen 1
0 5 10 15 20
0 5 10

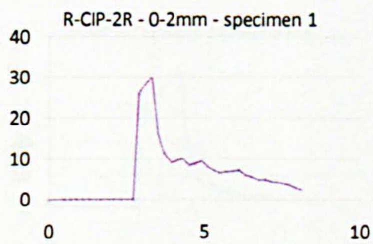
R-CIP-2R - 0-2mm - specimen 1
0 10 20 30 40
0 5 10

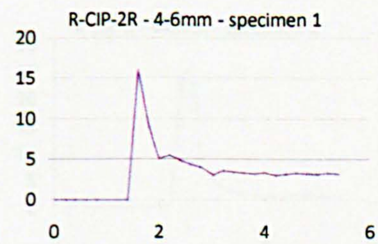
R-CIP-2R - 4-6mm - specimen 1
0 5 10 15 20
0 2 4 6

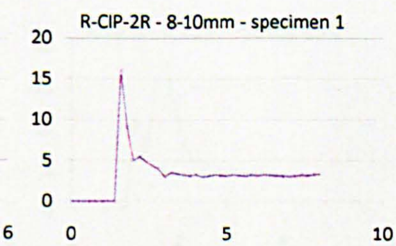
R-CIP-2R - 8-10mm - specimen 1
0 5 10 15 20
0 5 10

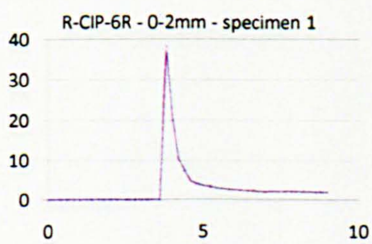
R-CIP-6R - 0-2mm - specimen 1
0 10 20 30 40
0 5 10

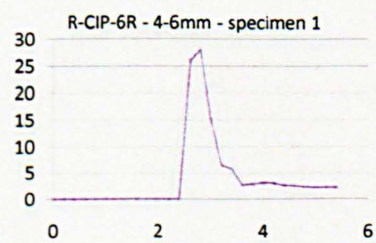
R-CIP-6R - 4-6mm - specimen 1
0 5 10 15 20 25 30
0 2 4 6

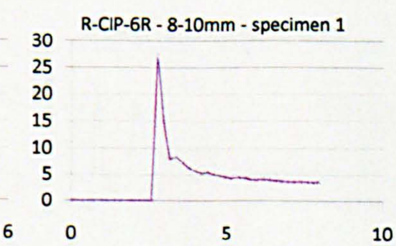
R-CIP-6R - 8-10mm - specimen 1
0 5 10 15 20 25 30
0 5 10

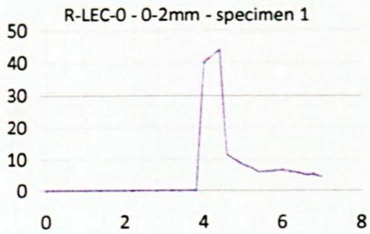
R-LEC-0 - 0-2mm - specimen 1
50 40 30 20 10 0
0 2 4 6 8

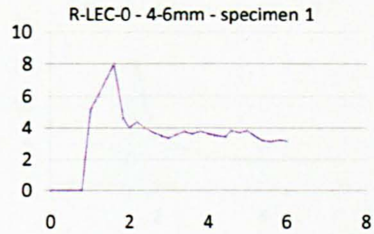
R-LEC-0 - 4-6mm - specimen 1
10 8 6 4 2 0
0 2 4 6 8

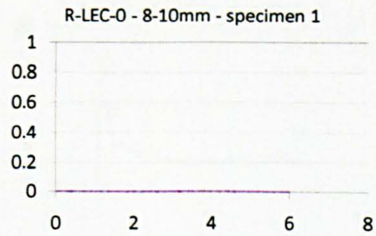
R-LEC-0 - 8-10mm - specimen 1
1 0.8 0.6 0.4 0.2 0
0 2 4 6 8

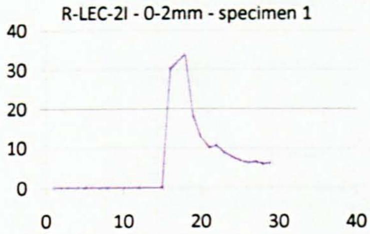
R-LEC-2I - 0-2mm - specimen 1
40 30 20 10 0
0 10 20 30 40

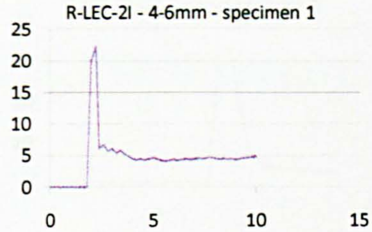
R-LEC-2I - 4-6mm - specimen 1
25 20 15 10 5 0
0 5 10 15

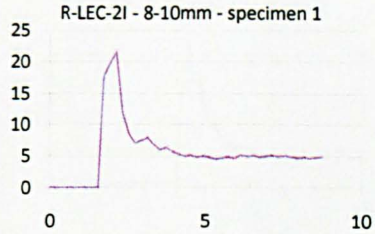
R-LEC-2I - 8-10mm - specimen 1
25 20 15 10 5 0
0 5 10

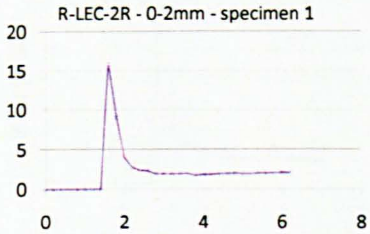
R-LEC-2R - 0-2mm - specimen 1
20 15 10 5 0
0 2 4 6 8

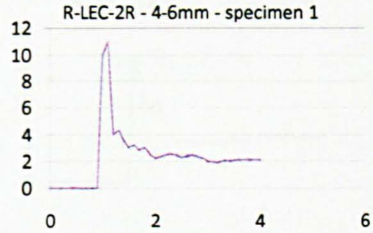
R-LEC-2R - 4-6mm - specimen 1
12 10 8 6 4 2 0
0 2 4 6

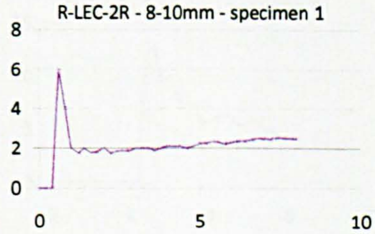
R-LEC-2R - 8-10mm - specimen 1
8 6 4 2 0
0 5 10

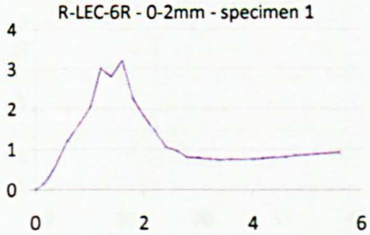
R-LEC-6R - 0-2mm - specimen 1
4 3 2 1 0
0 2 4 6

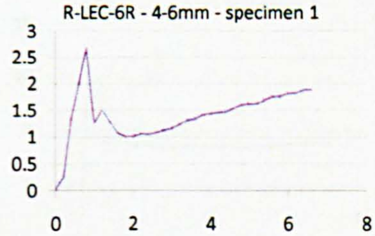
R-LEC-6R - 4-6mm - specimen 1
3 2.5 2 1.5 1 0.5 0
0 2 4 6 8

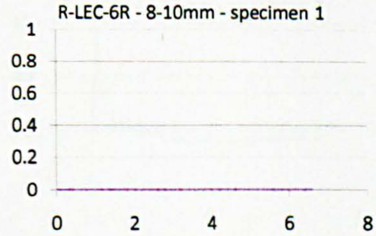
R-LEC-6R - 8-10mm - specimen 1
1 0.8 0.6 0.4 0.2 0
0 2 4 6 8

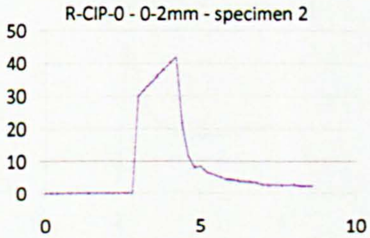
R-CIP-0 - 0-2mm - specimen 2
50 40 30 20 10 0
0 5 10

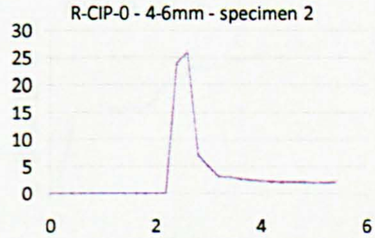
R-CIP-0 - 4-6mm - specimen 2
30 25 20 15 10 5 0
0 2 4 6

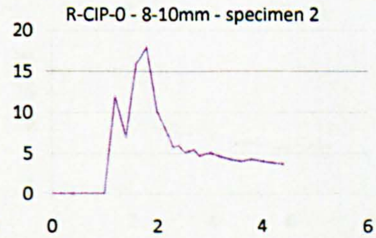
R-CIP-0 - 8-10mm - specimen 2
20 15 10 5 0
0 2 4 6

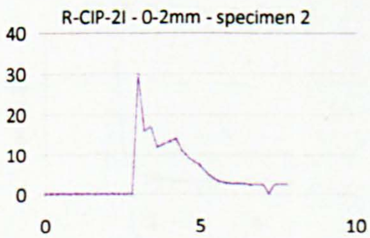
R-CIP-2I - 0-2mm - specimen 2
40 30 20 10 0
0 5 10

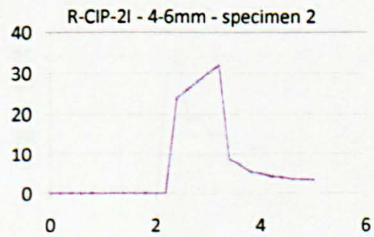
R-CIP-2I - 4-6mm - specimen 2
40 30 20 10 0
0 2 4 6

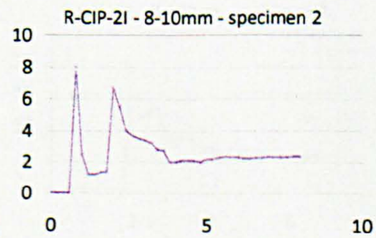
R-CIP-2I - 8-10mm - specimen 2
10 8 6 4 2 0
0 5 10

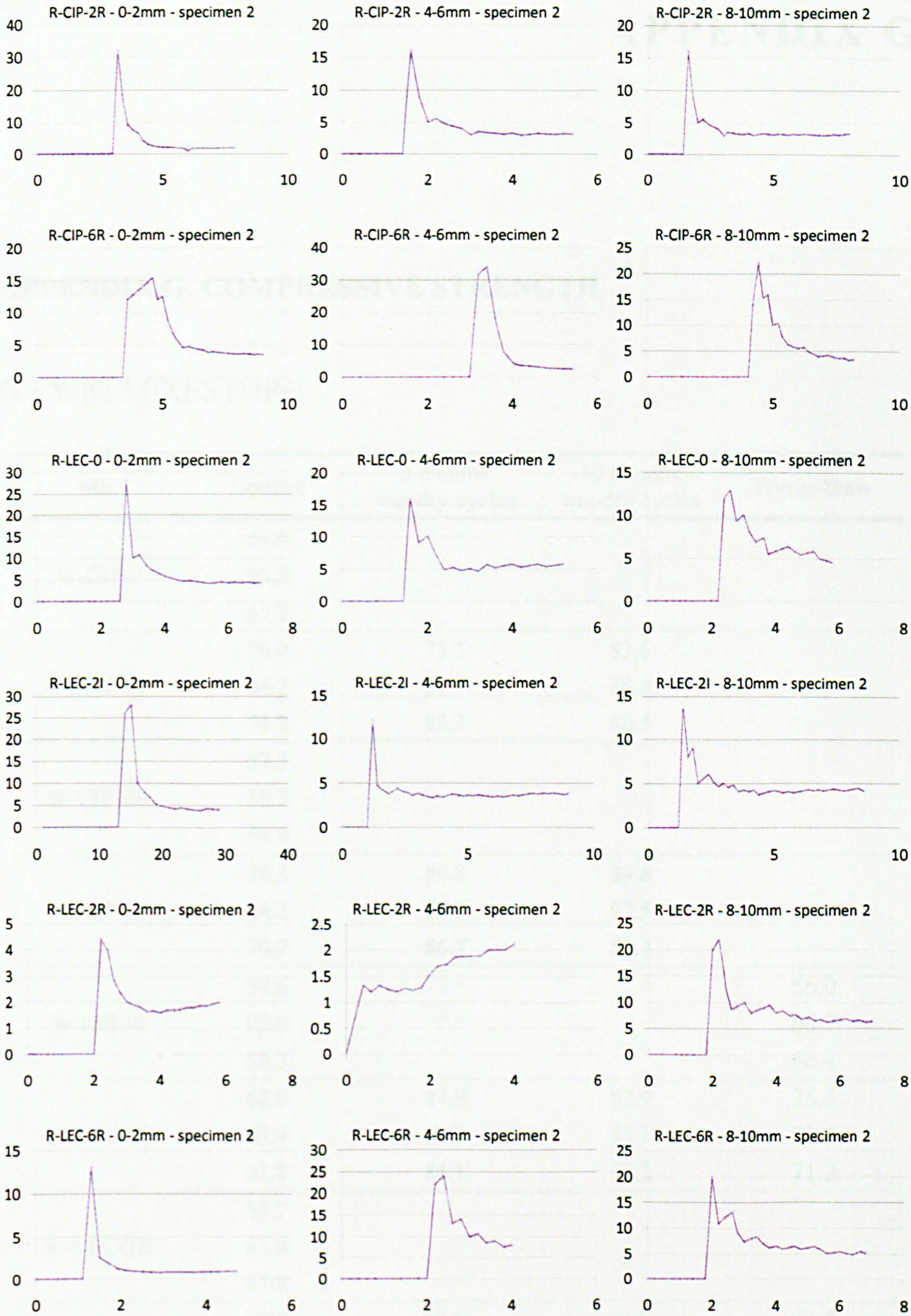
R-CIP-2R - 0-2mm - specimen 2
R-CIP-2R - 4-6mm - specimen 2
R-CIP-2R - 8-10mm - specimen 2
R-CIP-6R - 0-2mm - specimen 2
R-CIP-6R - 4-6mm - specimen 2
R-CIP-6R - 8-10mm - specimen 2
R-LEC-0 - 0-2mm - specimen 2
R-LEC-0 - 4-6mm - specimen 2
R-LEC-0 - 8-10mm - specimen 2
R-LEC-2I - 0-2mm - specimen 2
R-LEC-2I - 4-6mm - specimen 2
R-LEC-2I - 8-10mm - specimen 2
R-LEC-2R - 0-2mm - specimen 2
R-LEC-2R - 4-6mm - specimen 2
R-LEC-2R - 8-10mm - specimen 2
R-LEC-6R - 0-2mm - specimen 2
R-LEC-6R - 4-6mm - specimen 2
R-LEC-6R - 8-10mm - specimen 2

APPENDIX G

APPENDIX G. COMPRESSIVE STRENGTH

G.1 WET MIXES (MPa)

Mix	Control	5 months wet-dry cycles	10 months wet-dry cycles	Freeze-thaw
	61.6			
W-CIP-0	65.2			
	67.2			
	70.0	73.3	83.6	
W-CIP-2I	66.2	81.9	86.8	
	71.2	82.3	86.5	
	57.5			
W-CIP-2R	50.7			
	55.9			
	70.8	80.8	89.8	
W-CIP-6R	64.2	83.3	97.5	
	70.7	86.7	83.1	
	54.6			66.0
W-LEC-0	62.0			66.7
	59.3			66.4
	62.0	84.9	82.9	75.6
W-LEC-2I	63.4	83.3	85.1	72.4
	61.8	84.1	92.2	71.2
	59.7			
W-LEC-2R	61.8			
	61.8			
	70.6	93.6	93.3	92.5
W-LEC-6R	72.8	94.7	110.7	90.7
	70.9	107.8	101.5	78.8

G.2 RCC MIXES (MPa)

Mix	Control	5 months wet-dry cycles	10 months wet-dry cycles	Freeze-thaw
R-CIP-0	55.0			
	56.5			
	56.8			
R-CIP-2I	60.5	87.4	77.4	
	57.8	83.8	85.7	
	56.8	89.4	75.0	
R-CIP-2R	57.0			
	60.4			
	61.9			
R-CIP-6R	60.1	76.2	83.7	
	61.0	76.4	82.7	
	58.4	76.7	82.2	
R-LEC-0	49.8			11.0
	47.6			12.2
	47.3			10.8
R-LEC-2I	45.4	71.3	70.5	16.2
	46.2	70.4	68.3	15.7
	47.3	64.9	68.6	-
R-LEC-2R	50.4			
	47.6			
	50.2			
R-LEC-6R	42.2	68.1	71.0	60.2
	45.1	71.2	68.1	61.7
	47.6	68.9	65.9	65.6

APPENDIX H

APPENDIX H. FUNDAMENTAL OF CHLORIDE INGRESS

H.1 CHLORIDE INGRESS IN FULLY-SATURATED CONDITION

The value of $C(x,t_{SL})$ from Equation 32 (Section 10.2.1) is obtained according to Equation 12, in Section 3.2.1.3, which describes the chloride ingress in fully-saturated condition, based on a one-dimensional ingress of chlorides. Due to the geometric characteristics of concrete pavements (large horizontal area versus minimum vertical area), it is reasonable to assume that the ingress of chlorides is an one-dimensional process (vertically from the horizontal surface towards the interior of concrete).

The parameters that govern the equation are the diffusion coefficient, the time of exposure to chloride environment, the depth of the concrete and the surface chloride concentration of the concrete.

The chloride diffusion coefficient of concrete governs the transport of chloride ions into concrete (Section 3.2.1.3). As already reported by various authors (Saetta *et al.*, 1993; Xi and Bazant, 1999; Martín-Pérez *et al.*, 2001; Ababneh *et al.*, 2003; Val and Trapper, 2008; Kwon *et al.*, 2009), the chloride diffusion coefficient D_c [m^2/s] is influenced by various factors. The chloride diffusion coefficient can be estimated as follows:

$$D_c = D_{c,ref} \times f_1(t) \times f_2(g_i) \times f_3(H) \times f_4(T) \times f_5(C_f) \times f_6(w) \qquad \text{(H.1)}$$

Where:

$D_{c,ref}$= is the value of D_c at reference conditions (e.g. temperature, time of curing, relative humidity), measured by experimental tests

$f_1(t)$ = function that accounts for the age of concrete

$f_2(g_i)$ = function that accounts for the composite action of aggregates and the cement paste

$f_3(H)$ = function that accounts for the variations of relative humidity

$f_4(T)$= function that accounts for the variations of the temperature

$f_5(C_f)$ = function that accounts for the concentration of free chloride in the pore solution

$f_6(w)$ = function that accounts for the effect of cracks

Due to the lack of experimental results, models were developed from various authors to account for the various parameters that influence the chloride diffusion coefficient. Some of models are explained below.

Influence of age

Some of the most used *f(t)* models that account for the effect of age on the diffusion coefficient are explained as follows.

Some authors (Martín-Pérez *et al.*, 2001; fib, 2006; Val and Trapper, 2008) used the expression described in Equation H.2:

$$f(t) = \left(\frac{t_{ref}}{t}\right)^s \tag{H.2}$$

Where:

t_{ref} = reference time [usually 28 days]

s = age factor, depending on the mix proportions. Commonly used values of m vary from 0.2 to 0.6 (fib, 2006; Kwon *et al.*, 2009).

Kwon *et al.* (2009) used the method proposed by Luping and Gulikers (2007) to estimate the time-dependent diffusion. The equations are shown below.

$$f(t) = \left(\frac{1}{1-m}\right)\left(\frac{t_{ref}}{t \times 365}\right)^s \qquad t<30 \text{ years} \tag{H.3}$$

$$f(t) = \left[1 + \frac{30 \times 365}{t}\left(\frac{s}{1-s}\right)\right]\left(\frac{t_{ref}}{30 \times 365}\right)^s \qquad t \geq 30 \text{ years} \tag{H.4}$$

The diffusion coefficient after 30 years seems to stabilise, which explains the use of different equations.

Influence of composite action of aggregates and cement paste

The influence of composite action of the aggregates and the cement paste $f(g_i)$ is based on the composite theory proposed by Christensen (1979), shown in Equation H.5.

$$f(g_i) = D_{cp}\left\{1 + \frac{g_i}{\frac{1-g_i}{3} + \frac{1}{\frac{D_{agg}}{D_{cp}} - 1}}\right\} \qquad \text{(H.5)}$$

Where:

g_i = volume fraction of aggregates

D_{cp} = chloride diffusion coefficient of the cement paste

D_{agg} = chloride diffusion coefficient of the aggregates

D_{cp} and D_{agg} can be calculated based on the model proposed by Martys *et al.* (1994), shown in Equation H.6.

$$D_{cp} \text{ or } D_{agg} = \frac{2[1-(V_p - V_p^c)]}{S^2}\left(V_p - V_p^c\right)^{4.2} \qquad \text{(H.6)}$$

Where:

V_p = porosity

S = specific surface area = $\frac{surface\ area}{bulk\ volume}$

V_p^c = critical porosity (pore space that is first percolated) = 3% (Martys *et al.*, 1994)

It is important to note that not many authors account for the effect of composite action of aggregates and cement paste on the diffusion coefficient.

Influence of relative humidity

The model *f(H)* developed by Bazant and Najjar (1972) is commonly used to account for the humidity *H* of the concrete (H = 0 → 1). The model is shown in Equation H.7.

$$f(H) = \left[1 + \frac{(1-H)^4}{(1-H_c)^4}\right]^{-1} \qquad \text{(H.7)}$$

Where:

H_c = critical humidity level at which the diffusion coefficient drops halfway between its maximum and minimum value = 0.75 (75 %).

Influence of temperature

The expression that represents the influence of the temperature *f(T)* is based on the Arrhenius' law (Equation H.8).

$$f(T) = exp\left[\frac{U}{R}\left(\frac{1}{T_0} - \frac{1}{T}\right)\right] \quad \text{(H.8)}$$

Where:

U = activation energy of the chloride diffusion process [kJ/mol]

R = gas constant = 8.314E-3 kJ/mol.K

T_o = reference temperature = 296 K (23 °C)

T = temperature of the concrete [K]

The activation energy depends on the w/c ratio of the concrete. According to Page *et al.* (1981), U = 41.8 ± 4.0 kJ/mol for w/c = 0.4, U = 44.6 ± 4.3 kJ/mol for w/c = 0.5 and U = 32.0 ± 2.4 kJ/mol for w/c = 0.6.

Influence of the concentration of free chlorides in the pore solution

The movement of free chloride ions is restricted by the electrostatic field induced by the presence of other ions in the solution. According to Xi and Bazant (1999), the expression $f(C_f)$ that describes this effect is shown below.

$$f(C_f) = 1 - k_{ion}(C_f)^m \quad \text{(H.9)}$$

Where:

C_f = concentration of free chlorides in the pore solution [% by mass of concrete]

k_{ion} = constant = 8.333 (Xi and Bazant, 1999)

m = constant = 0.5 (Xi and Bazant, 1999)

Influence of cracks

Kwon *et al.* (2009) proposed the following empirical equation *f(w)*, based on data of two cracked wharves of South Korea, for the determination of the influence of cracks on the chloride diffusion coefficient (Equation H.10).

$$f(w) = 31.61w^2 + 4.73w + 1 \tag{H.10}$$

Where:

w = crack width [mm]

H.2 CHLORIDE INGRESS IN NON-SATURATED CONDITION

Even though a large number of studies consider the fully-saturation condition for modelling the chloride ingress into concrete, this simplified assumption does not apply to real conditions as explained next.

The chloride ingress into concrete is governed by three mechanisms: diffusion, convection and electric potential (Ababneh *et al.*, 2003). The diffusion involves the transport of ions in fully-saturated condition, as explained in Section 3.2.1.3. The convection is responsible for the transport of ions due to the movement of the pore solution by moisture gradient, and is described in this subsection. The electric potential exists only when an external electric potential (e.g. electric current for accelerated tests) is applied to the structure and, for this reason, is usually not accounted to described chloride ingress into concrete.

To account for the coupled influence of diffusion and moisture movement, the chloride ingress into concrete (in a one-dimensional configuration) can be described as follows (e.g. Val and Trapper, 2008):

$$\frac{\partial C_t}{\partial t} = \underbrace{D_c\left(\frac{\partial^2 C_f}{\partial x^2}\right)}_{\text{Diffusion}} + \underbrace{D_h C_f\left(\frac{\partial^2 H}{\partial x^2}\right)}_{\text{Moisture}} \tag{H.11}$$

Where:

C_t = total concentration of chlorides [kg/m^3 of concrete]

C_f = concentration of free chloride ions [kg/m^3 of pore solution]

H = pore relative humidity, ranging from 0 (0 %) to 1 (100 %)

D_c = chloride diffusion coefficient [m^2/s]

D_f = humidity diffusion coefficient [m^2/s]

t = time [seconds]

x = depth of concrete [m]

To solve the differential equation shown above, the first step is to account for the moisture movement effect alone, and then use the solution obtained from this analysis to solve the main equation shown above.

Moisture transport equation

The moisture transport in concrete, as a function of the gradient of the pore relative humidity *H* can be described as (e.g. Val and Trapper, 2008):

$$\frac{\partial w_e}{\partial h}\frac{\partial H}{\partial t} = D_h\left(\frac{\partial^2 H}{\partial x^2}\right) \tag{H.12}$$

Where:

D_h = humidity diffusion coefficient [m^2/s]

$\frac{\partial w_e}{\partial h}$ = moisture capacity

w_e = evaporable water content [m^3 pore solution/m^3 concrete]

The humidity diffusion coefficient depends on a series of factors, including age, temperature and humidity of concrete (Saetta *et al.*, 1993; Ababneh *et al.*, 2003; Val and Trapper, 2008). The parameter $\frac{\partial w_e}{\partial h}$ can be determined according to the sorption and adsorption isotherms[60] of concrete. Some models to predict the isotherms are detailed elsewhere (Saetta *et al.*, 1993; Ababneh *et al.*, 2003; Val and Trapper, 2008).

The solution of the non-linear equation is usually made numerically by finite-difference method. However, due to the fact that the parameters that influence the moisture transport into concrete are also non-linear (D_h and $\frac{\partial w_e}{\partial h}$ depend on the gradient of h), the numerical solution does not converge easily.

Moreover, the parameters D_h and $\frac{\partial w_e}{\partial h}$ are based on a large number of constants and variables that are not easy to obtain experimentally, which leads to various assumptions and a large degree of uncertainty of the model.

The non-saturated method to model the chloride ingress is more realistic in terms of describing most of the real conditions to which structures are exposed. Therefore, there is a need to

[60] Sorption and adsorption isotherms represent the relationship between water content and equilibrium humidity, for both processes of water penetration (sorption) and drying (desorption) of concrete.

understand the parameters that influence the model, especially when dealing with new concrete technologies, including the use of new cement types (such as the LEC) and the addition of recycled steel fibres into concrete.

Therefore, for practical implications, Fick's second law of diffusion was used in this thesis to predict the serviceability limit state of concrete pavements exposed to chloride environments, based on the fully-saturated condition.

Effect of biding capacity

Apart from the coupled effect of convection and diffusion, the models for non-saturated chloride ingress also account for the chloride binding capacity of the cement.

The threshold chloride limit (critical chloride content) of concrete is usually expressed as the total mass of chlorides per mass of concrete or per mass of cement. However, chloride-induced corrosion is only affected by the amount of free chlorides circulating in the concrete pore structure. Only the free chlorides are responsible for depassivation and corrosion initiation in RC structures (Luping and Nilsson, 1993).

The binding capacity of concrete is the slope of the relationship between free and bound chlorides ions in concrete, which is defined as binding isotherm (Val and Trapper, 2008). Two binding isotherms are commonly used to describe this relationship: Langmuir and Freundlich.

The Langmuir relationship is expressed by Equation H.13, while Freundlich relationship is expressed in Equation H.14.

$$C_{bc} = \frac{\alpha_L C_{fc}}{1+\beta_L C_{fc}} \tag{H.13}$$

$$C_{bc} = \alpha_F {C_{fc}}^{\beta_F} \tag{H.14}$$

Where:

C_{bc} = concentration of bound chlorides [% mass of cement]

C_{fc} = concentration of free chlorides [kg/m^3 solution]

α_L, α_F, β_L, β_F = binding constants that can be found by fitting the isotherms to experimental data using regression analysis

The binding constants are influenced mainly by the amount of C_3A in the cementitious material. As reported in section 6.3, C_3A reacts with chlorides forming chloro-aluminates compounds.

APPENDIX I

APPENDIX I. MATLAB SCRIPTS

I.1 CHLORIDE INGRESS

```
% this file calculates the chloride ingress in concrete due to fully-
saturated condition
Clear

%disp('Resistance Component:')
A_Cr=5.31, B_Cr=18.58,

%disp('Loading Component:')
mean_Dref=4.68, var_Dref=0.876
mu_Dref=log((mean_Dref^2)/sqrt(var_Dref+mean_Dref^2));
sigma_Dref=sqrt(log(var_Dref/(mean_Dref^2)+1));

mean_ur=4800, std_ur=700

A_a=5.8, B_a=3.87

Co=0.0
Cs=0.89
mean_CC=0.007, std_CC=0.0014

time=20

width=0

temperature=293

n=40000 % ('please type number of simulations =  ')

ur=normrnd(mean_ur,std_ur,n,1);
Cr=0.2+(2-0.2).*betarnd(A_Cr,B_Cr,n,1);
a=betarnd(A_a,A_a,n,1);
CC=normrnd(mean_CC,std_CC,n,1);
Dref=lognrnd(mu_Dref,sigma_Dref,n,1);

ft=(58/(time*365)).^a;

fT=exp(ur.*((1/293)-(1/temperature)));

fw=31.61*(width^2)+4.73*width+1;
```

```
Dm=Dref.*10^-12.*365.*86400.*ft.*fw.*fT;

X=2.*sqrt(Dm.*time);
Z=CC./X;
Y=erf(Z);
Ccl=Co+(Cs-Co).*(1-Y);
G=Cr-Ccl;

Cr1=mean(Cr);

%histfit(Cr), hold on
%histfit(Ccl)
%xlabel('Capacity'),ylabel('Frequency')
%legend('Cr', 'Ccl')

number_failures=sum(G<0)

Probability_of_failure=number_failures./n

%figure, histfit(G)
%xlabel('Safety Margin'),ylabel('Frequency')
%legend('G')
```

I.2 FREEZE-THAW

```
%this file calculates the reliability of frost-salt induced surface
scaling
clear

%number of simulations
n=36500;

%resistance temperature (assumed - Cai and Liu, 1998)
mean_Tr=270.5, min_Tr=268, max_Tr=273
TR=min_Tr+(max_Tr-min_Tr)*betarnd((mean_Tr-min_Tr)/(max_Tr-
min_Tr),(max_Tr-mean_Tr)/(max_Tr-min_Tr),n,1);

%ageing coefficient (LEC)
A_m=2.33, B_m=2.85
m=betarnd(2.33,2.85)

%time of exposure
time=22;
%NCP=cumulative number of cycles from previous years of exposure -
change
%manually
mean_NCP=4.45, std_NCP=0.445
NCP=normrnd(mean_NCP,std_NCP,n,1);

%ageing equation
fT=exp(m.*(1-((28/(time.*365)).^0.5)));
TR2=(TR-273).*fT;
TR3=TR2+273;

%concrete temperature (Sheffield, UK)
mean_Tair=275.9, std_Tair=3.2
Tair=normrnd(mean_Tair,std_Tair,n,1);
```

```
Tsky=(1.2.*(Tair-273)-14)+273;
ar=4.*0.9.*5.67E-8.*(((Tsky-Tair).^3)./2);
acv=6+4*4.12;
Tt=(Tair)+(ar./(ar+acv)).*(Tsky-Tair);

%number of corresponding accelerated freezing wet cycles
Ti=-15;
for i=1:n
if  Tt(i,1)<TR3(i,1)
    Nc(i,1)=((Tt(i,1)-273).^2)./((Ti).^2);
    else
    Nc(i,1)=0;
    end
end
Nc1=sum(Nc);

%number of effective freezing cycles
Nc2=Nc1/200;

%number of effective wet cycles
Nwd=85;
Nwfc=(Nc2.*Nwd)./(365/2);
N=Nwfc+NCP;

%('Scaling Resistance Component:')
mean_Scr=0.6, min_Scr=0.48, max_Scr=0.72
Scr=min_Scr+(max_Scr-min_Scr)*betarnd((mean_Scr-min_Scr)/(max_Scr-
min_Scr),(max_Scr-mean_Scr)/(max_Scr-min_Scr),n,1);

%histfit(Scr), hold on
%histfit(Sc1)
%xlabel('Capacity'),ylabel('Frequency')
%legend('Scr', 'Sc1')

%('Scaling Load Component:')
k=4
%1=W-LEC-0, W-LEC-2I; 2=W-LEC-6R; 3=R-LEC-0, R-LEC-2I; 4=R-LEC-6R

%for k=1
%    lSc=-0.0017.*(log(N))+0.0012;
%for k=2
%    lSc=-0.0028.*(log(N))+0.0023;
%for k=3
%    lSc=-0.0135.*(log(N))+0.008;
for k=4
    lSc=-0.0085.*(log(N))+0.0063;
    Sc=(1-(10.^lSc)).*100;
end

%model uncertainty due to full-saturated condition
mean_mu1=0.8, var_mu1=0.016
mu_mu1=log((mean_mu1^2)/sqrt(var_mu1+mean_mu1^2));
sigma_mu1=sqrt(log(var_mu1/(mean_mu1^2)+1));
mu1=lognrnd(mu_mu1,sigma_mu1,n,1);

Sc1=mu1.*Sc;

G=Scr-Sc1;
```

```
number_failures=sum(G<0);

Probability_of_failure=number_failures./n

%figure, histfit(G)
%xlabel('Safety Margin'),ylabel('Frequency')
%legend('G')
```

APPENDIX J

APPENDIX J. FATIGUE RESULTS

J.1 FLEXURAL STRENGTH CURVES CARRIED OUT AT UFRGS

J.1.1 W-CIP-0

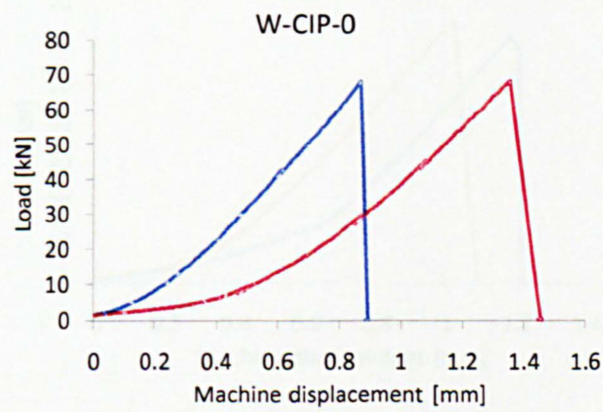

J.1.2 W-CIP-2R

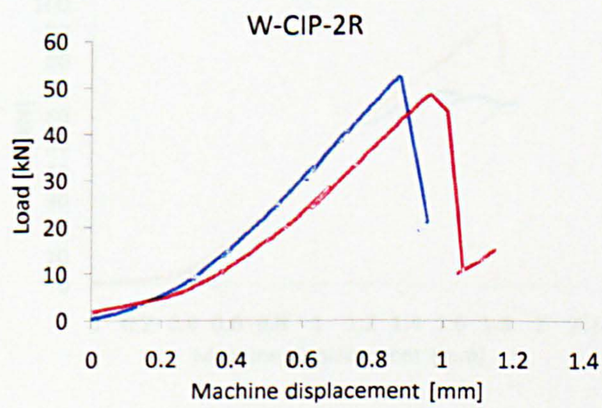

J.1.3 W-CIP-6R

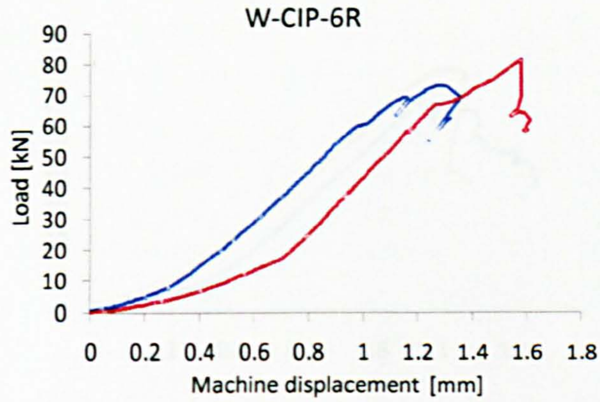

J.1.4 R-CIP-0

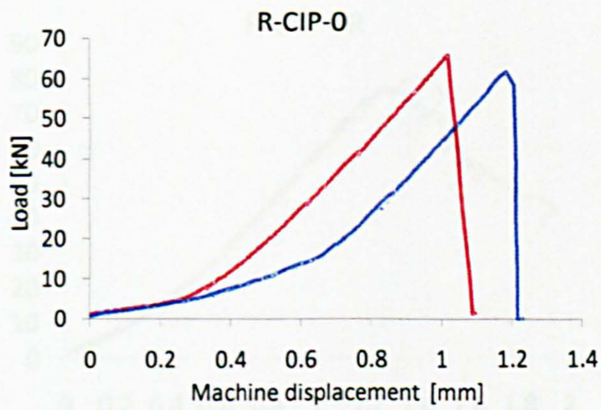

J.1.5 R-CIP-2I

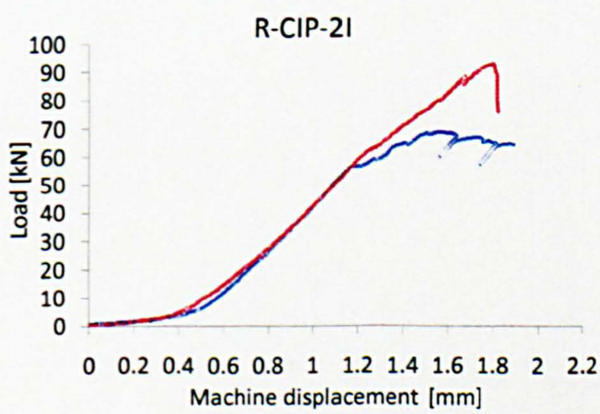

J.1.6 R-CIP-2R

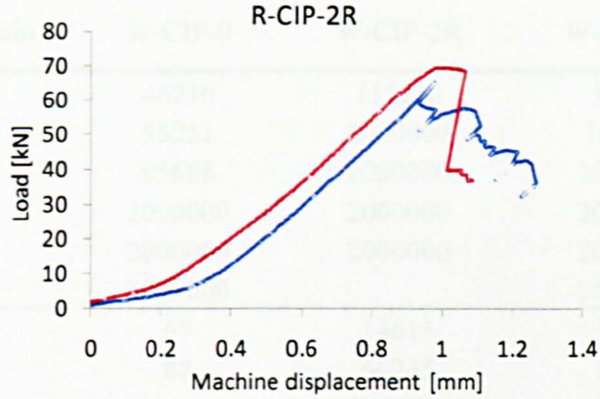

J.1.7 R-CIP-6R

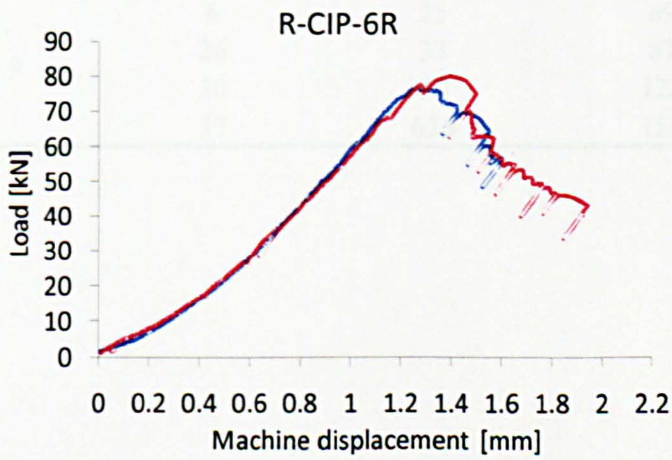

J.2 NUMBER OF CYCLES UNTIL FAILURE FOR WET MIXES

Stress ratio	W-CIP-0	W-CIP-2R	W-CIP-6R
0.5	46210	115210	99054
	55251	2000000	100882
	85668	2000000	2000000
	2000000	2000000	2000000
	2000000	2000000	2000000
	2000000		2000000
0.7	67	14615	1584
	88	60235	3467
	115	449974	5848
	176	1341698	18412
	276	2000000	366039
	2356	2000000	
0.9	6	25	69
	26	33	87
	30	50	123
	37	636	158

J.3 NUMBER OF CYCLES UNTIL FAILURE FOR RCC MIXES

Mix	R-CIP-0	R-CIP-2I	R-CIP-2R	R-CIP-6R
0.5	295400	74749	660300	2000000
	296050	120828	1227012	2000000
	756903	2000000	1227030	2000000
	1305150		1782000	2000000
	2000000		2000000	2000000
	2000000		2000000	2000000
0.6	-	-	-	2000000
				2000000
				2000000
				2000000
				2000000
0.7	1654	199520	7598	7974
	99175	298007	459236	8458
	136072	332650	837648	9798
	236910	654250	837746	10384
	402839		975678	23072
			1241372	235853
0.8	-	-	-	4402
				7788
				22930
				132204
				267337
0.9	1915	68	1	-
	1975	162	38	
	2056	42594	156	
	3791		278	

J.4 PROCEDURES FOR THE GRAPHICAL METHOD – PROBABILISTIC ANALYSIS

After ranking the specimens according to the number of cycles until failure per stress level, and after discarding some results based on the Chauvenet's criterion of rejection (see detailed information in Section 10.4), the graphs for the probabilistic analysis are plotted following the steps shown below:

Step 1) p_f – *log(N)* curves: The p_f – *log(N)* curves are plotted for each stress level investigated, by using data from Table J.1 (mix R-CIP-0), grouped vertically as shown by the red rectangles. The p_f – *log(N)* curves for mix R-CIP-0 is shown in Figure J.1.

Table J.1 – Number of cycles and probability of failure (mix R-CIP-0).

i	Stress level 0.5	Stress level 0.7	Stress level 0.9	p_f
1	756903	36850	1915	0.2
2	1305150	99175	1975	0.4
3	2000000	136072	2056	0.6
4	2000000	402839	3791	0.8

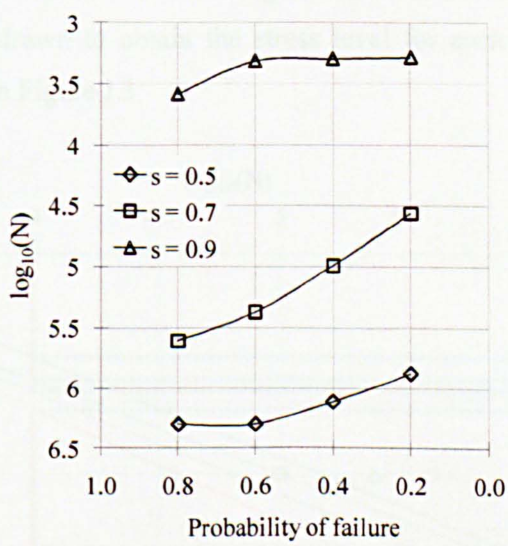

Figure J.1 – p_f – *log(N)* curves for mix R-CIP-0.

Step 2) *s* – *log(N)* curves: The number of cycles until failure is then plotted against the stress level according to the probability of failure for each rank. This is performed by using the data from Table J.1, grouped horizontally as shown by the blue rectangles. The *s* – *log(N)* curves for mix R-CIP-0 is shown in Figure J.2.

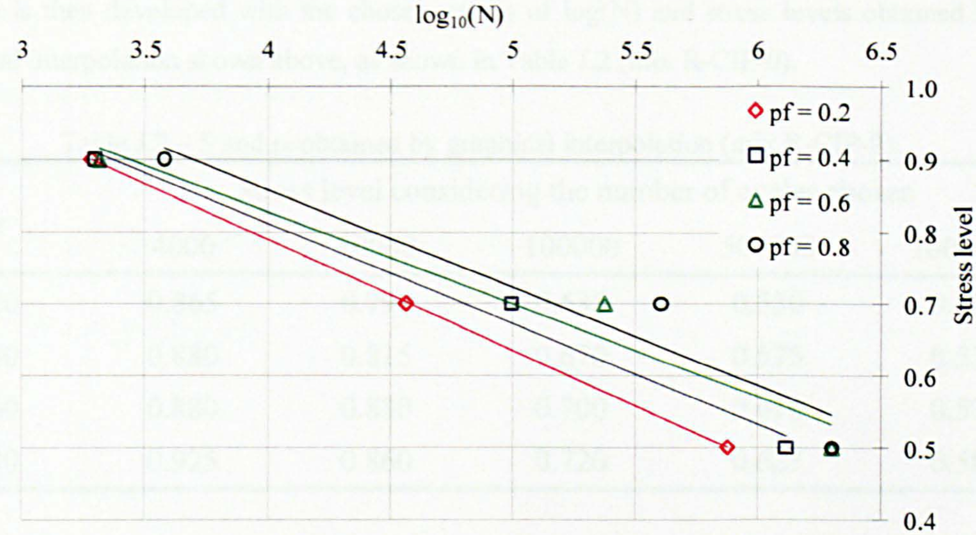

Figure J.2 – *s – log(N)* curves for mix R-CIP-0.

Step 3) *s* – p_f curves: by graphical interpolation of the *s – log(N)* curves obtained from step 2, the third graph correlating s and p_f can be plotted.

To obtain the values to plot the *s* – p_f curves, some specific number of cycles were selected: 4000, 10000, 100000, 500000 and 1000000. The number of cycles chosen may vary depending on the circumstances. A vertical line should then be drawn regarding all the number of cycles selected (in terms of log(N)). This is exemplified by the red line in Figure J.3, for 10000 cycles. The red vertical line should reach the linear regression lines for each probability of failure. Horizontal lines are then drawn to obtain the stress level for each probability of failure, as shown by the blue arrows in Figure J.3.

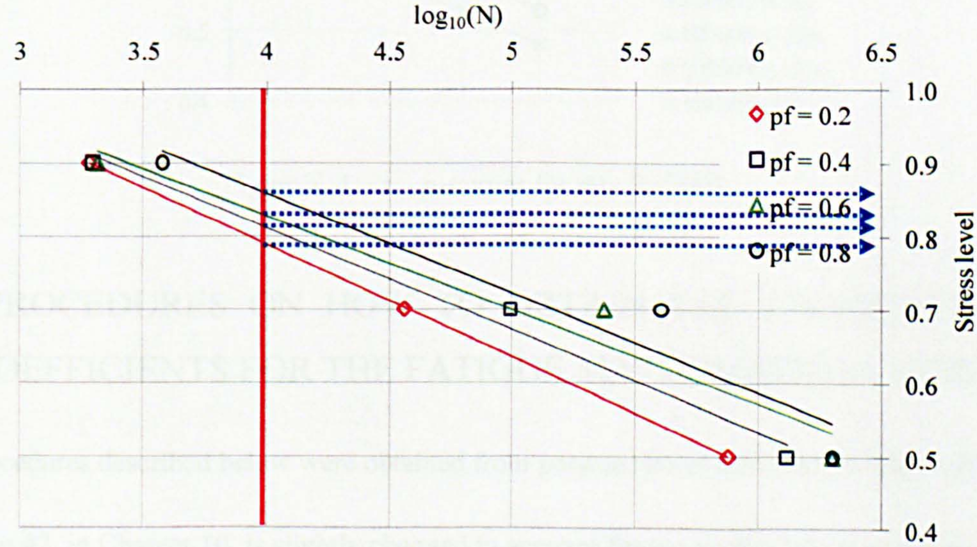

Figure J.3 – *s – log(N)* curves for mix R-CIP-0.

A table is then developed with the chosen values of log(N) and stress levels obtained by the graphical interpolation shown above, as shown in Table J.2 (mix R-CIP-0).

Table J.2 – S and p_f obtained by graphical interpolation (mix R-CIP-0).

p_f	Stress level considering the number of cycles chosen				
	4000	10000	100000	500000	1000000
0.20	0.865	0.790	0.635	0.530	0.480
0.40	0.880	0.815	0.670	0.575	0.530
0.60	0.880	0.830	0.700	0.610	0.570
0.80	0.925	0.860	0.720	0.625	0.585

Finally, the graph $s - p_f$ is then plotted (Figure J.4) based on the values shown in the above table. Graphs from Figures J.1, J.2 and J.4 are then gathered together as shown in Figure 254 to Figure 260 in Chapter 10.

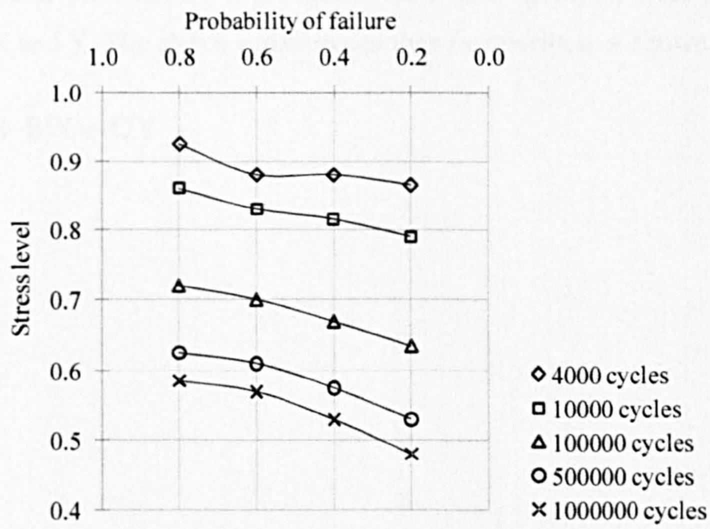

Figure K.4 – $s - p_f$ curves for mix R-CIP-0.

K.5 PROCEDURES ON HOW TO OBTAIN THE EXPERIMENTAL COEFFICIENTS FOR THE FATIGUE MATHEMATICAL MODEL

The procedures described below were obtained from personal notes provided by Singh (2010).

Equation 42, in Chapter 10, is slightly changed to account for the probability of survival instead of the probability of failure p_f. The probability of survival L is equal to $1 - p_f$. Equation 42 is then substituted by Equation J.1, described below.

$$L = 10^{-a(s)^{b}(logN)^{c}} \quad (J.1)$$

The above equation is subjected to a double log-operation as shown in Equation J.2.

$$\log(-logL) = \log(a) + b\log(S) + c\log(logN) \quad (J.2)$$

EquationJ.2 can then be written as shown in EquationJ.3.

$$\mathrm{Y = A + bX + cY} \quad (J.3)$$

Where:

$\mathrm{Y = \log(-logL)}$

$\mathrm{A = \log(a)}$

$\mathrm{X = \log(S)}$

$\mathrm{Z = \log(logN)}$

The number of cycles until failure is a function of S and L, which means that Z has to be determined from X and Y. The above equation can then be rewritten as shown in Equation J.4.

$$\mathrm{Z = A' + B'X + C'Y} \quad (J.4)$$

Where:

$\mathrm{A' = -\frac{a}{c}}$

$\mathrm{B' = -\frac{b}{c}}$

$\mathrm{C' = \frac{1}{c}}$

According to Singh (2010), it is more convenient to work with the averages of experimental values than with the original variables, and for this reason the following relationships can be formulated:

$$\mathrm{\sum Z = \sum A' + B'\sum X + C'\sum Y} \quad (J.5)$$

$$\mathrm{\frac{1}{n}\sum Z = A' + B'\frac{\sum X}{n} + C'\frac{\sum Y}{n}} \quad (J.6)$$

$$\mathrm{\bar{Z} = A' + B'\bar{X} + C'\bar{Y}} \quad (J.7)$$

By subtracting Equation J.7 from Equation J.4, the following expression is obtained:

$$Z - \bar{Z} = B'(X - \bar{X}) + C'(Y - \bar{Y}) \tag{J.8}$$

Equation J.8 is then substituted by Equation J.9.

$$z = b'x + c'y \tag{J.9}$$

Where:

$z = Z - \bar{Z}$

$x = X - \bar{X}$

$y = Y - \bar{Y}$

By means of least square normal equations, the following expressions are obtained:

$$b'\sum x^2 + c'\sum xy = \sum xz \tag{J.10}$$

$$b'\sum xy + c'\sum y^2 = \sum yz \tag{J.11}$$

The constants b' and c' can be calculated from the above equations, which is then substituted in Equation J.9 and in the modified form of Equation J.8, which takes us back to Equation J.3, where the coefficients a, b and c can be obtained.